A Dressing Solution for Burn Wounds: Antibacterial and Low-Adherent Wound Dressings

By

Tianyun Pu

A Thesis submitted to the Faculty of Graduate Studies of

The University of Manitoba

in partial fulfilment of the requirements of the degrees of

MASTER OF SCIENCE

Department of Textile Sciences

University of Manitoba

Winnipeg

ABSTRACT

Considering the infection and second trauma caused by dressing changes, development of antibacterial and low-adherent wound dressings is urgently needed. Silver ion is a widely used antimicrobial agent, but its cytotoxicity remains a problem. In this study, low-adherent PAM (polyacrylamide) hydrogel incorporated with less toxic AgNP (silver nanoparticle), was immobilized onto PET (poly(ethylene terephthalate)) substrates by an IPN (interpenetrating polymer network) method. The modified PET is effectively antibacterial and the surface is significantly less adherent than untreated PET. However, silver-resistant bacteria become a potential problem. Thus, ionic 5,5-dimethylhydantoin (DMH) analogues containing either a quaternary ammonium moiety or a phosphonate functional group were designed and synthesized. The DMH analogues were converted to antibacterial N-chloramine counterparts through chlorination to serve as potential alternatives to AgNP. The N-chloramine with a structural cation exhibited distinctly enhanced antibacterial functions both in solution and after immobilization on fabrics.

ACKNOWLEDGEMENT

The master's program at the Faculty of Human Ecology, University of Manitoba, has been a remarkable, challenging and fruitful learning experience for me. During my two years' of studies, I have received generous support and assistance from the people around me. Without their supports, my Master's thesis could not be revised and completed. I would love to express my sincere gratitude to those who have assisted, guided, and encouraged me.

In the first place, I express my deepest appreciation to my advisor, Dr. Song Liu, for his expert advice, wise guidance, consistent patience and kind encouragement in the past two years. Without his help and effort he has spent in our project, I could not finish this program in time.

Special thanks are extended to Dr. Lena Horne, Faculty of Human Ecology, Dr. Rick Holley, Faculty of Food Science, Dr. Juan Hinestroza, College of Human Ecology, Cornell University, and Dr. Sarvesh Logsetty, Faculty of Surgery for their valuable advice and guidance.

I am also indebted to all the colleagues, Dr. Lingdong Li, Wei He, Nan Zhao, Jiang Li, Abhilash Kulkarni and Chen Wu for their continued support and generous assistance. The friendship has helped me not only in research but also in daily life.

I acknowledge the financial support from the Manitoba Health Research Council (MHRC) and the Natural Sciences and Engineering Research Council of Canada (NSERC). I also acknowledge Dr. Rick Holley and Ms. Pat Kenyon for giving me permission and making arrangements for me to complete microbiology tests in the Faculty of Food Science. Thanks to Mary Pelton, who offered help in my academic writing.

Finally, I am truly grateful to my parents, Ms. Juan Cai and Mr. Anbin Pu, for their selfless love and encouragement in my study and life. Their love is always the best support for me to keep going.

LIST OF ABBREVIATIONS

ADMH: 3-allyl-5,5-dimethyhydantoin

AgNPs: Silver nanoparticles

AM: Acryamide

ATP: Adenosine triphosphate

ATR: Attenuated total reflectance

BP: Benzophenone

DI: Deionized

DLS: Dynamic light scattering

DNA: Deoxyribonucleic acid

DMH: 5,5-dimethyhydantoin

HA- MRSA: Healthcare associated Methicillin-resistant *Staphylococcus aureus*

HAIs: Healthcare associated infections

IPN: Interpenetrating polymer network

KI: Potassium iodide

MBA: N,N'-Methylene bisacrylamide

MRSA: Methicillin-resistant *Staphylococcus aureus*

PAM *:* Polyacrylamide

PET: Polyethylene terephthalate

MBAA: N-(2-methylbut-3-yn-2-yl) acrylamide

PBS: Phosphate buffered saline

PPS: Potassium persulfate

PTFE: Polytetrafluorethylene

PU: Polyurethane

QACs: Quaternary ammonium compounds

TEM: Transmission electron microscopy

TGA: Thermogravimetric analysis

TSA: Tryptone Soya Agar

UV: Ultraviolet

LIST OF TABLES AND SCHEMES

LIST OF FIGURES

1. LITERATURE REVIEW

1.1 Burn wounds and dressings

1.1.1 Burn wounds

Burn injury is one of the most common trauma caused by hot fluid, flame, electricity, chemicals and radiation. Burns are classified into four degrees from the least to the most serious. A first degree, for example a sunlight burn, makes the skin red and painful. In a second degree burn, the epidermis and parts of the dermis are damaged or destroyed. The entire epidermis and dermis are destroyed in a third degree burn. The most severe burn, fourth degree, causes damage to subcutaneous and deeper tissues such as muscles.[1,2]

Burn wound patients can suffer from pain, hypothermia, infection, femoral artery catheterization, disastrous organ failure and scar formation.[1] Large bacterial burden, great losses of body fluid and blood, a lack of nutritional supply and the second trauma can lead to delays and failures in wound healing. [4-7] Of all the problems hindering the healing of burns, infection is the leading cause of treatment failure.[8] It has been reported that 75% of the dead burn patients, who had more than 40% total body surface area burned, can be attributed to the infection-caused sepsis or other infection complications.[9] If not properly treated, burn patients can experience long periods of recovery, leading to financial burden for both patients and the health care system.[10] Prolonged periods of treatment can also lead to increased physical and mental suffering for patients. Thus, burn wound treatment is not only a physiological but also a psychological problem.[11] Reports show that of the entire two million burn victims each year in the United States, about 1% suffer severe

burns.[12] In India, more than seven million people annually suffer from burn injuries; nearly two hundred thousand of these injuries result in death.[13] Burn injuries are not confined to any specific location or region, but can occur anywhere in the world. Therefore, proper treatment for burn victims is crucial, not just for a single country, but for the betterment of the world.

The wound healing process has five overlapping stages: haemostasis, inflammation, migration, proliferation and maturation. Haemorrhage and clotting occur simultaneously in wounds. Bleeding activates haemostasis, which functions to prevent further blood loss. Inflammation involves both cellular and vascular responses and is characterized by increased blood flow. Protein-rich exudate releases serotonin and histamine; these two substances cause vasodilation to allow phagocytes to enter the wound and remove irreparably damaged tissue. At the stage of migration, epithelial and fibroblast cells move to the injured area to replace damaged or lost tissues. Cells regenerate and grow quickly over the wound. The proliferative phase occurs simultaneously with the migration phase. In this phase, there is an ingrowth of blood vessels and collagen is synthesized by fibroblasts. During the last phase, cellular connective tissue forms and the new epithelium is strengthened.[14,15,16]

1.1.2 Burn wound dressings

Dressings are materials that are used to cover and protect wounds. The purpose of applying dressings on burn wounds is to create optimal conditions to allow epithelial cells

to move, to enhance the healing process and to avoid damaging the wound by maintaining a moist environment and enabling effective oxygen circulation. [15,17] Many factors should be considered in choosing an appropriate wound dressing; these include depth of the burn, site and extent of the burn, the patient's ability to manage dressing, the associated pain and the urgency of healing time duration. Wound cleansing and debridement are necessary to create a good healing environment before applying a wound dressing. For first degree burns, no specific treatment is required to promote healing; however anti-flammatory drugs or aloe may be used to relieve pain and discomfort. For second degree burns, wound dressings and some antibacterial agents are needed. Severe burn injuries may require skin grafts; however, without appropriate and timely intervention, even superficial burns may result in deeper injuries.[2] Although there are many dressings available today, no single dressing is suitable for all kinds of wounds. A correctly chosen dressing will have a significant influence on the healing process. [14,18-21]

An ideal burn wound dressing should possess the following properties: debridement, prevention of rapid fluid loss, maintenance of a moist healing environment, timely removal of blood and excess exudates, infection control, low adherence and low frequency of dressing change. However, it is difficult to develop a dressing that meets all the above requirements. Based on their functions, dressings can be classified into antibacterial, absorbent, occlusive and adherent. As mentioned above, infection is always the leading problem in wound management. On the other hand, wound exudates from the wound may cause the problem of adherence upon drying. In such cases, dressings cannot

be easily removed resulting in a larger wound size and pain. [8,14,22] In the following sections, I will review some dressings that are effective in controlling infection or reducing second-trauma upon removal and as well as other dressings with excellent dressing features. [23,24]

1.2 Antibacterial wound dressings

1.2.1 Antibacterial agents used in wound dressing

Various antibacterial agents are used to kill bacteria to control infection in burn wound treatment.[25] Silver, in various forms, is the most common antibacterial agent used in wound dressings. QACs, N-choloramine,[26] honey, and chitosan have also been incorporated in wound dressings.

For centuries, silver has been used for bacterial inhibition in the process of water recycling and sanitization, in complementary health care, and in food.[27] In the 19th century, silver nitrate at 0.2% concentration was used to treat fresh burns. Silver sulphadiazine, made by combining silver nitrate and sodium sulphadiazine, was also introduced to treat burns; a 1 wt% in the hydrophilic cream was found to be effective in killing bacteria. However, a side effect of using silver, acute haemolytic anemia, occurred among patients. [28,29] The silver cation is highly reactive in a concentration between 5 and 40 mg/L.[28] It can damage bacterial cell walls and result in cellular structural changes. Silver ion can kill microbes by binding to intracellular proteins and inactivating them, can inhibit the synthesis of ATP (Adenosine triphosphate) and lead to DNA

(Deoxyribonucleic acid) denaturation.[30] To observe the killing mechanism of silver ion more directly, Feng et al. used TEM (Transmission electron microscopy) and X-ray techniques to facilitate the investigation. When *Escherichia coli* (*E.coli*) and *Staphylococcus aureus* (*S.aureus*) were treated with $AgNO_3$, the cytoplasm membrane detached from the cell wall. Subsequently, DNA and protein failed to function and finally the cell wall was damaged.[31]

AgNP, another form of silver element without an ionic charge, can be used as a catalyst, an optical sensor and an antibacterial agent.[32,33,34] The antibacterial activities of the silver ion and salts are well studied, but research about antibacterial mechanism of AgNP is relatively recent. [32] Different methods have been developed to synthesize and incorporate AgNP in some biomedical applications, and some reports have proven AgNP to be a potent antibacterial agent, that is effective against both Gram-positive and Gram-negative bacteria. [32,35-38]

Kittler et al. found AgNP was much less toxic to human cells than silver ion.[39] A concentration of silver ion higher than 1 μg/ml is toxic to human mesenchymal stem cells while the concentration of AgNP can be higher than 2.5 μg/mL. AgNP can destroy bacteria even at a nanomolar level while silver ion needs to be at a micromolar level. To kill silver resistant *E.coli*, the concentration of $AgNO_3$ should be higher than 1 mM while only 80 nM of AgNP is necessary for the same result. [38,40] Since AgNP is a less toxic antibacterial agent, it is also used to treat burns although the exact antibacterial mechanism of AgNP has not been clearly revealed to date.[39,41] The reduced nanosilver did

not show antibacterial activity towards *E.coli*, but when it was mixed with partially oxidized nanosilver, the mixture showed significant inhibition to the growth of *E.coli*. Thus, the antibacterial activity of AgNP is a result of surface oxidization as AgNP is sensitive to oxygen.[38]

QACs (Quaternary ammonium compounds) have been known for many years as efficacious biocides. Those with long alkyl chains, in particular, are used as antimicrobial agents or disinfectants for textiles. [42,43] QACs are active against a broad range of microorganisms such as fungi, Gram-positive and Gram-negative bacteria, and some viruses. The cationic ammonium group and the negatively-charged bacteria membrane are attracted to each other. Consequently, the interactions result in the formation of a surfactant-microbe complex that interrupts all the normal functions of the membrane.[44] However, after several washed, the concentration of QACs gradually decreases below minimum inhibition concentration. The most widely used QACs are monoquaternary ammonium such as alkyltrimethylammonium bromide, and diquaternary ammonium salts such as alkanediyl-α,ω-bis (dimethylalkylammonium bromide). Murugan et al. studied the antibacterial behavior of five novel insoluble bead-shaped, polymer-supported multiquaternary ammonium salts containing two to six quaternary ammonium groups. The QACs showed excellent antibacterial activity against *S.aureus, Klebsiella pneumonia* and *Pseudomonas aeruginosa* (*P.aeruginosa*). Murugan et al. also found that the antibacterial activity increased as the number of QACs in the structure increased.[45] However, there are also reports of bacterial resistance to QACs.[46,47]

N-halamines are compounds containing one or more nitrogen-halogen covalent bonds formed by the chlorination or bromation of imide, amide or amine groups. N-halamine compounds, of which N-chloramine is one form, can provide instant and complete kill of a broad-spectrum of microorganisms. The antibacterial property is based on Cl^+. Two mechanisms can be used to explain the antibacterial activity of N-chloramine. One mechanism is that free chlorine is released into water and then forms HClO or ClO^-. The other is that chlorine binds directly to acceptor regions in bacteria and greatly influences their enzymatic and metabolic processes. Worley et al. found that the antibacterial activity mainly attributed to the second mechanism because the dissociated chlorine is limited.[48] N-halamines possess stability that is suitable for long-term use, storage and regeneration. N-chloramine can be achieved by the reaction between sodium hypochlorite solution and imide, amide or amine groups. N-halamines have been used in water treatment and incorporated into cellulose-containing fabrics, polyester fibers and polyamide. [49,50,51] Although no research has directly addressed N-halamine in wound dressing, it has been grafted onto fibers or fabrics so it may be used in wound dressing.[50,51]

In addition to the antibacterial agents mentioned above, natural substances such as honey, chitin and chitosan also exhibit antibacterial activity. Honey has been reported to have the ability to treat burn wounds due to its antibacterial activity. [52,53,54] It contains hydrogen peroxide and plant derived chemicals such as bioflavonoids, which account for the antibacterial activity of honey towards some major wound-infecting bacteria such as

MRSA (methicillin-resistant *Staphylococcus aureus*). The bioflavonoids in honey have the ability to inhibit nucleic acid synthesis.[55] Chitin and its derivative, chitosan, are capable of accelerating the healing processes at the systemic, cellular and molecular levels. Chitosan possesses the properties of nontoxicity, biocompatibility and biodegradability. It has been proposed that the interaction between the positive charge in chitosan and the negative charge in the bacterial cell wall may lead to the disruption of membrane.[56,57] Due to its polycationic structure, the antibacterial activity of chitosan is similar to that of QAC. Although chitosan itself is an antimicrobial agent, it is also able to effectively deliver extrinsic antibacterial agents to control infection.[58]

1.2.2 Methods for depositing antibacterial agents onto substrates

1.2.2.1 Depositing silver onto materials

Since silver exhibits antimicrobial activity against a broad range of microorganisms, methods of depositing silver onto materials are important for a desired antibacterial medical product.

In recent research, AgNPs were impregnated onto different materials by a reducing agent accompanied by a stabilizer. Dong et al. designed a one-step method to deposit AgNPs uniformly to nylon fiber. The reaction was driven by the carboxylic acid group of sodium citrate on the surface of AgNPs and the amide group of the Nylon 6 fiber. The Ag^{+} was reduced by sodium borohydride. Stabilized AgNPs (8nm) self-assembled on the surface of the Nylon 6 fiber at pH 5 or 6. After the fiber was treated with 108 mg/L AgNP

solution (0.01g treated fabric) and challenged 1 ml 10^7 CFU/mL *E.coli*, the log reduction was 5 after 2 hours of contact and even reached 6-7 logarithm after 24 hours. The antibacterial activity is strong and fast.[59]

Zhang et al. prepared a nano-silver colloidal solution by mixing $AgNO_3$ aqueous solution with an aminoterminated hyperbranched polymer (HBP-NH_2) aqueous solution in which HBP-NH_2 played a role in reducing the silver ion and stabilizing AgNP. A cotton fabric was then immersed in AgNP (18nm) solution; particles were assembled on cotton because of the hydrogen bonding between amide and hydroxyl groups. The cotton treated with 120 mg/L AgNP solution (0.75g treated fabric) killed 99.87 % *S. aureus* and 99.77 % *E.coli* after 18 hours of contact with 70 ml 10^5 CFU/mL bacterial suspension. Even with an increased Ag load, the efficacy increased only slightly.[60] These results show that even with similar AgNP concentration, a larger sample mass, less bacteria colony and longer contact time, the antibacterial activity of the silver-coated cotton is weaker than the silver treated nylon fiber. [59] The efficacy difference could be attributed to the difference in AgNP sizes. Thus, the importance of smaller particle size in antibacterial activity is notable. Vimala et al. used a three-step process to prepare a chitosan-silver nanocomposite film. The silver ions were reduced by both poly(ethylene glycol) and chitosan and the resultant AgNPs (12 nm) were stabilized by the two reducing agents. The chitosan-silver nanocomposite film showed great antibacterial efficacy in the Kirby Bauer diffusion test.[61] However, the film-based antibacterial material is suitable only for slightly exudating wounds because the film is good at water vapor and oxygen

permeation but not water absorption.

There are also many reports regarding the synthesizing of AgNP and hydrogel composites through less toxic methods. A number of synthetically varied methods were developed by incorporating metal ions into sol-gels, polyelectrolyte multilayer films, and porous polymers.[61] Recent trends show that a gel is a proper and promising structure for the synthesis of metal nanoparticles with small diameters. [62,63]

Murthy et al. designed the first semi-IPN (interpenetrating polymer network) hydrogel silver nanocomposite. The polyacrylamide/poly(vinyl pyrrolidone) hydrogel was synthesized by a redox free radical polymerization. AgNPs (around 3 nm) were incorporated by reducing silver ions that diffused into the hydrogel from a silver nitrate solution. *E.coli* can grow around pure semi-IPN hydrogel, while hydrogel-silver nanocomposites can inhibit the growth of *E.coli*.[64] Varaprasad et al. prepared poly(acrylamide)/poly(vinylalcohol) hydrogel-silver nanocomposites and the AgNPs were only around 2 to 3 nm. The results of antibacterial tests show that the AgNP-bonded hydrogel can kill more *E.coli* than silver ion-bonded hydrogel. These results indicate that much smaller AgNPs could be synthesized in a hydrogel structure. Although the antibacterial assessment method is different from that used to evaluate fabric and fiber, the antibacterial test results reveal the excellent antibacterial efficacy of AgNP. Thus, the prepared AgNP-hydrogel composites are promising antibacterial materials for the incorporation of tiny AgNPs.[65]

The above reports all addressed the synthesis of AgNP containing hydrogel that can

be used as antibacterial material, wound dressing applications and even water-based applications. However, none of these methods considered grafting a silver-containing hydrogel onto another material. An ideal dressing should not only be suitable and effective to treat the burn, but it also needs to be handled easily.[15] The antibacterial activity of a silver-containing dressing can be affected by its conformability.[66] Therefore, some textile fabrics may be suitable substrates since they are quite flexible and conform to the wound contour, enabling water/vapor exchange and act as a barrier to prevent bacterial invasion. A knit fabric structure possesses better extension and flexibility than either woven or nonwoven structures. However, the yarns and loops in a weft knitted fabric unravel from the edge when the fabric is cut while those in a warp fabric do not. Thus, a knit fabric, especially a warp knitted structure is suitable for using in a wound dressing. Even when the dressing needs to be cut according to the wound size, the structure is run-resistant and will maintain its integrity.

1.2.2.2 Depositing QACs onto materials

Since fabrics finished with QACs were found to have low durability because of gradual leaching, some efforts were made to improve the bonding between QACs and fabrics. Polymerizable QACs with acrylate or methacrylate groups in the structure have been synthesized. Under certain conditions, the synthesized QACs could be polymerized into a polymer network with a polycationic structure. The QACs moiety could be chemically bonded to the main polyacrylate chain. Thus, the polymerized coating can be

immobilized on the fabric surface, vastly increasing the fabric's durability and wash resistance in comparison with QACs. The microorganisms can be killed by contact. [67,68]

Sol-gel technology has also been applied in QACs immobilization. An organic-inorganic structure was formed to render a nanocomposite polymer. The colloid solution consisted of $Si(OR)_4$ and QACs or $Rx\text{-}Si(OR)_3$ with incorporated QACs. When the alkoxy groups hydrolyzed, (-SiOH) groups can further condense with each other or with the (-OH) groups in fibers. The covalent bond between -SiOH groups and -OH groups in fibers provide improved durability and wash resistance for the nanocomposites on the finished fibers.[69]

1.2.2.3 Depositing N-halamines onto materials

Much work has been done to immobilize the N-halamine onto different polymers. Liu et al. grafted acrylamide and methacrylamide to cotton cellulose. When chlorinated by sodium hypochlorite, the products demonstrated durable and regenerable biocidal functions against 10^5-10^6 CFU/mL *E.coli* suspension and the log reduction reached 5 after 120 min of contact for treated cotton.[70]

N-halamine could also be successfully on polyester. Ren et al. synthesized two N-halamine siloxane precursors and immobilized them onto polyester. When exposed to bleach solution, the polyester specimens were challenged with 10^6 CFU/mL *S. aureus* and *E.coli*.[71] Compared to the previous report,[70] the treated polyester killed bacteria much faster than the treated cotton with just a 30 min contact with bacterial suspension. In

addition to cotton and polyester fibers, Sun et al. grafted 3-allyl-5,5-dimethyhydantoin (ADMH) onto different fibers such as Nomex®, Kermel® and a PBI/Kevlar® blend using heat induced copolymerization. The antibacterial activity was achieved by exposing the grafted fibers to a NaClO solution. Those fibers with N-chloramine were powerful against both Gram-positive and Gram-negative bacteria.[72] Liu et al. grafted ADMH onto PET (Polyethylene terephthalate) fabric, but little could be grafted. The fabric killed 10^5-10^6 CFU/mL *E.coli* at a contact time of 2 hours.[73] The antibacterial activity was not as efficient as Ren's work. It is probable that the amount of ADMH grafted onto the surface was limited as the grafting percentage was only about 0.7%, leading to less convertible N-H bonds to become N-Cl bonds upon exposure to sodium hypochlorite.

From the research on depositing N-halamines onto materials, materials with amide, amine and imide groups could react with normal bleach solution, conveniently activating the antibacterial function. Even when the antibacterial efficacy of fiber or fabric becomes weak due to the leaching of active chlorine, the materials will regain their antibacterial property through rechlorination.

1.2.3 Antibacterial dressings

Chitosan can stimulate cell proliferation, help natural blood clotting and block nerve endings to relieve pain. Chitosan is biocompatible, biodegradable, nontoxic and antibacterial. Furthermore, it can be processed into hydrogels, nanofibers, sponges and membranes. For example, Mi et al. designed a chitosan membrane that could be used as a

wound dressing. The membrane was composed of a top layer supported by a sponge-like sub-layer. It showed good oxygen permeability and fluid drainage ability, and blocked the penetration of bacteria due to the dense top layer. In addition, since chitosan is an antibacterial agent, it can kill the bacteria in the wound.[74] When chitosan is combined with hydrogel, the dressing could stop bleeding within 30 seconds confirming the hemostatic ability of chitosan. [75] However, the low mechanical property of a chitin/chitosan based sponge remains a problem until new tissue forms and matures. Furthermore, chitosan dressings are not always effective in killing bacteria or controlling bleeding. Thus, the incorporation of coagulant and silver are needed.[76]

For several reasons the interest in incorporating honey into a wound dressing is increasing. The high viscosity of honey can from penetrating a wound bed.[77] In addition, honey stimulates cytokines, reduces wound odor and rarely causes eschar. [78,79] The effectiveness and advantages of a honey dressing, as reviewed by Molan, include rapid healing, reduced odor, less pain and accelerated epithelization. However, it is difficult to keep the honey in place on a wound as it gradually flows to other sites. Sting was also observed in some clinical trials.[80]

By incorporating silver ion into alginate fibers, a highly absorbent antibacterial alginate wound dressing can be produced. The dressing is a nonwoven structure having good swelling capacity. When in contact with wound exudates, the fibers swells, resulting in reducing the space between fibers. Thus, the bacteria carried in wound exudates are trapped between the fibers; the released silver ions subsequently deactivate bacterial cells.

Researchers showed that the alginate dressing obtained 100% antibacterial activity after 5 hours of contact with *P.aeruginosa* and *E.coli.* However, bacterial concentration was not clearly given in the research. The silver content could reach 2.18 μg/mL in human serum after 30 minute release,[81] which is relatively higher than the maximum concentration of silver ion that does not cause cytotoxicity.[39]

Aquacel® Hydrofiber dressing is a soft nonwoven silver-containing wound dressing composed of sodium carboxymethylcellulose fibers. The dressing can reduce pain and effectively kill bacteria, is easy to remove and cost effective. However, it shows cytotoxicity in some in *vitro* studies.[82] Likely, the silver ions combine with the chlorine in the exudates to make the silver lose its antibacterial property after prolonged contact.

A hydrophilic polyurethane dressing called Contreet Foam® is able to sustain a release of the silver ion and absorb a great deal of exudates. Consequently, it is typically used for wounds having a high bacterial burden and high exduates. The hydroactive silver ions are released from the dressing and function on the bacteria as the dressing absorbs exudates. About 56% of the ulcer area can be reduced, however 80% of patients reported stinging for the first 0 to 2 hours after the dressing was applied. It is possible that the content of silver in this dressing is relatively high causing discomfort.[30,83] To summarize, the antibacterial activity of silver-containing wound dressings has been recognized, but cytotoxicity remains a problem.

Instead of using silver ions, Acticoat® is a wound dressing with a nanocrystalline silver (Ag_2O and Ag_2CO_3) coated layer and a rayon/polyester layer. It claims to have a

faster bacteria-killing rate when compared to silver nitrate and silver sulphadiazine. Acticoat Flex 3® is a polyester knit product with high flexibility and stretch properties. It allows fluid transport into the secondary dressing and maintains good contact to the wound bed. However, patients experienced stinging in the first few hours probably because of the high silver dosage in the dressing. The wound bed also became colored from the released silver particles. The biggest problem for Acticoat® is the adherence to the skin and the need to be wetted before removal.[84,85,86]

1.3 Atraumatic wound dressings

1.3.1 Atraumatic surface and dressings

Vital to the healing process are dressings that do not cause trauma or damage to the wound or the skin--atraumatic dressings. Hydrogel dressing, hydrocolloids, alginates and soft silicone coated dressing are considered to be nonadherent wound dressings since they have the ability to prevent drying of exudates by maintaining a moist layer around the wound.[22] Consequently, the dressing does not adhere to the wound. The soft silicone dressing is adherent to the intact skin but not to the moist surface of the wound.[87]

Hydrocolloid dressings are wound management products generally used for lightly to moderately exuding wounds. They are obtained from gel-forming materials combined with elastomers and adhesives. Usually, carboxymethylcellulose, gelatin and pectin are widely used as gel forming agents.[88] Currently available products include Aquacel™, Granuflex™ (ConvaTec, Hounslow, UK) and Tegasorb™ (3M Healthcare, Loughborough, UK). In one study, hydrocolloid dressing and another dressing were chosen to treat

lacerations and abrasions. Patients who used the hydrocolloid dressing experienced less pain and less analgesia. Furthermore, they could carry out daily activities even when they had dressings on wounds.[89] The desirable advantages of hydrocolloid wound dressings include its ability to absorb wound exudates, and not to cause pain to patients. However, an occlusive outer cover may affect the infected wound because oxygen is needed for rapid healing.[15]

The main features of wound dressing containing polymeric organic silicone compounds are good absorption, atraumatic removal and less pain. For example, Mepitel®, which is a silicone-coated wound dressing used in second degree burns, is a polyamide net. It is low-adherent and causes little pain and damage when removed from a wound. A burn treatment study comparing Mepitel® and silver sulfadiazine cream showed that healing time was shorter for those using Mepitel® than for those using silver sulfadiazine, and the silicone in the dressing provided easy removal of the dressing from the wound. However, the dressing leaves imprints on the skin if pressure is added on the dressing.[90] Mepilex Ag®, a dressing composed of a Safetac soft silicone wound contact layer, film backing and a foam pad, does not cause trauma upon removal and minimizes risk of maceration. Film backing allows moisture vapor to permeate into the dressing although it is waterproof, and the foam pad plays a role in absorbing exudates. In addition, Mepilex Ag® contains antibacterial silver sulfate. The product has been proved effective in treating partial-thickness burns and newly grafted burn wounds. Although the dressing showed broad-spectrum antibacterial activity, the antibacterial agent in the dressing is

silver sulfate that can lead to cytotoxicity because of the presence of silver ion. The dressing does not exhibit antibacterial activity without a moist environment.[91,92,93]

Alginate dressings are produced from the calcium and sodium salts of alginic acid. The alginate dressing can be produced in two different forms: freeze-dried porous sheets, or flexible fibers. When in contact with wound exudates, alginate can form a gel, limit wound secretion, and avoid being infected by bacteria.[94] The multivalent Ca^{2+} ions in alginate dressing can exchange with Na^{+} in exudates and form a protective film of gel to maintain moisture and healing temperature.[95] There are some alginate products such as Sorbsan™, Kaltostat™. And Comfeel Plus™, which is a type of hydrocolloid/alginate dressing. Not only are alginate dressings easily removable without causing pain or destruction of granulation tissue, they are also biodegradable.[96] However, alginate dressing cannot be used on dry wounds or those covered with necrotic tissue because the wound could become dehydrated and thus delay healing. Alginate dressings are usually used for moderate to heavily exuding wounds.[15]

Hydrogels are excellent structures to shelter proteins and cells without altering their characteristics and properties. They are solid and jelly-like three dimensional polymeric materials of which up to 90% is water. Hydrogels are hydrophilic and are highly absorbent natural or synthetic polymers which possess a degree of flexibility highly similar to natural tissue.[97] Their end-uses include tissue engineering (to create scaffolds to repair damaged tissues), environmental interventions (pH/temperature sensitive material), drug release systems.[98] Now research and development of hydrophilic materials

(hydrogels) for temporary skin covers or as wound dressings are becoming a subject of great commercial interest. [99,100] Hydrogels can imbibe water and biological fluids, maintain a moist environment for wounds and create a low-adherent interface between dressing and wound.

Antibacterial agents could be incorporated into hydrogels to make them bactericidal. Hydrogels are made of synthetic polymers such as poly(methacrylate), polyacrylamide and polyvinylpyrrolidine. These are insoluble, swellable and hydrophilic materials. When hydrogel dressings contain almost 70-90% water, they cannot absorb much exudates, and therefore hydrogel dressings can be used to treat lightly or moderately exuding wounds. Hydrogel dressings are suitable for dry or necrotic wounds because they are able to rehydrate dead tissue and promote autolytic debridement. Hydrogel dressings have high patient acceptability due to the promoted moisture for wound healing, nonadherence, less pain, expedited re-epithelisation and no residue. The only problem of hydrogel dressings is their low mechanical strength. The tensile strength of 1 mm thickness PVA-hydrogel is 0.04 MPa and that of a superabsorbent polysaccharide hydrogel based on a pullulan derivate ranges from 0.663 to 1.097 MPa. [100,101] However, the tensile strength of polyester/cotton blend fabric can be higher than 10 MPa which is far beyond that of a hydrogel.[102] During clinical application, the dressing should be handled carefully.[103]

1.3.2 Evaluation of adhesive force test between wound and dressings

Adherence of dressings to wounds, as mentioned above, is a problem of burn wound

management. There is a need to test adhesive force when the dressing is peeled from wounds. Analysis can be undertaken to determine the dherence property of dressings and the patient discomfort during the wound dressing change. The following are relevant research about adhesive force tests.

Kiatamnuay et al. adhered silicone rubber strips to human skin using Epithane-3 (E3) or Secure^{2} Medical Adhesive (SMA). Skin-Pre Uni-Solve adhesive remover was also applied 1 day before testing. An Instron TM-M was chosen to peel off the dressing at the rate of 100mm/min.[104] Dykes et al. tested adhesive force and discomfort of 6 wound dressings by removing the dressing at an angle of 135° and a constant speed of 1500mm/min. The subjects used an electronic visual analogue scale to assess the discomfort level. The Mepilex Border® dressing was given a significantly lower discomfort score than others indicating that the Mepilex Border® dressing causes less pain for the patients.[105] A similar method was also reported by Klode et al. using European standard EN1939:2003 'Self- adhesive tapes–Determination of peel adhesion properties'.[106] Another human model was adopted in Dykes's research where volunteers were treated with methylene blue for 60 minutes so the stratum corneum on the skin could be evenly stained. Then a dressing was applied to the forearm and peeled off after 24 hours. The dye left on skin was analyzed by a spectrophotometer. The less dye left indicated the dressing is less adherent. Volunteers were aged from 19-53 and random skin sites were chosen which indicates test validity.[107] However, these methods are generally used for wound dressings and adhesives which are applied to healthy human skin. We

need to directly observe the adhesive force between wound dressing and wound.

To better analyze the dressing adherence through biological testing, Xu et al. cultured human fibroblasts with the concentration of 4×10^4 cells/mL on dressing samples for 4 hours. Then samples were washed with PBS solution and quantified with MTT method. The fewer viable cells attached to the surface indicated a less adherent property.[108] Since adherence is caused by exudates drying and cell in-growth, the cell adhesion test mainly focused on the material, regardless of exudates. The cell adhesion test is an appropriate to test adherence, but the method does not consider the wound healing mechanism. Therefore, a wound model is a better way than the cell adhesion test. Dong et al. adopted a device to measure peeling force continuously between the graft and full-thickness wound on mice. This device could conduct a reproducible, controlled and constant rate peeling process. [109] The adhesive property was expressed as peeling force per area unit. However, since a slight contraction occurred during the healing process, the dimension of the graft may change so the full peeling forces need to be reported.

1.4 Conclusion

Infections and adherence, which could lead to delayed healing, have become serious problems in burn treatment. Thus, it is essential to introduce an antibacterial function as well as a low-adherent surface into wound dressings. Different antibacterial agents have been used to control infection and different wound dressings are widely available in burn wound treatment. Silver-containing dressings demonstrate excellent antibacterial activities, but silver ions have cytotoxicity. Some bacteria were found to have a silver-resistant gene, which is a potential problem for future use of silver dressings. Therefore, there is a need to develop a new biocide. Hydrogels are nonadherent materials and AgNPs have been incorporated into them. To develop a more conformable dressing, textiles can be used to serve as a substrate for silver containing hydrogels.

2. HYPOTHESES AND OBJECTIVES

A burn is a type of injury to the skin caused by heat, electricity, chemicals, light, radiation or friction. It can occur in any age group or any society. About 75% of the mortality in burns owes to infection.[110] Large burn infections may cause lethal problems and are the main reason for the failure of burn treatments, accompanied by problems such as pain, exudates fluid, monitoring electrolyte imbalances, and improper nutrition.[111] Wound dressings are widely used during burn treatments.[19] Silver containing dressings exhibit good performance because silver is effective in infection control and has been used for more than 200 years. [28,30,112,113] However, silver ion can inhibit the synthesis of ATP and lead to DNA denaturation and it is also toxic to keratinocytes and fibroblasts.[114] AgNP is cytotoxic to cells when its concentration is higher than 30 mg/L but for ionic silver, it is toxic to cells only at 1 mg/L.[41,115] Moreover, AgNP is effective in killing bacteria even at a nanomolar level, but Ag^{+} should be used at a micromolar level to achieve the same antibacterial efficacy. As for current wound dressings, there is a silver ion containing wound dressing that is nonadherent and antibacterial, but silver ion is not an ideal antibacterial agent. Dressings with AgNP still present some problems such as adherence, which means tissue cells will stick and grow into the dressing. There is no research about combining hydrogel and silver onto other substrates such as fabrics, which conform to different parts of the human body, to achieve atraumatic and antibacterial properties.

Although AgNPs-coated wound-care dressings are successful in reducing the

bacterial burden in burn wounds and in preventing infections, several bacterial stains including *E.Coli* K-12, O157:H7, MRSA 133/03 have been reported to be silver-resistant.[116,117] The emergence of silver-resistant bacterial strains requires frequent monitoring of the occurrence of that kind of bacteria. Thus, new biocides are a necessity. Besides silver, QACs and N-halamines are two other categories of biocides that can be used to control infection. Although bacteria-resistance was found against QACs, [118,119] there have been no reports of bacterial resistance against N-chloramines. Whereas it is difficult to develop a new category of biocides, studying the possible synergistic effect among existing biocides could be rather useful. We found poly(2-(N-chloroacrylamido)-2-methylpropane-1-sulfonic acid) (poly(CAMPS)) had a lower antibacterial efficacy than poly(N-chloro-N-(1,3-dihydroxy-2-(hydroxymenthyl) propan-2-yl) acrylamide) (poly(CTHMA)) even with higher active chlorine due to the negative charge in the poly(CAMPS) compound structure that repels the negative charges on cell walls.[70] It is possible that the antibacterial performance can be boosted by combining both cationic and N-chloramine moieties. If long chain QAC is combined with N-chloramine, it may produce a synergistic antibacterial activity.

The following are the rationales of this thesis.

1. Researchers have already found the antibacterial activity of AgNPs in wound dressing as well as in hydrogel polymer composites. We hypothesize that when a polymer is grafted onto a substrate and AgNPs are incorporated into that polymer, the modified substrate could also be antibacterial;

2. Hydrogels have been found to have a nonadherence property so we hypothesize a layer of hydrogel on the surface of PET fabric could markedly reduce the adherence to the wound;
3. Since there are no reports of bacteria resistance against N-chloramine, and positive charge in biocide could attract negatively charged bacteria, we hypothesize that by combining cationic moiety with N-chloramine, there could be a synergistic effect for the new biocide.

To sum up, the objective of this project is to design a wound dressing that is both atraumatic and antibacterial. Since hydrogel can create an atraumatic surface, and knit fabric has good stretch ability and conformability, by grafting AgNPs containing hydrogel onto a knit fabric could solve the adherence problem and provide antibacterial activity to a dressing with less cytotoxicity. However, the untreated knit PET fabric with the same structure as Acticoat^{TM} Flex 3 is difficult to obtain. Thus, a plain woven PET fabric was used in the research because it is cheaper and much easier to obtain than the knitted one. To develop a new biocide that is effective and non silver resistant, the possible enhanced antibacterial activity of combining both cationic charged center and N-chloramine was to be studied. The specific objectives of this project are to:

1. Graft polyacrylamide (PAM) onto PET fabric to achieve a low-adherent surface and enable self-assembly of AgNPs;
2. Control the AgNPs size and water absorbing capacity of the hydrogel to achieve an optimal bacterial killing rate and low-adherence;

3. Graft a potent antibacterial biocide on PET/cotton and study the potential boosting effect of QACs with N-halamine.

Findings from this study would be beneficial in understanding the antibacterial activity of both AgNPs and the new biocide which containing both N-chloramine and QACs. The adherence property would be evaluated.

3. MATERIALS AND EXPERIMENTS

3.1 Materials

Acrylamide (AM), N,N'-Methylene bisacrylamide (MBA, crosslinker), benzophenone (BP, photoinitiator), silver perchlorate ($AgClO_4$), sodium citrate ($Na_3C_6H_5O_7 \bullet 2H_2O$), sodium borohydride ($NaBH_4$) , PET plain woven fabric (#777H) , cotton print cloth (#400) were purchased from Testfabrics, Inc. (West Pittiston, PA), PMBAA-PET were prepared according to a published article,[120] methanol (Fisher), Milli-Q water, synthesized compounds were prepared in our lab.

3.2 Experiments

3.2.1 Surface modification of PET

It has been reported that amides can form dimeric hydrogen bonds with Citrate-Stabilized AgNPs so to enable their self-assembly. PAM was chosen to be embedded on PET. The first step of surface modification is to graft acrylamide onto PET. Briefly, PET (10 × 6 cm) was first swollen in a methanol solution (15 mL) of AM, MBA and BP for 1 hour under continuous shaking (40 ^{o}C, 90 rpm). **Table 1** lists the concentrations of AM, MBA and BP. Then, the swollen PET was exposed to UV (ultraviolet) irradiation (365 nm) to initiate the polymerization. Afterwards, the fabric went through 24 hours soxhlet extraction in water to get rid of loosely attached polymer and monomer. PAM IPN formed as shown in **Scheme 1** (b), part of the network is embedded in PET fabric (the broken blue lines), and part of it protrudes out (solid blue

lines). The modified PET is called PAM-PET-1, PAM-PET-2 and PAM-PET-3 according to increasing monomer concentration.

Immobilization percentage (IP)=$(W_1-W_0)/W_0 \times 100\%$ (1)

where W_1 and W_2 are the weights of the original and grafted fabrics, respectively.

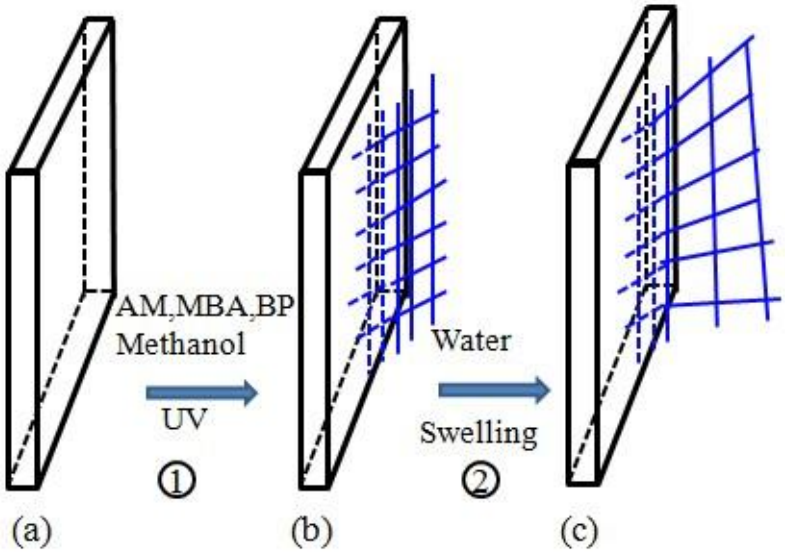

Scheme 1. Formation of PAM interpenetrating polymer network on PET fabric. (a) untreated PET fabric, (b) PAM-PET, (c) PAM-PET after swelling.

Table 1. Concentrations of monomer, crosslinker and initiator in the surface modification of PET.

Samples	Concentration (mol/L)		
	Monomer	Crosslinker	Initiator
	AM	MBA	BP
PAM-PET-1	3	0.45	0.055
PAM-PET-2	3.6	0.45	0.055
PAM-PET-3	4.5	0.45	0.055

3.2.2 Preparation of silver nanoparticles

AgNPs were synthesized by reduction of sodium citrate stabilized Ag^+ with sodium borohydride. Briefly, 2 mM $NaBH_4$ and 0.6 mM trisodium citrate was prepared in Milli-Q water with continuous stirring in an ice bath until all the chemicals dissolved. Then 0.2 mL 15 mM $AgClO_4$ solution was slowly added into 59.2 mL trisodium citrate and sodium borohydride mixture. The solution appeared to be gold-yellow as AgNPs formed in it. Following 3 hours stirring at room temperature, all the AgNPs solution was purified to remove soluble salts by using centrifugal ultrafiltration (3K). The suspension was stored at 4 ^oC for later use.

Prepared solution was added into 1M HCl to adjust pH value to 6 to assemble AgNPs onto PAM-PET-(1, 2, 3). About 30 mL prepared solution was used for 3 cm^2 fabric and shake for 3 hours to allow AgNPs self-assembly. All the samples with AgNPs can be referred to as PET-Ag and PAM-PET-Ag-(1, 2, 3).

3.2.3 Swelling kinetics study

The kinetics of the swelling process was investigated by means of weight test at room temperature. All the samples were cut into 2×2 cm and around 0.2 g is needed for each sample. PET and PAM-PET-(1, 2, 3) were weighed after they reach equilibrium in dessicator by an electronic balance (0.0001 g) and then totally immersed in DI water. The samples were taken out after certain time duration (0 min, 2 min, 4 min, 6 min, 10 min, 15 min, 20 min, 30 min). A centrifuge with the speed of 2800 rpm was used to remove the

excess water on the surface for 30 s. All the samples were weighed again quickly.

Swelling ratio = $(m_t-m_0)/m_0 \times 100\%$ (2)

m_t is the weight of sample after t min swelling in water, t =0, 2, 4, 6, 10, 15, 20, 30 min

m_0 is the weight of sample before swelling

3.2.4 Peeling force test

In this project, an in *vitro* model was chosen to mimic the environment between human skin and wound dressing.[121] Basically, 50 wt% gelatin (gelatin from porcine, type A, Fisher) was used because of its relatively low moisture and high tensile strength, which are necessary during peeling test. A PTFE (polytetrafluorethylene) window frame, with 16×60 mm^2 area for gelatin casting, is molded for gelatin casting. All the fabric samples (3×10 cm^2) were soaked in DI water for 5 min and spread on a clean bench; one frame was placed onto one piece of fabric. Gelatin powder was dissolved in DI water at 70 ^oC then it was poured into the window frame. All the samples were dried at 35 ^oC which is close to normal human body temperature. After drying, the PTFE window was removed from all the specimens, and an Instron 5956 machine (Instron, MA, USA) was used to peel gelatin off from the sample at a constant rate of 100mm/min with 180 ° peeling angle to mimic the peeling process in dressing removal. Five highest peaks were chosen to obtain the average peeling force. Peeling energy per unit area is expressed in this thesis as

$$\theta=\frac{2P}{b} \quad (3)$$

where P is the average peeling force and b is the width of the gelatin strip, unit J/m^2

3.2.5 Grafting polymerization of MBAA onto cotton swatch

To study the boosting effect of QACs and N-halamine, we chose both hydrophobic and hydrophilic fabrics for surface modification. PMBAA-PET was prepared in the laboratory. As cotton is quite hydrophilic and is able to absorb a large amount of water, pure organic solvent is not necessary. Thus, water and water soluble initiator can be used in cotton surface modification. The solution of the monomer MBAA (1.92 g, 14 mmol), in mixed solvent (acetone 8 mL + DI water 32 mL), was added into initiator potassium persulfate (PPS, 0.43 g, 1.6 mmol). After the complete initiator dissolution, a piece of cotton fabric (10 × 10 cm) was dipped in the resulting solution and padded twice at a required expression (150% wet pick up). The padded fabric was dried at 60 ^{o}C for 10 min, cured at 105 ^{o}C for 30 min, and then immersed in a large amount of water to remove water soluble chemicals. The fabric was then extracted with methanol in a Soxhlet-extractor for 24 hours to remove ungrafted monomers. Afterward, the fabric was air dried and stored in a desiccator for 24 hours to reach constant weight. The resultant modified fabric was named as "PMBAA-grafted-cotton" (PMBAA-g-cotton). Percentage graft was calculated from the following equation:

$$\text{Graft Percentage (\%)} = (W_2-W_1) / W_1 \times 100\% \qquad (4)$$

where W_1 and W_2 are the weights of the original and grafted fabrics, respectively.

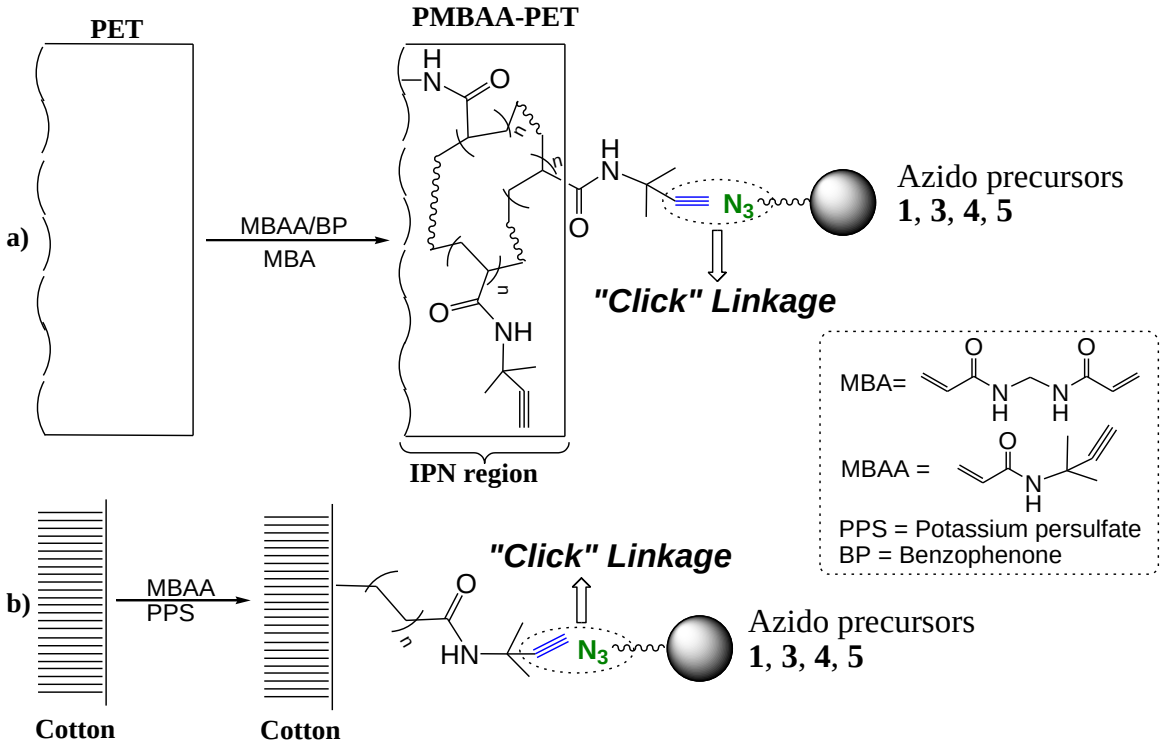

Scheme 2. **MBAA grafting and immobilization of azido-precusors onto (a) PET and (b) cotton via "click" reaction.**

3.2.6 "Click" linkage between synthetic precursors (1, 3, 4, 5) and PMBAA-PET/PMBAA-g-Cotton

PMBAA modified PET (PMBAA-PET) was obtained by forming a surface interpenetrating network of PMBAA and PET following the reported protocol.[121] The "click" reaction between the synthetic precursors and PMBAA-PET was performed following a previous protocol. These synthetic azides were covalently bonded onto PMBAA-g-cotton in a similar way. PMBAA-g-cotton fabric (1.2 g, grafting percentage=1.1%) was first immersed in 20 mL mixed solvent (t-BuOH/H_2O = 1:1, v/v) containing equivalent amounts of synthetic azides (calculated based on totally PMBAA on grafted cotton). Then Na ascorbate (40% mol) and Cu^{2+} (10% mol) were added to initiate the "click" reaction. After 1 hour of shaking with Wrist Action Shaker (Burrel Scientific, PA, USA), the fabric was taken out and washed thoroughly with DI water and ethanol. The rinsed cotton was then air dried overnight and stored in desiccators until use. The obtained fabrics that were endowed with specific precursors were named as PMBAA-PET-(1, 3, 4, 5) or PMBAA-g-cotton-(1, 3, 4, 5).

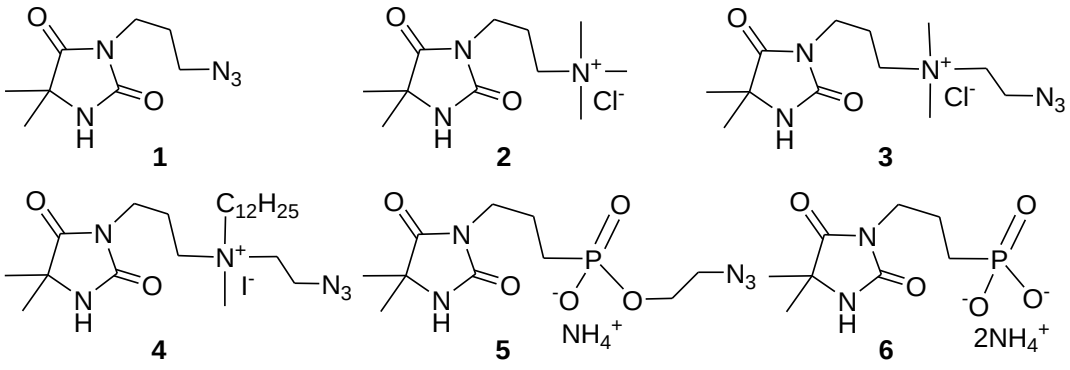

Scheme 3. Structures of N-chloramine precursors used in this research.

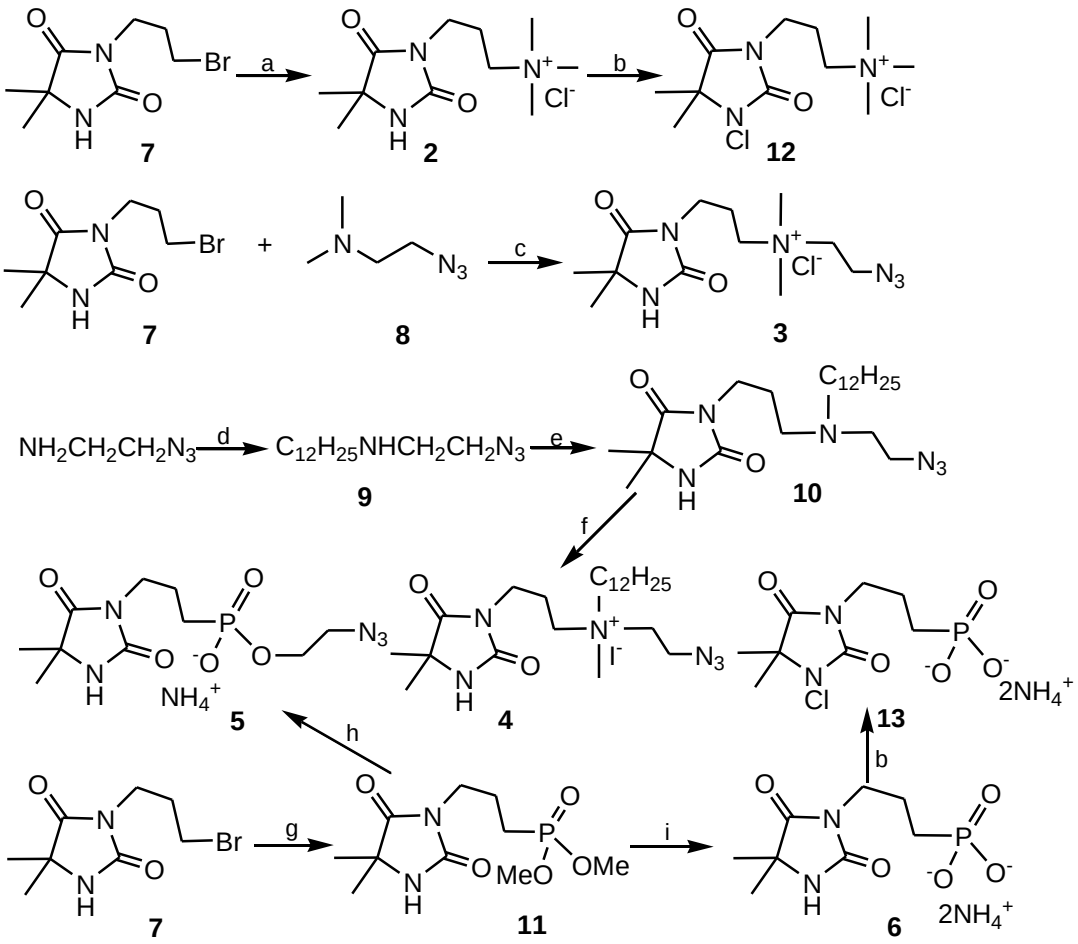

Scheme 4. Chemical synthesis of 2-6.

3.2.7 Chlorination and titration of PMBAA-PET-(1, 3, 4, 5) and PMBAA-g-Cotton-(1, 3, 4, 5)

3.2.7.1 Chlorination

Both "click" modified PET and cotton fabrics were chlorinated by simply immersing in sodium hypochlorite solution with a solid/liquid ratio of 1:50 (w/w). The concentration of bleaching solution varied from 15 ppm to 1,500 ppm as needed. After continuously shaking for 30 min, the samples were rinsed with plenty of DI water thoroughly and then air dried overnight for titration analysis or antibacterial assay.

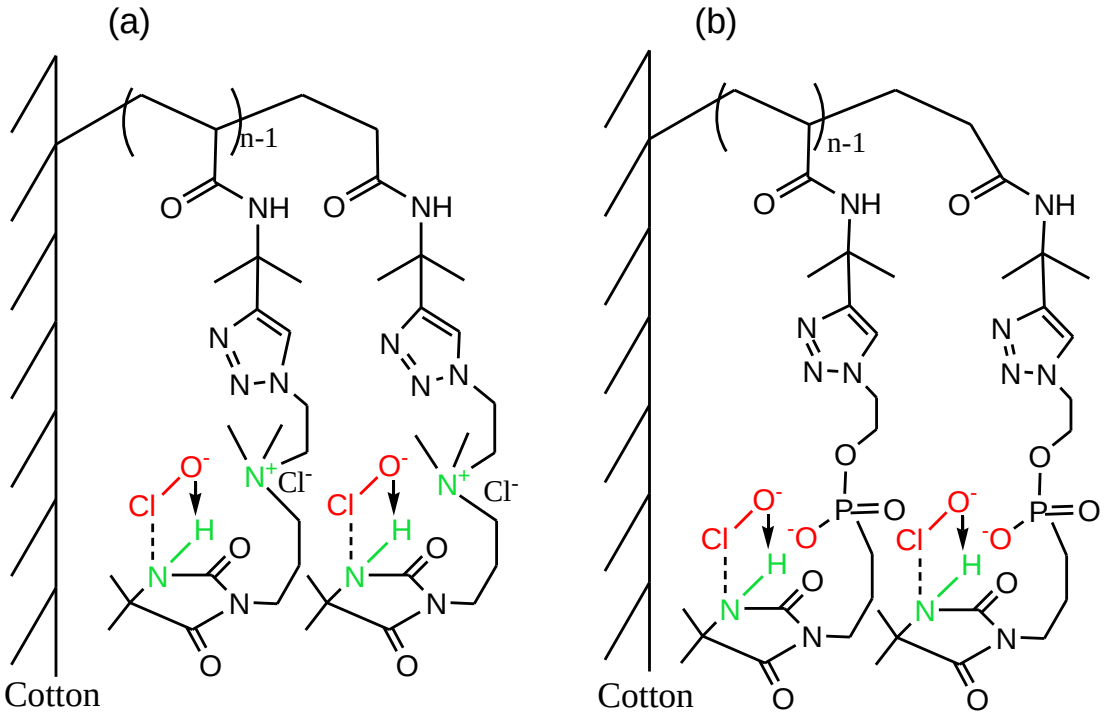

Scheme 5. Chlorination process on precursor grafted cotton.

3.2.7.2 Analytical titration of NaClO

The amount of active chlorine was quantified by titration. First, the NaClO bleach solution, which is used to chlorinate PMBAA-PET- (1, 3, 4, 5) and PMBAA-g-Cotton (1, 3, 4, 5), was titrated. Iodometric titration was used in which potassium iodide (KI) formed as a result of oxidation by chlorine.

Starch indicator was prepared by dissolving 1 g soluble starch powder in 2-3 mL cold DI water then the cold starch solution was added to 100 mL of boiling DI water. The starch solution was cooled down for later usage. This solution was be re-prepared every two weeks approximately. Sodium thiosulfate $Na_2S_2O_3$ volumetric solution 0.1mol/L was diluted 100 times using volumetric flask. Acetic acid 99.8% for analysis was diluted to 5% (pH=4) as buffer. NaClO bleach solution was diluted for 100 times with volumetric flask and waited to be titrated. Thermo Scientific pH/conductivity Benchtop meter is needed.

The buret was rinsed with $Na_2S_2O_3$ solution three times and filled with $Na_2S_2O_3$ solution. 1 mL diluted NaClO solution was added to 30 mL DI water. The solution was under continuous stirring around 300 rpm. Then about 1 g KI and 1 mL acetate buffer were added to the beaker and a yellow to yellow-orange color appeared as the KI dissolved. The start reading in the buret was recorded before titrating. The electrode was set up erectly in the beaker and electric potential mode (mv) was observed by using a conductivity benchtop meter. $Na_2S_2O_3$ was slowly added into the solution while observing the color change. The color began to fade as more $Na_2S_2O_3$ was added. When the color of the solution in the beaker was close to the color of straw (pale yellow), 3-4 droplets of the

starch solution (1%) were added. Then the color of the solution immediately changed to dark blue or purple. The endpoint of this titration is the point at which the solution just turned to colorless, or when the electric potential showed a sudden drop. The ending reading was recorded in the buret. Titration for NaClO solution was performed in triplicate.

Available chlorine concentration of the NaClO bleach solution

$[Cl^+]$ (ppm)= $35.45 \times (V_e - V_s) \times 100$ (5)

V_e and V_s is the endpoint and start point of the titration.

3.2.7.3 Analytical titration of active chlorine on fabrics

All the samples after the click reaction were chlorinated in sodium hypochlorite solution with different concentration at room temperature for 30 min. An iodometric titration method was adopted to quantify the active chlorine in the samples right after the air-dry process. Around 0.26 g to 0.27 g of PET fabric, 0.15 to 0.16 g of cotton fabric was usually used and cut into small pieces, 10 ml 0.001 mol/L $Na_2S_2O_3$ volumetric solution and 30 mL DI water were added into the beaker with fabric in it. The active chlorine was quenched by $Na_2S_2O_3$. The solution was under continuous stirring for 30 min and the beaker was sealed with parafilm. After stirring, iodine volumetric solution 0.0005 mol / L was used to titrate the remaining $Na_2S_2O_3$.

We added 2 ml acetic buffer into the beaker and began stirring again. The buret was filled with iodine solution and iodine was added drop by drop into beaker. When the

reading of electric potential tended to be stable, one drop was carefully added into the beaker until the reading jump occurred. The start reading and end reading were recorded at the beginning and in the end for one titration process. A beaker with only 10 mL $Na_2S_2O_3$ and 30 mL DI water should be titrated first as control.

The active chlorine concentration of the fabric samples was then calculated from the following equation:

Active chlorine concentration $[Cl^+]$ (ppm)$=35.45\times(V_1-V_2)\times N\times 1000/(2\times W)$ (6)

where V_1 is the volume (mL) of the iodine solution consumed in titrations of blank sodium thiosulfate solution, V_2 is the volume of iodine solution consumed when titrate fabric sample. N is the normality of iodine solution and W is the weight of the samples in grams.

3.2.8 Antibacterial assay

3.2.8.1 Assessment of PAM-PET-Ag-(1, 2, 3)

To evaluate the antibacterial activity of PAM-PET-Ag-(1, 2, 3), the Suspension Test was carried out.[122] Both untreated PET, PET-Ag and PAM-PET-Ag-(1, 2, 3) were tested. All samples with the size of 1×1 cm^2 piece were needed. Healthcare associated (HA)-Methicillin-resistant *Staphylococcus aureus* (MRSA) 40065 and Pseudomonas aeruginosa 73104 were chosen as challenging organisms because they are the main bacteria causing infections in burn wounds.[3,123] MRSA is Gram positive, and *Pseudomonas aeruginosa* is Gram negative; thus AgNP containing sample would be

tested on different kinds of bacteria. Briefly, the culture process is introduced in previous research.[124] All samples were soaked in 5 mL bacterial suspension with a concentration of 10^6 CFU/mL. Put the vials with bacteria suspension and samples into an incubator at 37 ^oC for 4 hours. After 15 min, 30 min, 60 min, 120 min and 240 min the vials and 100 μL solution of each sample were taken out and diluted 10-fold and then transferred onto an agar plate, which had been divided into four sections. Then the solution was diluted for 10-fold and transferred to the next section. Each sample was tested in triplicate. An analysis of variance was used to check for statistical differences among the test results, and statistical significance is considered at $p \leq 0.05$.

Percentage reduction of bacteria (%) = (A - B)/A ×100 (7)

Log reduction= Log (A/B) (8)

Where A is the control bacteria concentration and B is the bacteria concentration after certain time contact.

3.2.8.2 Assessment of compounds (12) and (13)

Tryptone Soya Agar (TSA) was used for bacterial culture. After subculture from stock, bacteria were allowed to grow at 37 ^oC for 18-20 hours to obtain logarithmic-phase cultures. Biocidal activity of bleached **12** and **13** were completed as follows. The 20 mL bacterial suspension (10^6–10^7 CFU/mL) in a centrifuge tube was added into 30 μL of **12** or **13** solutions (0.28 M stock solution) to achieve a final 15 ppm [Cl^+]. Timing of the exposure to the disinfectant was started immediately with the addition agent **12** or **13**. At

predetermined contact times (5 min, 10 min and 20 min), 1.0 mL aliquots were withdrawn and added to an equal volume of 0.02 N sodium thiosulfate in PBS (0.05 M, pH 7.0). The quenched suspension was serially diluted, and 100 μL of each resulting dilutions were placed onto nutrient agar plates. After being incubated at 37 ^{o}C for 24 hours, viable bacterial colonies on the plates were counted. Bacterial reduction was reported according to equations 7, 8. In the equations, A is the number of bacteria retrieved from bacterial control (CFU/mL), and B is the number of bacteria retrieved from **12** or **13** (CFU/mL).

3.2.8.3 Assessment of chlorinated PMBAA-PET-(1, 3, 4, 5) , PMBAA-g-cotton-(1, 3, 4, 5)

Antibacterial assessment for chlorinated PMBAA-PET-(1, 3, 4, 5) was carried out against a clinical isolate of MDR-*E. coli* (#70094). Antibacterial properties of chlorinated PMBAA-g-Cotton-(1, 3, 4, 5) were examined against clinical isolates of MDR-*E. coli* (#70094) and HA-MRSA (#77090, healthcare-acquired) respectively. The click-modified fabrics PMBAA-g-Cotton-(1, 3, 4, 5) were first cut into four small pieces (diameter = 4.8 cm), two of which were put together in a sterilized container. Then 0.5 mL bacterial suspension (10^5–10^6 CFU/mL) was placed onto these two fabric surfaces, and sandwiched by another two portions of the identical fabrics. Immediately another 0.5 mL bacterial suspension was dispensed on the whole fabric set. After a contact time of 5 min at room temperature, 100 mL of 0.03% sodium thiosulfate aqueous solution was added to

the container to neutralize any active chlorine. The mixture was then vigorously shaken for 2 min followed by ultrasonic treatment for 5 min. An aliquot of the solution was removed from the mixture and then serially diluted and 100 μL of each dilution was placed onto a nutrient agar plate. The same procedure was also applied to the bleached untreated cotton and bleached PMBAA-g-cotton. Viable bacterial colonies on the agar plates were counted after incubation at 37 ℃ for 24 hours. Bacterial reduction is reported according to the equations 7, 8. In this case, A is the number of bacteria counted from bleached pristine cotton and B is the number of bacteria counted from modified cotton fabrics.

Non-contact killing test was carried using the following protocol. Chlorinated cotton and chlorinated PMBAA-g-cotton-3 were cut into small pieces and sealed in a nylon bag respectively. The bags containing cotton fabrics were immersed in 10 mL PBS (Phosphate buffered saline) (0.05 M, pH 7.0) and continuously shaken using vortex stirring. At the predetermined time of 5 min and 10 min, 2.0 mL aliquots were taken out by a syringe equipped with a nylon filter membrane (0.45 μm, Fisher) and mixed with 0.5 mL bacterial suspension (10^5-10^6 CFU/mL). The mixture was left to stand for 5 min before 12.5 mL 0.03% sodium thiosulfate aqueous solution was added to quench the "released" active chlorine. Afterward, the bacterial suspension was serially diluted, and 100 μL of each resulting dilutions were placed onto nutrient agar plates. After being incubated at 37 ^{o}C for 24 hours, the viable bacterial colonies on the plates were counted.

3.2.9 Characterization

Attenuated total reflectance (ATR): The ATR spectra were collected and all the samples were scanned at 16 cm^{-1} resolution. A background-corrected spectrum was analyzed according to characteristic peaks in spectrum.

Transmission electron microscopy (TEM): TEM was used to observe the AgNPs which had been deposited on PAM-PET fabric. From the images, the particle distribution in solution can be viewed and the average diameter of the AgNPs were measured and calculated.

Dynamic light scattering (DLS): The hydrodynamic size of silver nanoparticle was measured, QS 3.00mm cuvette was cleaned by 2% Hellmanex, 5% acetic acid and milliQ water then dried with air flow. Transferred 200 μl AgNPs solution to cuvette and run the test at 20 ^{o}C. The software Zatasizer summarized statistics according to the intensity of light scattered. Size distribution by volume was analyzed.

Thermogravimetric analysis (TGA): TGA test was carried out with TGA 2050 analyzer (Linseis, Germany) to quantify the silver content on fabric. Temperature increased at 10 ^{o}C/min up to 1000 ^{o}C at an oxygen atmosphere and percentage change of fabric mass was plotted against temperature. The residue mass percentage equals to the percentage of AgNPs on the tested sample.

3.2.10 Statistical analysis

In the study, antibacterial tests and peeling force test were performed in triplicate.

The results are expressed as means ± standard deviations. All the data were analyzed by two-sample t-test. Values of $p<0.05$ were considered significant.

4. RESULTS AND DISCUSSION

4.1 Deposition of AgNPs containing PAM hydrogel on PET

4.1.1 Immobilization of PAM on PET

To develop a low-adherent surface, we immobilized AM on PET by IPN method, which is supposed to polymerize functional monomer and crosslinker in the swollen surfaces of the polymers to form an interlocking structure and durably immobilize the functional groups. In-situ photoinduced polymerization under UV follows the diffusion of acrylamide monomers, crosslinkers and photoinitiators into the polymer substrate and then polymer network forms on the surface. As reported in previous publications,[125] the photoinitiator BP can generate free radicals when exposed to ultraviolet and initiate polymerization.

During the experiment, the polymer formed on the PET fabric after irradiation for one hour. The feel of fabric was different with soft untreated PET because of the polymer. As shown **Figure 1**, the amide group on modified fabric can be confirmed by some characteristic peaks in the spectrum. Spectrum (a) is untreated PET, Spectrum (b) is PAM-PET-3, the last one is the subtraction spectrum between PAM-PET-3 and untreated PET, which provides a magnified view of the differences between untreated PET and PAM-PET-3 sample. For both untreated PET and PAM-PET-3, peak at 1713.05 cm^{-1} was assigned to C=O in ester. No obvious new peaks could be seen from spectrum (b); however in spectrum (c), there were two new peaks located at 1654.33 cm^{-1} and 1620.42 cm^{-1}, which are characteristic amide I and II peaks of PAM. The ATR spectra confirm the

successful immobilization of PAM on PET.

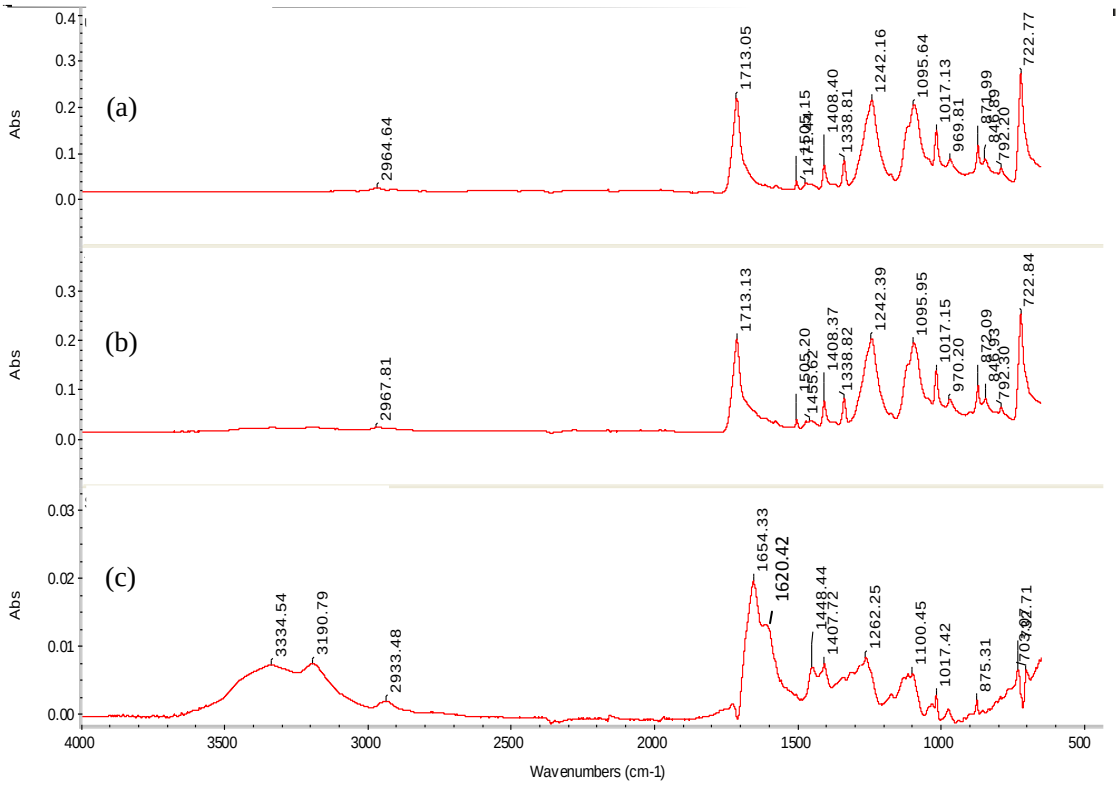

Figure 1. ATR spectra of (a) untreated PET, (b) PAM-PET-3, (c) subtracted spectrum of PAM-PET-3 and untreated PET.

4.1.2 Incorporation and distribution of AgNPs

During the preparation of AgNPs, sodium citrate and $NaBH_4$ were dissolved in Milli-Q water. As $AgClO_4$ was added drop by drop, a color change was observed as AgNPs formed in the solution. When reacting with the reducing agent $NaBH_4$, the $AgClO_4$ drop immediately became black and then turned to gold yellow along with continuous stirring, which indicated AgNPs formation. Before self-assembly onto PAM-PET-(1, 2, 3), the size of AgNP was investigated by both DLS and TEM. Distribution of AgNPs was first evaluated by DLS, a very helpful and versatile technique. As shown in **Figure 2**, there is only one sharp peak in the curve at 13.18 nm (analyzed by Zetasizer). Although DLS result displayed the distribution of particles, those smaller than 6 nm did not exist in DLS graph. Since TEM is a more direct technique to observe particles and DLS only shows the volume distribution, we also carried out TEM to analyze prepared AgNPs.

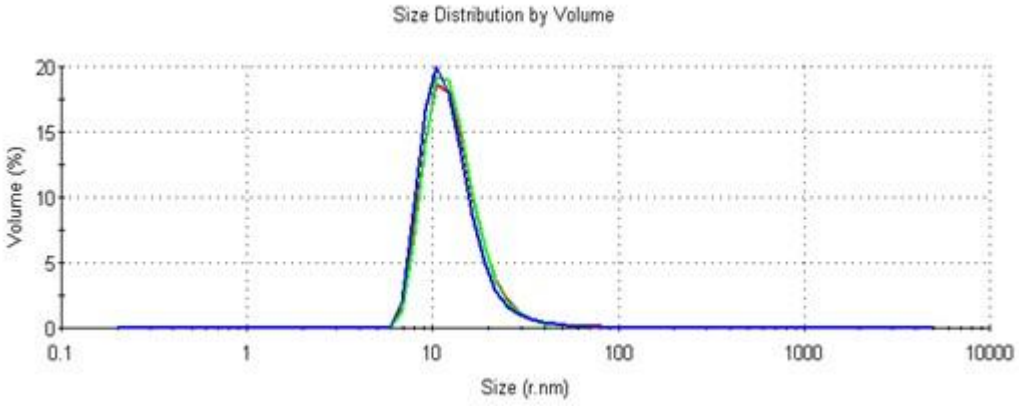

Figure 2. Size distribution by volume recorded by DLS.

The following TEM pictures give a more straightforward illustration of the distribution, shape and size of AgNPs. **Figure 3** (a) shows the particle distribution in solution is uniform and no big cluster or aggregated particles could be seen. The size of the AgNPs could be measured from **Figure 3** (b). According to TEM images, smaller particles were observed and measured (**Figure 4**). It is probable that DLS is not sensitive enough to detect small particles which are less than 6 nm in size.[126] The corresponding TEM image (**Figure 3** (b)) revealed that AgNPs are around 1-20 nm and the average diameter of AgNP was 6.74 nm. Some relatively bigger particles were surrounded with a bunch of tiny ones. The DLS showed only one broad peak biased to larger particles because those small ones are undetectable by this technique.

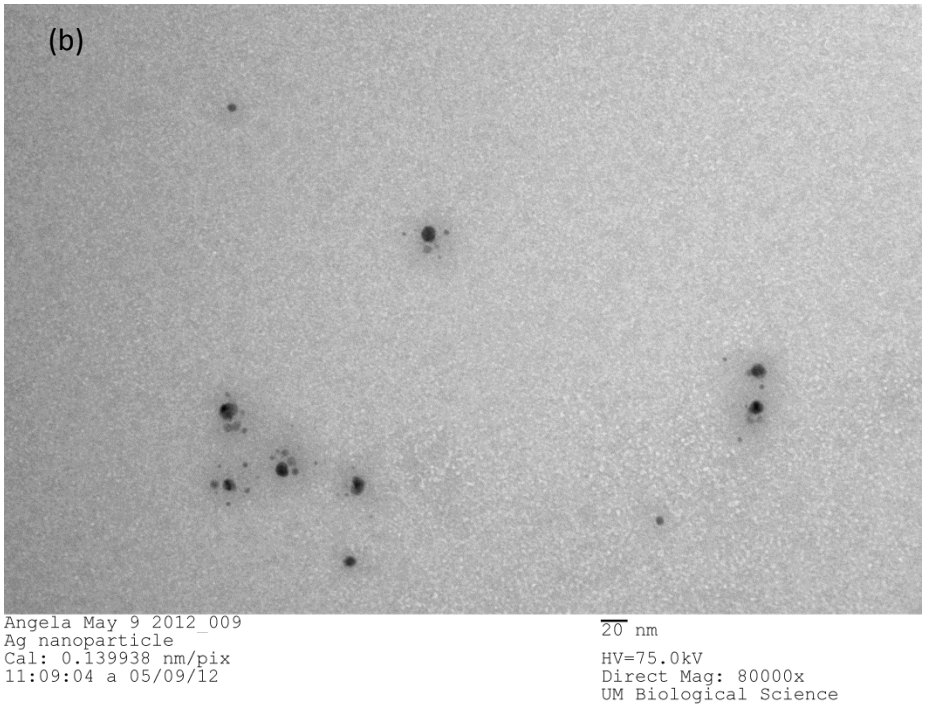

Figure 3. TEM images. Magnification of images: (a) 40,000×, (b) 80,000×.

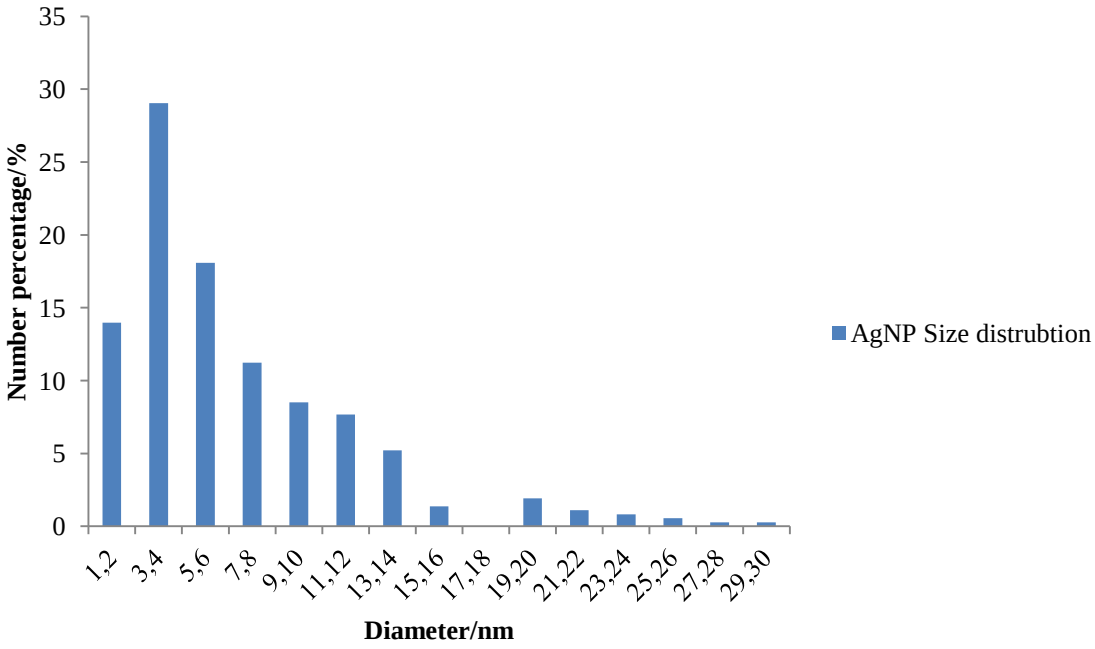

Figure 4. AgNPs size distribution of TEM images.

The prepared AgNPs solutions were later used for silver self-assembly on PAM-PET fabric by hydrogen bonding which was achieved between carboxylic groups in soudium citrate and amide moieties. Through interfacial dimeric hydrogen bonding, AgNPs were successfully assembled. The fabric was dark brown with particles on it while the untreated samples remained white with only limited quantities adsorbed between fibers (**Figure 5**). Because of numerous AgNPs, the PAM-PET-Ag-3 was shiny as metal (**Figure 6**) and the mass percentage of loaded silver was analyzed by TGA (**Figure 7**). PET served as a control sample and the silver percentages of PAM-PET-Ag-3, as an example, was the mass change difference between control sample and modified sample. The mass change of untreated PET was 98.39% and that of PAM-PET-Ag-3 was 94.61% and therefore, the silver content in PAM-PET-Ag-3 was 3.78%, which was higher than

PET-Ag (1.77%), PAM-PET-Ag-1 (3.02%) and PAM-PET-Ag-2 (2.90%).

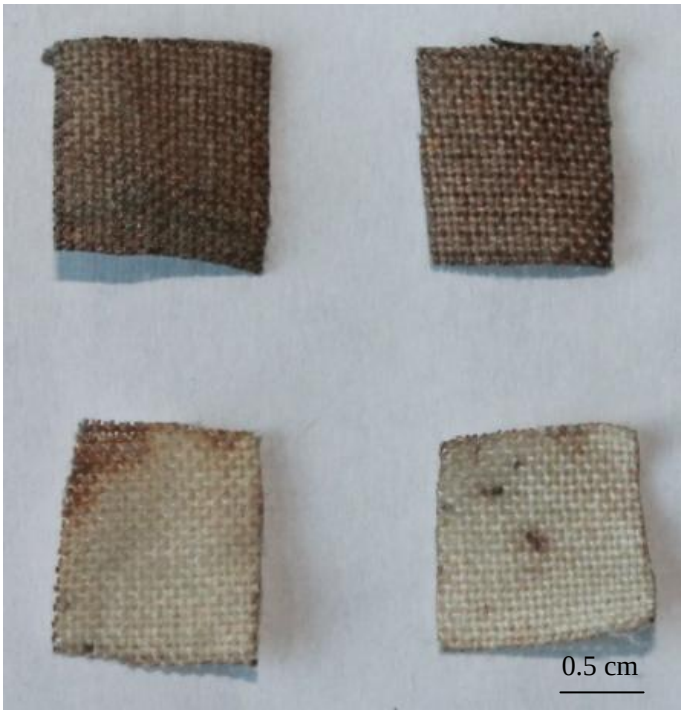

Figure 5. AgNPs assembled on PAM-PET-3 (1st row) and untreated PET (2nd row).

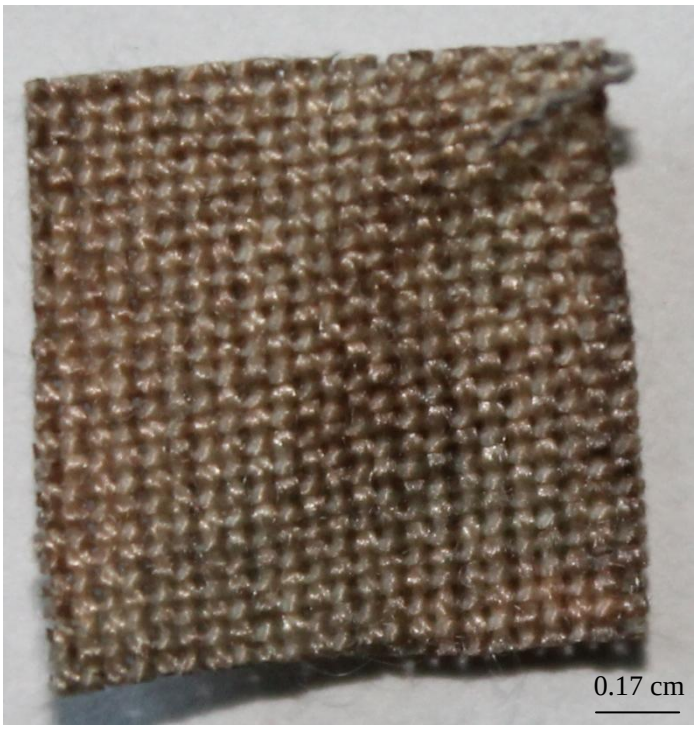

Figure 6. AgNPs assembled on PAM-PET-3. Magnification of image: 9×.

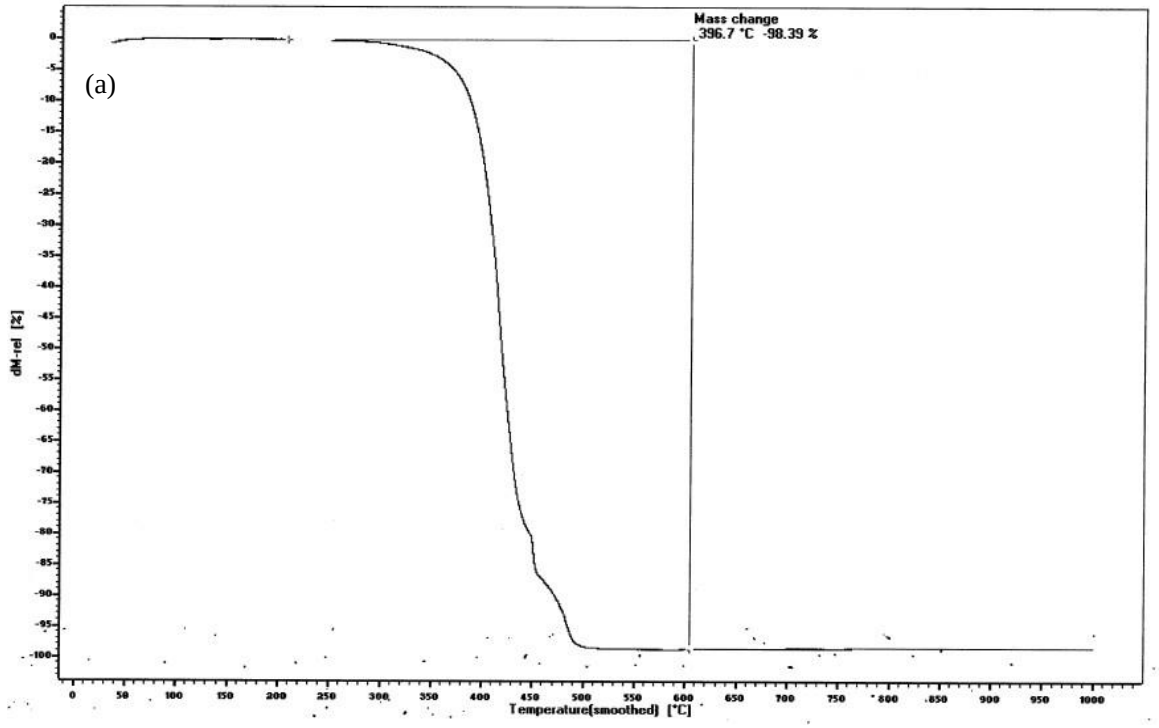
(a)
Mass change
396.7 °C -98.39 %
dM-rel [%]
Temperature(smoothed) [°C]

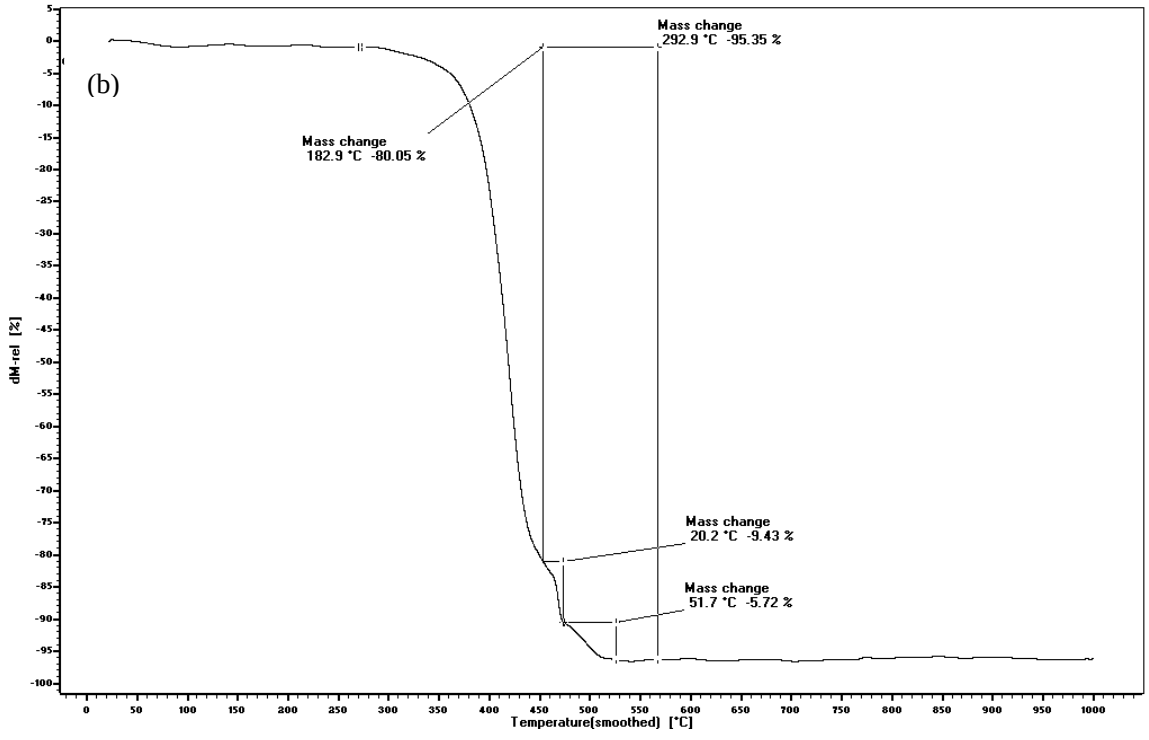
(b)
Mass change
292.9 °C -95.35 %
Mass change
182.9 °C -80.05 %
Mass change
20.2 °C -9.43 %
Mass change
51.7 °C -5.72 %
dM-rel [%]
Temperature(smoothed) [°C]

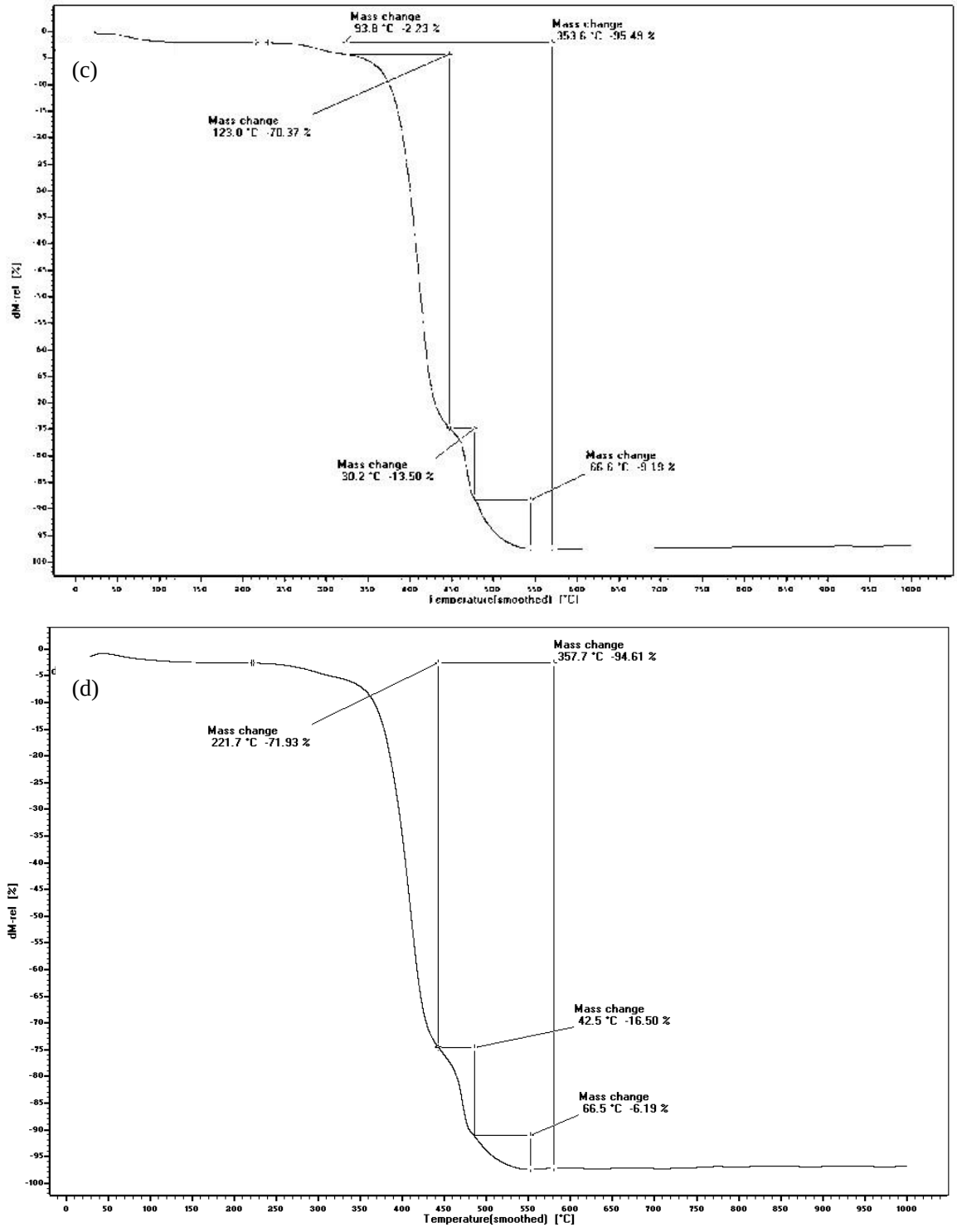

Figure 7. TGA curves of untreated (a) PET, (b) PAM-PET-Ag-1, (c) PAM-PET-Ag-2, (d) PAM-PET-Ag-3.

4.1.3 Swelling kinetics study of PAM-PET-(1, 2, 3)

As hydrogels can provide a moist environment, prevent fluid loss and absorb excessive water, the swelling kinetics of hydrogels needs to be studied to observe how fast that hydrogel can form on the modified PET fabrics. Acrylamide was used as a monomer in photoinitiated polymerization because it is a common monomer to be polymerized to form hydrogel, which is capable of swelling and deswelling reversibly. Thus, the PET fabric grafted with PAM is quite hydrophilic. The swelling capacity of modified PET with grafted PAM was studied and untreated PET in the study was a control sample. The swelling percentage of PET should be deducted from that of PAM-PET-(1, 2, 3) and the resulted swelling data was contributed by the immobilized PAM hydrogel.

Given there is a lot of excessive water on the fabric which should be removed by centrifugation during swelling kinetics experiment, it is essential to study the proper time duration in centrifugation. Both untreated PET and PAM-PET-1 were drenched in DI water for 30 min and put in centrifugation tubes with cotton at the bottom to absorb water. The samples were then weighed after 4 s, 10 s, 30 s, 300 s and 600 s centrifugation. It is easy to find that the swelling percentage dropped dramatically for both untreated PET and PAM-PET-1 during the 4 s to 30 s centrifugation (**Figure 8**). Some water molecules existed between fabric pores, and the rest was stored between fibers by capillary effect as well as in the polymer network. The slope of the curve from the point of 30 s became much less steep, so we conclude that the water molecules adsorbed on the surface were

eliminated by centrifugation according to the curve. It was the IPN in the PAM-PET-1, we believe, that contributed to the swelling percentage difference that resulted from the subtraction of untreated PET from PAM-PET-1. Though the swelling percentage kept dropping after 30s, it is probable that the air flow (caused by high speed and longstanding centrifugation) in the tubes caused the water molecules to evaporate gradually. It also could be concluded from **Figure 8** that PAM-PET-1 had a better ability to conserve more water than untreated PET. In the following experiments, 30 s was chosen as the suitable centrifugation duration.

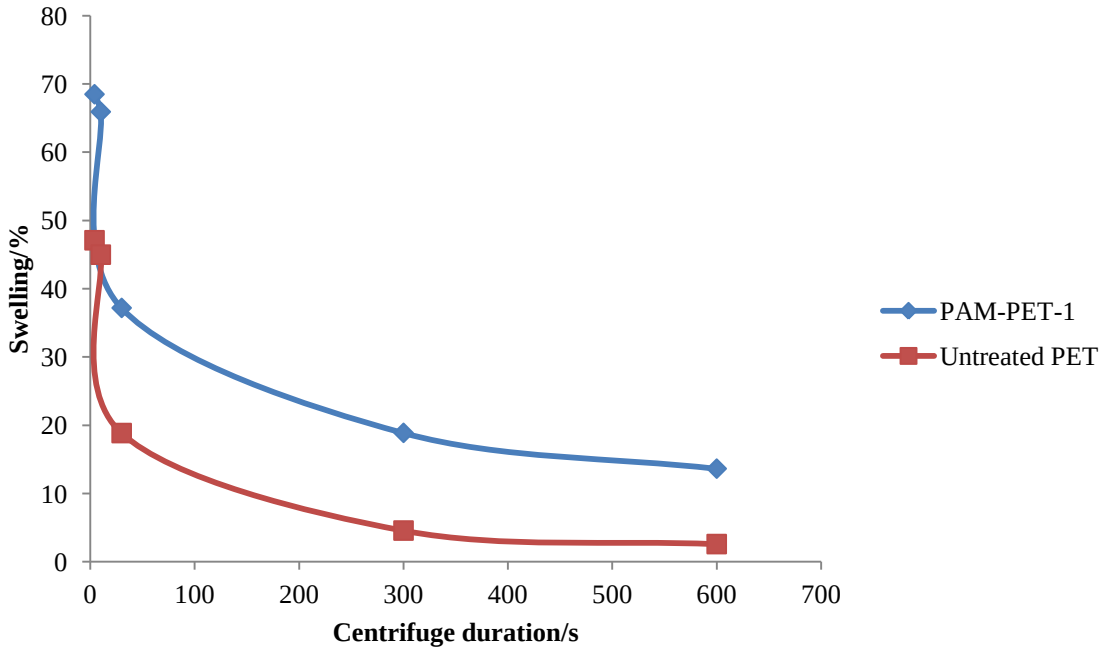

Figure 8. Swelling percentage versus centrifugation time.

The swelling kinetics was conducted after setting the centrifugation time. In this study, both untreated PET and PAM-PET-(1, 2, 3) were dried after extraction under room temperature over night and equilibrated in a vacuum desiccator for 24 hours to reach a constant weight. Then IP of each fabric (**Figure 9**) was obtained according to equation 1. All specimens were totally immersed in adequate DI water and redundant water was removed by 30 s centrifugation. The swelling percentage of untreated PET and PAM-PET-(1, 2, 3) was obtained according to equation 2.

Although PET is hydrophobic due to the benzene ring and ester group in the structure, the resulted 14.7% swelling could be considered as water absorbed into the fabric structure by capillary action. As fabric is a porous material and the space between fibers is rather narrow, the adhesive force of water to solid surface is greater than the cohesion between liquid molecules, then the capillary action occurs. Although PET is hydrophobic and cannot be spontaneous wetted, it can be wetted by external mechanical forces. Thus, the solid-liquid interface increases and capillary force drives the water molecules to the narrow space between fibers.[127] Consequently, water can be stored between yarns and fibers. Therefore, the swelling percentage observed in untreated PET can be attributed to capillary action. Moreover, AM is water soluble and the carbonyl group in the structure would form hydrogen bonding with water molecules. It can be used to explain the higher swelling ratio for all the PAM-PET samples.

As for PAM-PET-(1, 2, 3), the curve in **Figure 10** determined that the higher concentration of monomer AM used in PET modification resulted in the higher swelling

ratio. During the surface modification, the weight of monomer solution picked up by the fabric was controlled by using an electronic balance. To prepare more uniform specimens, the mass of solution picked up in fabric was set as 150%. As the monomer concentration increased, the mole percentage of monomer in solution relatively increased in solution; therefore, more AM was grafted onto the PET surface. The immobilization percentage was calculated according to equation (1). PET that swelled in solution with 4.5M AM yielded in 13.78% IP (**Figure 9**). Principally, a polymer consisting of more hydrophilic moieties swells more. As expected, PAM-PET-3 was found with the highest swelling percentage. On the other hand, the mole percentage of crosslinker MBA decreased with the increase of monomer concentration, leading to lower crosslinking density of the formed polymer network. Hence, larger pores were obtained in the polymer network, and hence retained more water in the network structure.

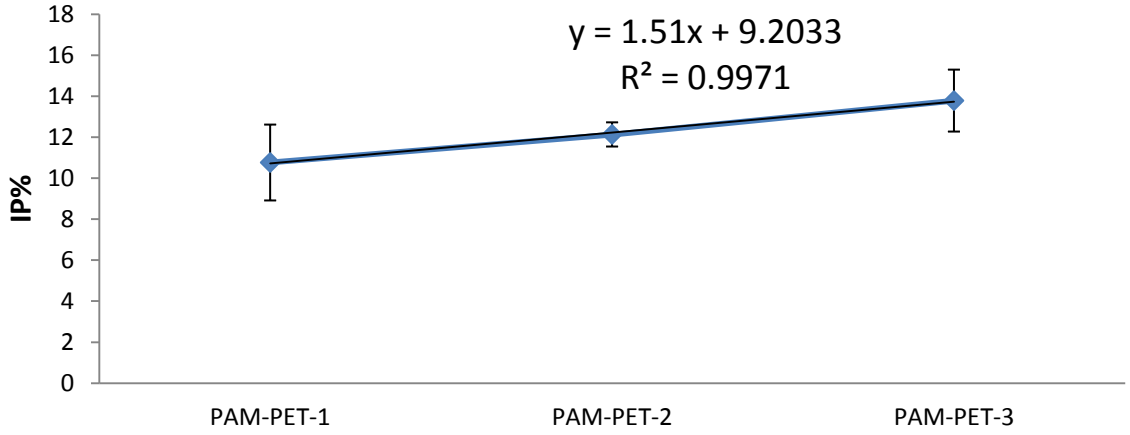

Figure 9. Immobilization percentage (IP) of PAM-PET-(1, 2, 3).

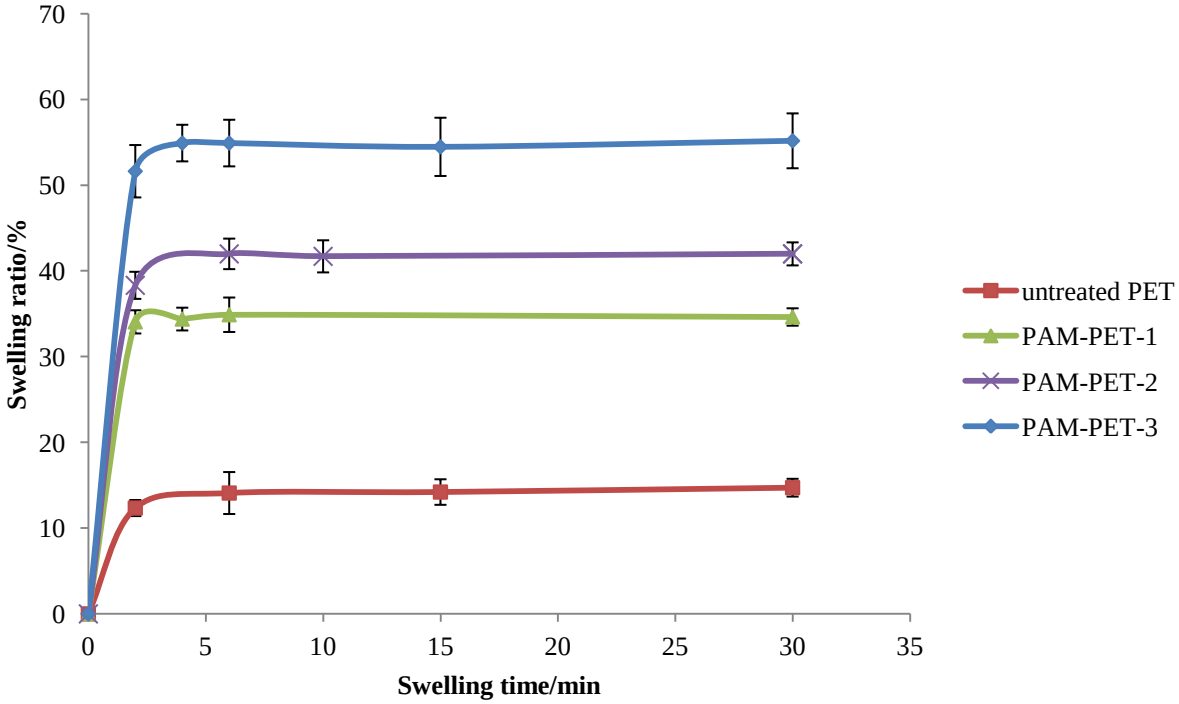

Figure 10. Swelling kinetics of untreated PET and PAM-PET-(1, 2, 3).

4.1.4 Peeling force test for untreated PET and PAM-PET-(1, 2, 3)

The importance of studying peeling energy for wound dressing lies in how to lower peeling energy so as to greatly relieve pain and reduce trauma to newly formed fibroblast and keratinocytes around the wounds. To evaluate the adherence of both untreated and modified PET, the test method using a gelatin model was adopted.

Gelatin is derived from collagen in pig skin and it is a mixture of peptides and proteins. As a proteinaceous material, gelatin was used as an *in vitro* stimulant of the protein-rich wound surface. It melts to the liquid state when heated and solidifies when cooled. This property makes gelatin an appropriate material for an adhesive after casing onto fabric. Adhesive works as it penetrates small pores of the substrate. When penetrating into fabric, gelatin gets in contact with fine fibers, and then adheres the fine fibers together when gelatin is solidified. The strength of the adherence depends on the surface area of the fabrics that can come into contact with gelatin as well as the surface properties of the fabrics.

Peeling energy can be quantified and analyzed with an Instron, and the peeling energy of untreated PET, Acticoat^{TM} Flex 3 (Acticoat^{TM}) and PAM-PET-(1, 2, 3) were tested. The commercial dressing, Acticoat^{TM}, is a widely used dressing in burn treatment. Although silver incorporated in Acticoat^{TM} can kill bacteria so as to protect the wound from being infected, while adherence is still a problem. The gelatin model quantified the peeling energy and PAM-PET-3 was demonstrated to be the least adherent. Generally, the peeling energies of PAM-PET-(1, 2, 3) were lower than untreated PET. Since all the

fabric strips were wet before gelatin casting, the polymer network was swollen by restoring water and there was a thin hydrogel layer on the specimen. The fabric pore size was smaller than the dry piece so as to control gelatin penetration. The less penetration means that a smaller superficial area with a small amount of fiber is available for the gelatin to bind. Consequently the peeling force is decreased. It is known that hydrogel swells and acts like a reservoir, as well as helps maintain a moisture environment so that more water molecules were left in PAM-PET-(1, 2, 3) than untreated PET after the same drying duration. The peeling energies increased when gelatin hardened with water loss. Herein samples with more water molecules in fabric may contribute to less hardened gelatin, which can also be used to explain the lower peeling energies for PAM-PET-(1, 2, 3).

All fabric-gelatin strips were removed from the oven and then gelatin was peeled off from fabric samples with 180^{o} peeling angle to mimic the peeling process and decrease the damage to skin in surgery. Although the peeling energies of Acticoat^{TM} and PAM-PET-1 were close to each other, the morphologies of samples after peeling test were quite different (**Figure 11**). There were only some residues left on PAM-PET-1 at the edge but there was even a layer of gelatin on Acticoat^{TM}. The gelatin at the edge of the whole gelatin strip was thinner and harder than in other parts, thus it was difficult to be peeled off after drying. The peeling energy of Acticoat^{TM} could not be precisely measured because the peeling was not an interfacial debond between gelatin and the substrate, but between gelatin itself.

As shown in **Figure 12,** the peeling energy of untreated PET was the highest (6439.79 Jm^{-2}, 16 hours) among all the samples. The peeling energies of PAM-PET-(1, 2, 3) gradually decreased as the AM concentration in PAM-PET-(1, 2, 3) increased. The peeling energy dropped to 4105.53 Jm^{-2} for PAM-PET-3 which is 36.2% decline compared with untreated PET. It reveals that PAM polymer network can promote the nonadherent property of wound dressing in terms of lowering peeling energy, especially when dressing had been under body temperature for 16 hours. This also coincides with the swelling data that PAM-PET-3 provides more hydrophilicity. Furthermore, there was no data for Acticoat after 16 hours drying because the fabric broke during the peeling process. Generally, knit fabric has better flexibility, easier extension but lower fabric strength compared with plain weave fabric. The differences among all the samples were smaller if they were dried within 6 hours.

Figure 13 plots the peeling energies of all the five specimens as a function of drying time: 2 hours, 4 hours and 6 hours. Overall, untreated PET showed the highest peeling energy (997.35 Jm^{-2}) when dried only for 2 hours. Because of the increased hydrophilic moieties on modified PET fabrics, the peeling energies with 2 hours drying decreased to 734.13 Jm^{-2}, 678.99 $Jm-^{2}$ and 479.60 Jm^{-2} for PAM-PET-(1, 2, 3) respectively. With the extension of drying time, adhesion rose accordingly. Acticoat^{TM}, which has a different fabric structure, showed a close peeling energy to untreated PET. However, a gelatin layer remained on Acticoat^{TM}, which indicated that the intact gelatin strip is difficult to be removed.

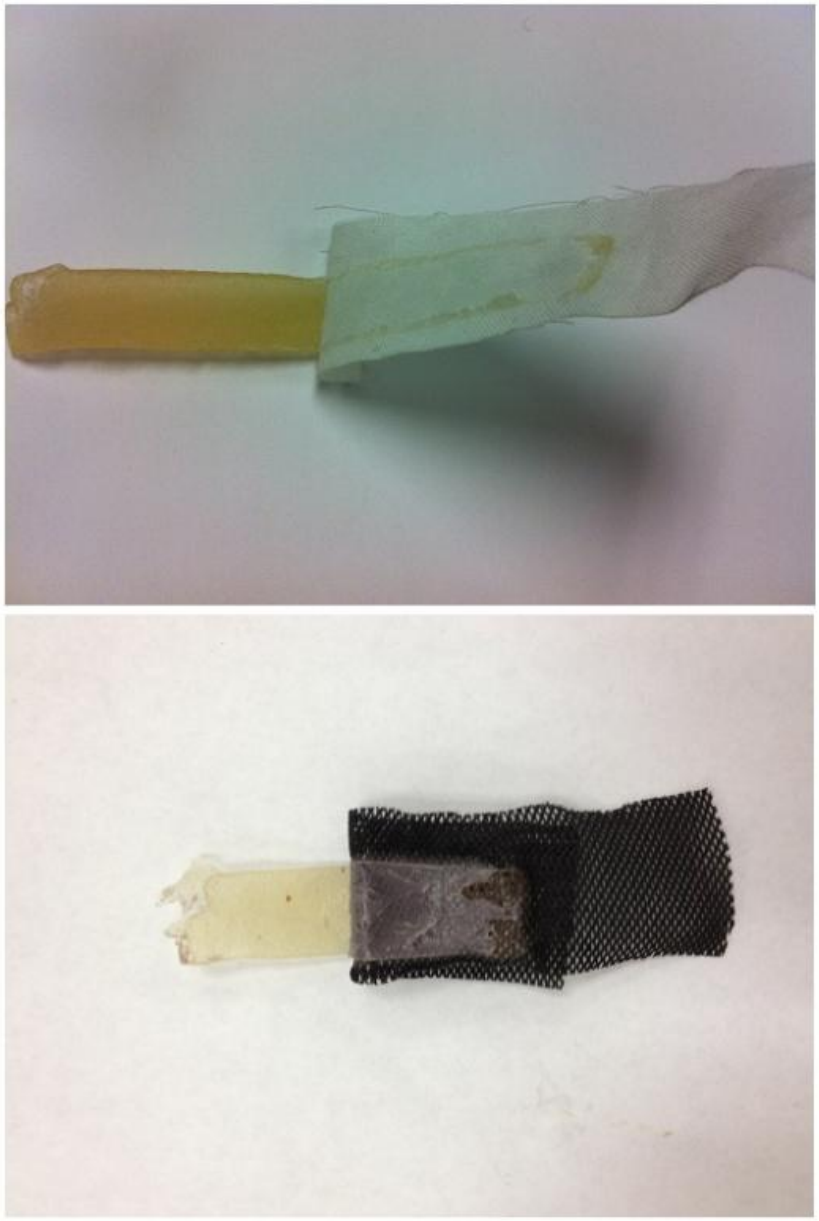

Figure 11. PAM-PET-1 and Acticoat™.

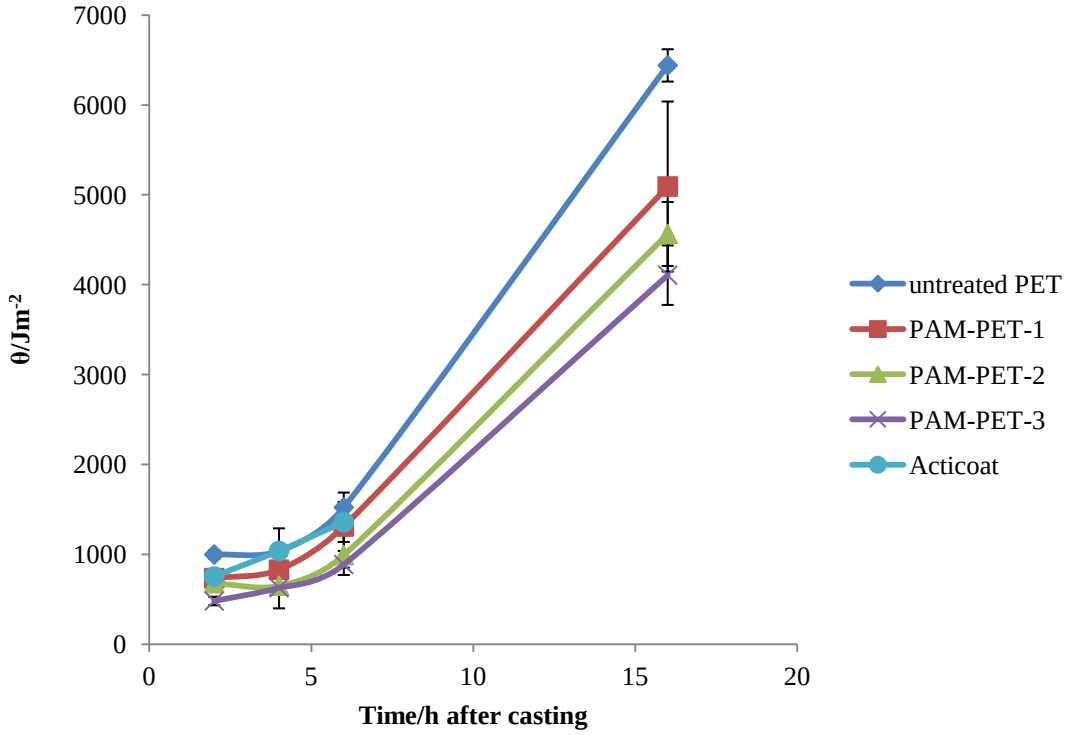

Figure 12. Peeling energies of untreated PET, PAM-PET-(1,2,3) and Acticoat™ tested by dry method. Drying duration: 2 h, 4 h, 6 h and 16 h.

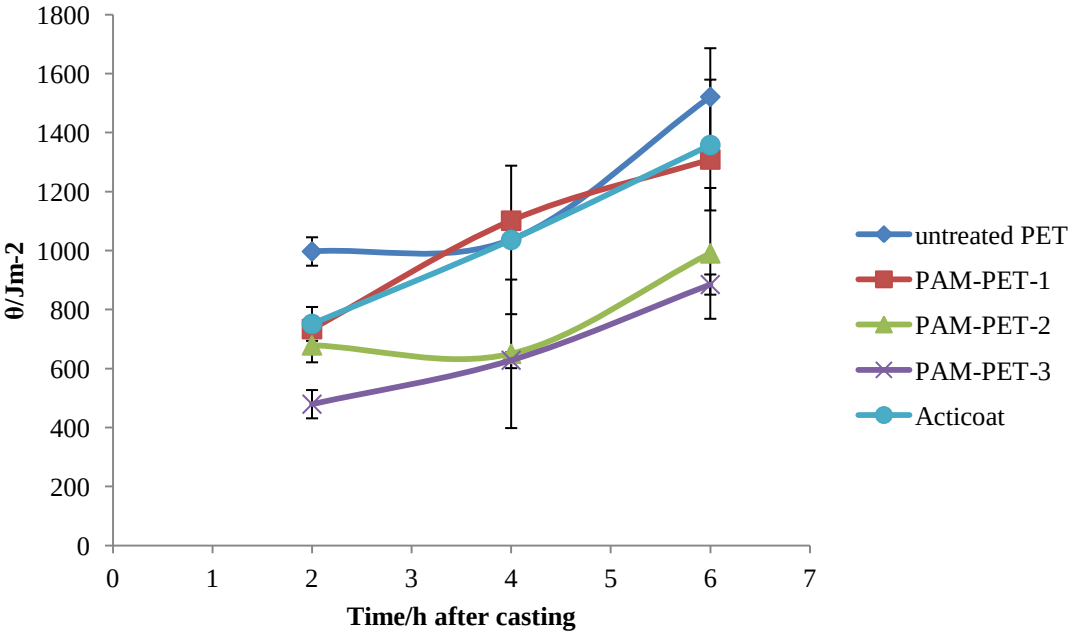

Figure 13. Peeling energies of untreated PET, PAM-PET-(1, 2, 3) and Acticoat™ tested by dry method. Drying duration: 2h, 4h, and 6h.

Thomas suggested that the peeling energy exceeding 300-400 Jm^{-2} is not suitable on a drying wound.[128] Even though the modified PET samples were less adherent than untreated PET, the peeling energies were still about 10 times higher than the above limit. There is an urgent need to further decrease the peeling energy. Taking the hydrophilicity and the swelling capacity of PAM-PET-(1, 2, 3) fabric into account, we added 500 μl DI water onto the dressing and allowed it to penetrate into the fabric for 2 min. This method is termed a wet method, as opposed to the previous method (termed a dry method) where peeling was carried out immediately after the drying of the PET/gelatin specimen in oven. Using the wet method, the IPN formed on fabric could swell with water molecules. As previous publications reported, water and organic solvent can play a role in debonding adhesives and substrates.[129] Peeling energy dropped for all specimens after various drying durations (**Figure 14**). Taking the specimens after 16 hours drying for example, peeling energies of untreated and PAM-PET-(1, 2, 3) in **Figure 14** were 2322.87 Jm^{-2}, 2028.45 Jm^{-2}, 1726.22 Jm^{-2} and 1207.86 Jm^{-2}. Compared to those dried for 16 hours in the dry method, peeling energy decreased by 63.94% on untreated PET using wet method, 60.16% on PAM-PET-1, 62.18% on PAM-PET-2 and 70.58% on PAM-PET-3. The difference between the dry method and the wet method was significant ($p<0.05$) for all the samples. According to the swelling kinetics data, PAM-PET-3 was the most hydrophilic and swelled by absorbing water molecules into IPN, therefore, the pore size became smaller again during swelling making it easier for the gelatin to be peeled off. It is reasonable to

expect that after a dressing is left on an acute wound over night, wetting the dressing before peeling could decrease the peeling force and reduce pain for the patients.

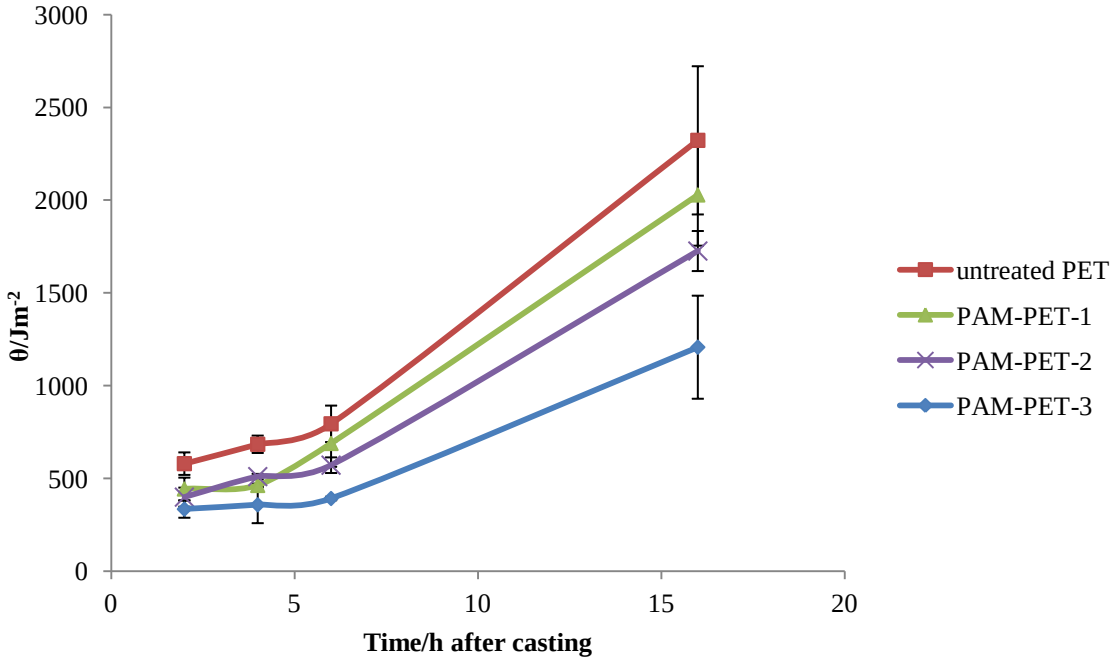

Figure 14. Peeling energies of untreated PET, and PAM-PET-(1,2,3) tested by adding 500µl DI water ahead of peeling. Drying duration: 2h, 4h, 6h and 16h.

Surfactants are well-known in decreasing the surface tension of water to allow easier wetting of surfaces. Foam forming surfactant 2% chlorhexidine gluconate solution (Huntington) was chosen to test if it has the potential to further reduce peeling energy. 2% chlorhexidine gluconate solution was added to the back of fabric, and the gelatin-fabric strip was soaked in 0.9% saline for 10 min, 20 min and 30 min. The control group was prepared by just drenching dried gelatin-fabric samples in DI water for an equivalent time. Samples were analyzed after 16 hours drying. As shown in **Figure 15**, the peeling energy of untreated PET, either by using water or surfactant, dropped drastically compared to

that of using the dry method. After 10 min water soaking, the peeling energy of PET declined from 6439.78 Jm^{-2} to 1669.29 Jm^{-2} and it further decreased to 1078.60 Jm^{-2} after 30 min soaking. However, the peeling energy reached 1055.02 Jm^{-2} after 10 min surfactant soaking which was much lower (significant different) than that of water soaking. There was no significant difference ($p \leq 0.05$) between different soaking time durations using surfactant (**Figure 15**). It is probable that the PET has a hydrophobic surface and the surfactant has a remarkable impact on the wetting of PET and 10 min is enough for the surfactant containing water to diffuse into the gelatin and PET interface. When the soaking time was extended to 30 min, the peeling energy of water soaked PET was approaching that of surfactant soaked PET. It indicates that given a longer soaking time, there is a similar effect using water to reduce peeling energy.

Figure 16 shows the peeling energies of PAM-PET-3 by using water and surfactant. The peeling energy decreased from 4105.53 Jm^{-2} to 856.65 Jm^{-2} after 10 min water soaking and it decreased to 803.15 Jm^{-2} using surfactant. Different from PET, there was no significant difference between peeling energies of water soaked and surfactant soaked PAM-PET-3. It can be explained that PAM-PET-3 is much more hydrophilic than untreated PET, surfactant does not speed up soaking on a quite hydrophilic surface. Moreover, no significant difference was observed between various soaking durations using water. It is because IPN swells within 5 min, which is less than soaking time, and reaches full swelling capacity. Nevertheless, the pre-wet duration should be short so as not to cause maceration in human skin, since the newly formed cells and tissues around

wound are very sensitive and tender. The effectiveness of surfactant was demonstrated because of shorter soaking time and relatively lower peeling energies.

In general, the dressings are not changed within a couple of hours so the study of peeling energy, after 16 hours of drying, is more critical than short drying duration. **Table 2** summarizes the peeling energies of different samples and reduction in percentages of peeling energies with different peeling methods. The peeling energies in "Dry method" implicate the importance of surface modification in providing a less adherent surface on PET fabrics. The reduction percentages in "500 μL DI water" reveal sharp decreases in peeling energies after wetting the samples with 500 μL water for 2 min which enables the PAM IPN to swell. And those displayed in "Surfactant soaking 10 min" reveal that a surfactant can be used to further decrease peeling energies of both untreated PET and PAM-PET-3. Take PAM-PET-3 as an example, when treated with surfactant for 10 min, the peeling energy showed 87.53% decrease compared to PET (Dry method). Although 803.15 Jm^{-2} is still not ideal, according to Thomas, the enhancement is obvious and prominent. [128] Compared to Andrew's work[121], the peeling energies of PAM-PET-(1, 2, 3) were much higher than Lyofoam®, Micropore® and Melolin®. It is probable that the gelatin used in this project was 50 wt% rather than 40 wt% and it contained less water. Therefore, the gelatin on the fabric strips was drier than that on commercial dressings. Given the swelling capacity of PAM-PET-(1, 2, 3), the peeling energy, take PAM-PET-3 for example, was below that of Lyofoam® and Micropore® with the addition of surfactant before peeling.

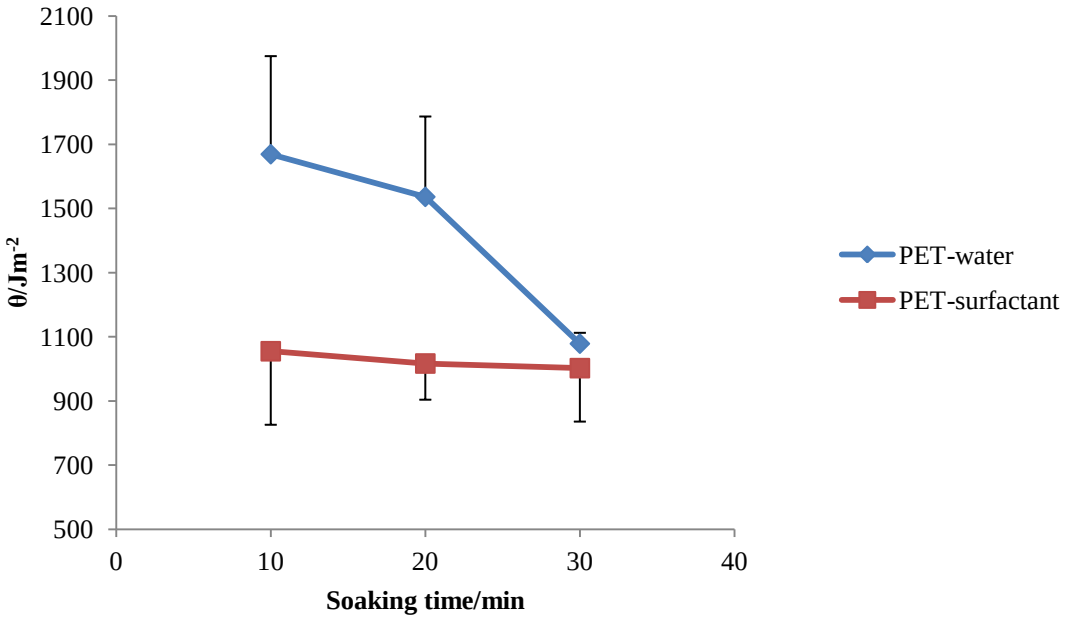

Figure 15. Peeling energy of untreated PET tested by adding DI water/surfactant ahead of peeling. Drying duration: 16 h.

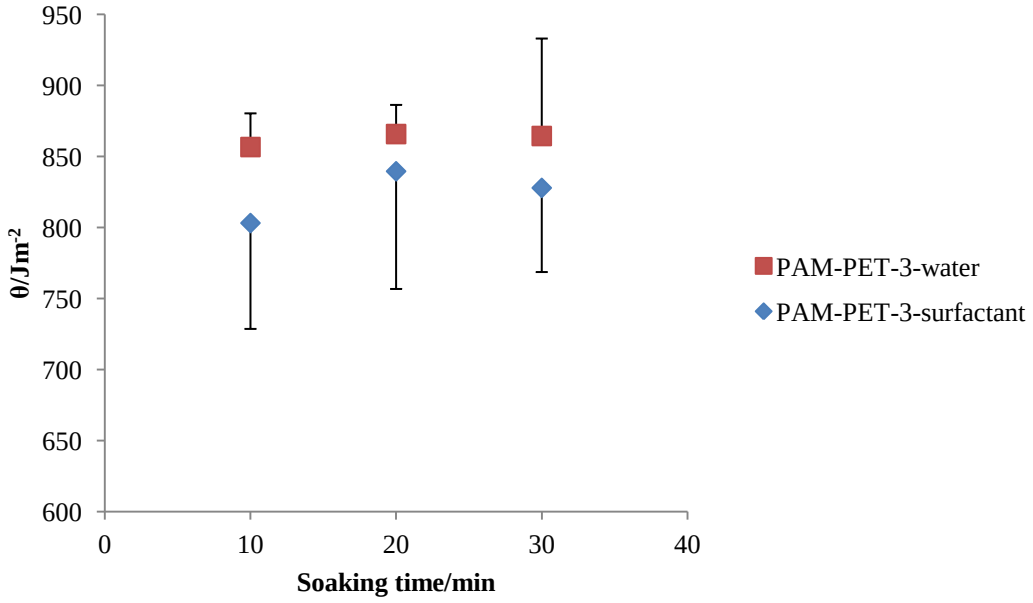

Figure 16. Peeling energy of PAM-PET-3 tested by adding DI water/surfactant ahead of peeling. Drying duration: 16 h.

Table 2. Peeling energy by different treatments and reduce percentage[1,2].

Sample	Dry method		500 μl DI water		Water soaking 10 min		surfactant soaking 10 min	
	θ	Reduce %	θ	Reduce %	θ	Reduce %	θ	Reduce %
PET	6439.78	N/A	2322.87	63.93	1669.29	74.08	1055.02	83.62
PAM-PET-1	5091.99	20.93	2028.45	68.50	N/A	N/A	N/A	N/A
PAM-PET-2	4564.13	29.13	1726.22	73.19	N/A	N/A	N/A	N/A
PAM-PET-3	4105.53	36.25	1207.86	81.24	864.42	86.58	803.15	87.53

[1]All samples were dried for 16 h

[2]All the reduce percentages were based on PET dry method.

The antibacterial dressing was impregnated with AgNPs, and the possible negative effect on nonadherence was studied as the incorporation of AgNPs may compromise the nonadherence. PAM-PET-Ag-3 was used to test the swelling percentage and peeling energy (Dry method). The swelling of PAM-PET-Ag-3 was 39.24±0.83% and the peeling energy of PAM-PET-Ag-3 was 4861.09±20.21Jm^{-2}. Both the swelling percentage and the peeling energy were between PAM-PET-(1, 2). The amide groups that were available to bind water molecules became less because some amide groups participated in forming hydrogen bonding with carbonyl groups, which are in sodium citrate stabilized AgNPs. Moreover, the space of polymer network was occupied by numerous AgNPs which also prevent water storage to some extent. The peeling energy increased but it was still lower than untreated PET. The incorporation of AgNPs did compromise the swelling and nonadhenrence.

4.1.5 Antibacterial assay for PAM-PET-Ag-(1, 2, 3)

AgNPs are considered non-toxic environmentally friendly antibacterial material and have been used as antibacterial agents in some commercial antibacterial wound dressings. Three silver impregnated samples, PAM-PET-Ag-(1, 2, 3) were used in this study, with PET-Ag as the control sample. The results are summarized in **Table 3**.

It is obvious that PAM-PET-(1, 2, 3) showed efficient antibacterial activity against *P.aeruginosa* and *S.aureus* (**Figure 17, Figure 18**), and over 90% of the bacteria were killed within the first hour of incubation. There is a marginally lower antibacterial activity within 1 hour of incubation in the case of Gram-positive MRSA. Overall, a 6.53 log reduction was achieved after 4 hours incubation in killing Gram-negative *P.aeruginosa* and more than a 6 log reduction in killing Gram-positive MRSA was observed. It is well known that AgNPs and silver ion could poison the respiratory enzymes, components of the microbial electron transport system and some proteins. The antibacterial difference between the two bacteria is probably due to the structural differences of Gram-positive and Gram-negative bacteria. The outer membrane of Gram-negative bacteria is composed of tightly packed lipopolysaccharide and protein, but there is a dense peptidoglycan cell wall outside the plasma membrane of MRSA which makes it more resistant to AgNPs.[122]

Previous studies showed that the smaller AgNPs possess better antibacterial activity because of a higher surface area.[130] The particles assembled on PAM-PET-(1, 2, 3) were shown in TEM images ranging from 1-30 nm, and most of them were between 1-6 nm.

The AgNP content percentages of PAM-PET-(1, 2, 3) were 3.04%, 2.90% and 3.78% respectively. PET-Ag also showed 27.45% killing in *P.aeruginosa* and 31.56% in HA-MRSA. The antibacterial activity of PET-Ag can be attributed to the very few AgNPs in the PET fabric (**Figure 5**). With regard to modified PET fabrics, there was no significant difference between PAM-PET-Ag-(1, 2, 3) in the 15 min and 30 min antibacterial activities in killing *P.aeruginosa*, but the reduction in percentages of PAM-PET-Ag-(1, 3) were significantly different ($p<0.05$) with 60 min, PAM-PET-Ag-(1, 3) were significantly different with 120 min contact, and the difference between PAM-PET-(2, 3) were also statistically significant. Although the PAM-PET-Ag-3 killing efficacy with 120 min contact was higher than PAM-PET-Ag-(1, 2), the reduction in percentages of PAM-PET-Ag-(1, 2) reached 99.95%. The more effective antibacterial efficacy of PAM-PET-Ag-3 may due to the slightly higher silver content. In the case of killing HA-MRSA, there was no significant difference between PAM-PET-Ag-(1, 2, 3) at each contact time. This is because the MRSA is more resistant to silver and the silver percentage in PAM-PET-Ag-3 was not capable to exhibit an outstanding killing efficacy. Due to the negative effect of AgNPs in nonadherence property, the PAM-PET-Ag-3 can be loaded with less silver to get a less adherent surface but with a competitive antibacterial efficacy.

Table 3. Antibacterial activities of PET-Ag and PAM-PET-Ag-(1, 2, 3)[a,b].

Sample	Bacteria	Contact time/min						
		15	30	60	120		240	
		Reduce %	Reduce %	Reduce %	Reduce %	Log_{10}	Reduce %	Log_{10}
PET-Ag	1	16.67±4.50	26.47±7.78	30.39±3.39	18.63±4.49	N/A	27.45±8.98	0.14
	2	12±2.67	26.22±4.07	30.67±4.62	33.33±2.67	N/A	31.56±6.71	0.16
PAM-PET	1	47.06±5.09	55.88±7.78	98.42±0.12	99.95±0.002	3.3	100	6.53
-Ag-1	2	31.56±5.55	40.44±8.57	92.98±1.26	99.86±0.02	2.85	100	6.57
PAM-PET	1	43.12±4.49	59.80±6.12	98.17±0.13	99.95±0.008	3.3	100	6.53
-Ag-2	2	30.67±2.67	38.67±4.62	91.91±1.56	99.85±0.02	2.82	100	6.57
PAM-PET	1	36.27±7.40	51.96±8.99	97.89±0.14	99.97±0.003	3.52	100	6.53
-Ag-3	2	32.44±8.15	44.89±5.55	92.35±1.20	99.83±0.02	2.77	100	6.4

[a] 1: *P.aeruginosa* 73104, 2: HA-MRSA 40065

[b] The concentration of *P.aeruginosa* 73104 is $3.4*10^6$ CFU/mL

The concentration of MRSA 40065 is $3.75*10^6$ CFU/mL

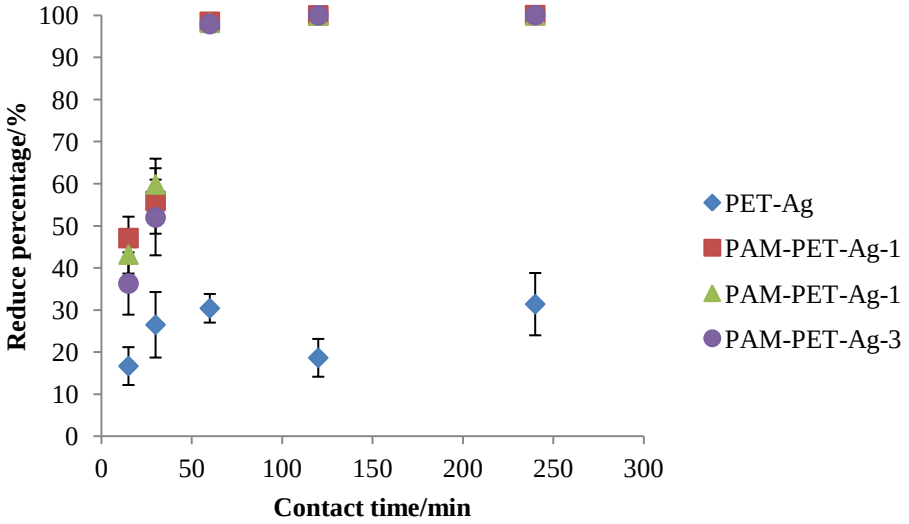

Figure 17. Antibacterial reduction for PET-Ag and PAM-PET-Ag-(1, 2, 3). Bacterium challenged: *P.aeruginosa* 73104.

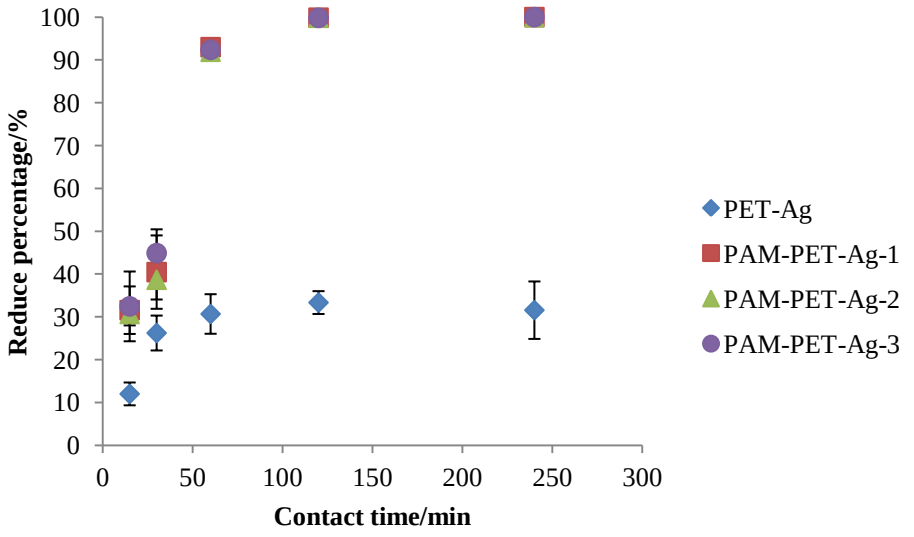

Figure 18. Antibacterial reduction for PET-Ag and PAM-PET-Ag-(1, 2, 3). Bacteria challenged: HA-MRSA 40065.

4.2 Antibacterial performance of ionic DMH derivatives in solution and after being immobilized on fabrics

A dressing that is both antibacterial and atraumatic was prepared in the previous part. The AgNPs containing dressing exhibited good antibacterial activity towards both Gram-positive and Gram-negative bacteria. However, bacteria resistance to silver has been reported and it may be a problem for infection control in the future. So we planned to develop a new biocide that was effective even with a small amount and did not cause bacteria resistance. And therefore, the material with the strong and powerful new biocide on the surface could also serve as a protective layer in the previously designed dressing to prevent wound infection.

4.2.1 Model study-Antibacterial performance of ionic DMH derivatives 12 and 13

To test the hypothesis that introducing a positive charge into the structure of N-chloramine may enhance its antibacterial efficacy, compound **2**, a hydantoin derivative with cationic charge, was synthesized and converted to its N-chloramine counterpart (compound **12** in **Scheme 3**). Compound **6**, a hydantoin derivative with anionic charge, was also synthesized and converted to N-chloramine (compound **13**) for comparison. Both compounds **2** and **6** were used to serve as controls.

E.coli is a typical Gram-negative bacterium and *S.aureus* a typical Gram-positive bacterium. In the model study we investigated the antibacterial performance of small molecules **12** and **13** against three strains for each bacterium at the concentration of 15

ppm. As shown in **Table 4**, **12** demonstrated a total kill of all six bacterial strains within 5 min whereas no significant reduction was observed for **13** at the same time frame. For **13**, total kill or >3 log reduction was only achieved at the contact time of 20 min except for MRSA #77090. It indicated that as compared with negative charge, positive charge contributed to a faster bacterial killing by the N-chloramine compound. The fact that >3 log reduction or total kill (except MRSA # 77090) can still be achieved by **13** after extending the contact time to 20 min led us to a conclusion that the negative charge just impedes the killing kinetic without compromising the overall antibacterial capacity of **13.**

Table 4. Antibacterial efficacy of 12 and 13 against 3 *E.coli* and 3 MRSA strains[1].

Bacteria[a]		Synthetic compounds[b]	Bacteria reduction at various contact times (min)					
			5		10		20	
			%	Log_{10}	%	Log_{10}	%	Log_{10}
Gram-negative	*E.coli* ATCC 25922	**12**	100	6.63	100	6.63	100	6.63
		13	28.5±3.4	0.15	99.96±0.00	3.40	100	6.63
	MDR-*E.coli* (#70094)	**12**	100	6.17	100	6.17	100	6.17
		13	35.6±1.9	0.19	66.8±0.5	0.48	100	6.17
	MDR-*E.coli* (#95882)	**12**	100	6.67	100	6.67	100	6.67
		13	4.6±1.2	0.02	99.75±0.02	2.59	99.94±0.03	3.24
Gram-positive	MRSA ATCC33592	**12**	100	6.60	100	6.60	100	6.60
		13	6.2±0.9	0.028	98.83±0.12	1.94	99.94±0.01	3.19
	MRSA (#70527)	**12**	100	6.76	100	6.76	100	6.76
		13	32.5±3.5	0.17	99.78±0.00	2.97	100	6.76
	MRSA (#77090)	**12**	100	6.16	100	6.16	100	6.16
		13	37.1±10.6	0.2	52.8±4.5	0.33	74.2±0.5	0.59

[1]Inoculum concentration: 1.46-5.87*10^6CFU/mL

4.2.2 Design and synthesis of "clickable" ionic antibacterial precursors

In view of the encouraging model study in solution, we grafted DMH derivatives onto PET and studied the synergistic effect between immobilized QACs and N-halamine. We have already prepared PMBAA-PET containing an alkyl handle, which allows easy immobilization of azido compounds by using "click" chemistry. To construct ionic azido precursors, DMH, a positive or negative charge and an azide functional group are necessary. Since chemical modification of the methyl group of DMH involved intense synthetic chemistry usually with low yield,[131] the DMH segment was designed as to be the terminal part of the final structure. Either a positive or a negative charge can serve as a bridge linking two terminal functional groups (DMH and azide). Linear azido precursors with cations were designed as **3** and **4** based on synthesis of **1** which has been reported in another paper.[132] As for the negative charge moiety, it needs to act as a shoulder pole to carry the azide handle and the DMH moiety at each end. So phosphoric acid, the commonly used triprotic acid, was herein adopted and the final azido precursor with anion was designed as compound **5**. It's important to mention that we introduced a C-P bond into the structure because the resultant phosphonate (C-P) is more stable compared with alkyl phosphates (C-O-P) especially when treated with trimethylsilyl bromide (TMSBr) for methyl deprotection.[133] All the precursors were synthesized in our laboratory by Dr. Lingdong Li.

4.2.3 Immobilization of "clickable" ionic antibacterial precursors on PET

Attachment of **1, 3, 4** and **5** on PET surface was completed by in advance forming an interpenetrating network (IPN) of poly-MBAA (PMBAA, **Scheme 2**) on PET surface (named as PMBAA-PET) followed by "click" linkage reaction.[120] After the covalent immobilization, all PET samples were chlorinated to activate their biocidal function. **Table 5** outlines the antibacterial results of "click"-modified PMBAA-PET against MDR-*E.coli*(#70094). PMBAA-PET samples clicked with various hydantoin derivatives (**1, 3, 4** and **5**) were loaded with similar amounts of active chlorine (around 430 ppm). PMBAA-PET-**3** showed the best antibacterial efficacy which might be due to the cationic charge in **3**. However, only 23.2% bacterial reduction was observed, the worst efficacy among all clicked samples, was achieved on PMBAA-PET-**4** which possesses both N-chloramine and long chain QAC moieties. This was unexpected and intrigued us to conduct contact angle measurements.

Results of contact angle measurement show that PMBAA-PET-**4** is still quite hydrophobic with a contact angle of 107.1±4.1 degree, similar to PMBAA-PET. The surface energy of PMBAA-PET-**4** sample is not high enough to cause the bacterial suspension to spread on its surface. Even a beaker was loaded on the top of the fabric assembly onto which bacterial suspension was dispensed to help create an intimate contact; minute beads of bacterial suspension might still exist on the hydrophobic surface hindering the contact killing process. For the more hydrophilic samples such as PMBAA-PET-**3**, however, bacterial suspension spread over the surface immediately after being dispensed to

ensure a sufficient contact with the immobilized biocides. Therefore, differences in the biocidal efficacies of all the samples are confounded by their differences in hydrophilicity and surface charges (negative, neutral, and positive). The sequence of antibacterial strength: PMBAA-PET-**3** > PMBAA-PET-**1** > PMBAA-PET-**4** corresponds to their hydrophilicities as denoted by contact angles (undetectable, 90.8±5.6 and 107.1±4.1). Although we can clearly see that PMBAA-PET-**3** demonstrates the most potent biocidal efficacy among all the samples, no convincing conclusion can be drawn about the effect of the cation center of PMBAA-PET-**3** on its biocidal efficacy. To eliminate the effect of substrate hydrophobicity on the antibacterial efficacy, we decided to graft **1, 3, 4**, and **5** onto a hydrophilic cotton substrate.

Table 5. Antibacterial efficacy of PMBAA-PET after "click" linkage modification.

Modified PET Sample	Active chlorine (ppm)	Reduction of MDR-*E.coli* [a]	Contact angle (After chlorination)
PET	0	0	122±8.1
PMBAA-PET	132±23	0	106.4±7.3
PMBAA-PET-**1**	427±19	46.4%	90.8±5.6
PMBAA-PET-**3**	433±23	97.7%	UD[b]
PMBAA-PET-**4**	434±25	23.2%	107.1±4.1
PMBAA-PET-**5**	423±31	43.6%	78.1±10.1

a) Inoculum concentration was 1.02×10^7 CFU/mL, % reduction after a contact time of 5 min;

b) Undetectable (too hydrophilic to be detectable)

4.2.4 Immobilization of "Clikable" ionic antibacterial precursors on Cotton and chlorination progress

To bind the synthetic azido precursors on cotton fabrics, PMBAA was also grafted onto cotton via PPS initiated radical polymerization.[134] In ATR spectrum of PMBAA-g-cotton (**Figure 19** (a)), a new peak appeared at 1647 cm^{-1} characteristic of carbonyl stretch C=O of amide in PMBAA. N-H stretching gave rise to a broad peak centered at 3421 cm^{-1} in the spectrum of PMBAA-g-cotton (**Figure 19** (a)). ATR results implied successful grafting of PMBAA onto cotton. The subtraction spectrum provided a clearer vision of grafted functional groups.

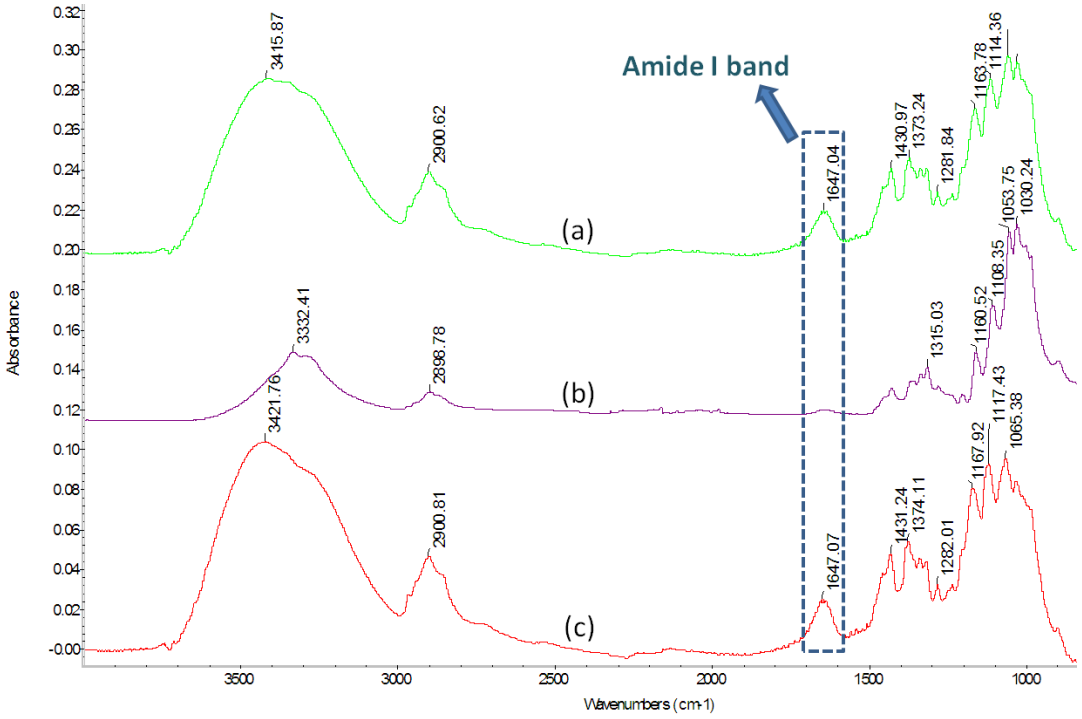

Figure 19. ATR spectra of (a) PMBAA-*g*-cotton (percentage graft = 1.03%); (b) untreated cotton; (c) subtracted ATR spectrum of PMBAA-g-cotton and untreated cotton.

Synthetic azido-precursors **1, 3, 4** and **5** were attached on PMBAA-*g*-cotton in the presence of Cu^{2+}/Na ascorbate at room temperature. Afterwards, a chlorination process was carried out converting those clicked cotton samples into corresponding N-chloramines. Since cotton fabric is hydrophilic, a small change of available chlorine in the chlorination solution can result significant variation of active chlorine on the modified cotton samples. Therefore, we studied the chlorination kinetics of those "click"-modified cotton fabrics.

Based on the previous study,[70] the chlorination reaction could be regarded as in first-order relationship with the amide concentration according to equation :

$$v = -d[\text{amide}]/dt = k\,[\text{NaClO}][\text{amide}] \qquad (9)$$

where v is the chlorination reaction rate, k is the rate constant and t is the reaction duration.

Since NaClO for chlorination is in excess, k [NaClO] can be regarded as constant k'. Integration of equation 9 gives equation 10:

$$\ln\{[\text{amide}]_t/[\text{amide}]_0\} = -k't \qquad (10)$$

where $[\text{amide}]_t$ is amide concentration at the reaction time of t, $[\text{amide}]_0$ is the total amide of hydantoin on cotton (which can be calculated from the graft percentage 1.1%) and $k' = k\,[\text{NaClO}]$. The yield of the click linkage reaction was regarded as 100%, and t was 1800 s. Therefore, based on the obtained active chlorine levels when the available chlorine ([NaClO]) was between 500 ppm and 2400 ppm (**Figure 17)**, the k' in the equation 10

could be calculated as shown in **Table 6**.

Table 6 shows that *k* of PMBAA-*g*-cotton-**3** (*k*(**3**)) was the highest among all the samples. The chlorination of PMBAA-g-cotton-**3** proceeded at a much higher rate due to the attraction between the positive charge in **3** and the negatively charged chlorination species ClO^-. However, the similarly positively charged PMBAA-g-cotton-**4** had only a comparable *k* and even lower active chlorine loadings than PMBAA-g-cotton amide bond of which could also be converted to N-chloramine (as shown in **Figure 20**). It was probably due to increased hydrophobicity of PMBAA-g-cotton-**4** and the steric hindrance of the introduced dodecyl chain impedes the formation of hydrogen bond between amide hydrogen and hypochlorite oxygen which has been proposed to be the transition state of the chlorination of amides.[135] To test this hypothesis, we subsequently prepared lauryl azide and attached the long chain azide onto PMBAA-*g*-cotton via the "click" chemistry method. The active chlorine loading on the obtained cotton sample, termed as PMBAA-g-cotton-lauryl chain, was also plotted as a function of the available chlorine of the sodium hypochlorite solution (**Figure 20**). The active chlorine loadings on PMBAA-g-cotton-lauryl chain were lower than both PMBAA-g-cotton and PMBAA-g-cotton-**4** over the full range of available chlorine (250-2500 ppm). This confirmed that the long alkyl chains retard the chlorination of either acyclic amide of PMBAA or the cyclic amide of DMH. In addition, it is notable that total active chlorine loadings on PMBAA-g-cotton-**3** were more than double of that of all other modified cotton fabrics when the available chlorine was greater 500 ppm, meaning that the positive charge

center contributed to not only faster chlorination but also higher equilibrium active chlorine loading.

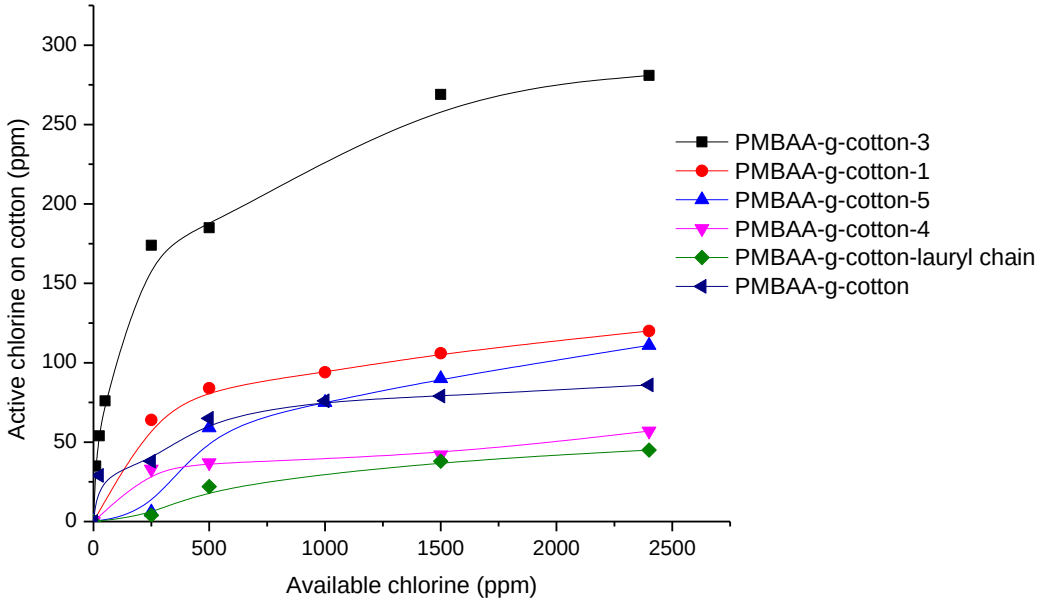

Figure 20.Chlorination progress versus available chlorine in NaClO solution. Reaction duration: 30min.

Table 6. Rate constant (k) for the chlorination of modified cotton samples.

Modified cotton	PMBAA-g-cotton	PMBAA-g-cotton-**1**	PMBAA-g-cotton-**3**	PMBAA-g-cotton-**4**	PMBAA-g-cotton-**5**
Rate constant *k* ($L.mol^{-1}.s^{-1}$)	7×10^{-5}	1×10^{-4}	4×10^{-4}	7×10^{-5}	2×10^{-4}

4.2.5 Antibacterial activities of modified cotton fabrics

Given enough contact time (120 to 180 minuts), cotton fabrics with active chlorine as low as 48 ppm resulted in a 5 log reduction of k-12 *E. coli*. [70] Differences in the antibacterial efficacies of the cotton samples may not be distinguishable if a longer contact time contact was allowed. Also, according to the model study, cationic charge center majorly contributes to a quick kill of bacteria. Thus, short contact time of 5 min was adopted in the antibacterial test.

Table 7 shows that only a negligible percent reduction of **MDR-*E.coli* (**#70094**)** was observed on PMBAA-g-cotton samples within 5 minutess of contact (**Table 7**). This finding accords with previous findings that t-Butyl acrylamide grafted cotton could neither be easily chlorinated nor demonstrate effective biocidal efficacy. [70] It is because the methyl substitution adjacent to N-Cl structure impedes effective chlorine transfer from N-Cl biocide to biological receptors on bacteria. As shown in **Table 7**, the biocidal efficacy of PMBAA-g-cotton-**1** was around half of that of PMBAA-g-cotton-**3** (with 35±3 ppm active chlorine) even when the latter's active chlorine was much lower (120 vs. 35 ppm). This confirmed the boosting effect of the cationic charge center on the biocidal efficacy of N-chloramine. PMBAA-g-cotton-**5** only gave comparable efficacy as with PMBAA-g-cotton-**1**, indicating negligible or no contribution to the biocidal effect from the negative charge. Considering the significantly enhanced antibacterial activity of chlorinated PMBAA-g-cotton-**3**, we proposed the possible boosting mechanism as depicted in **Scheme 6**. *E.coli* cells are covered with a lipopolysaccharide layer of 1-3 nm

thickness and is hence negatively charged. The negatively charged shell can be arrested by the cation in **3** through electrostatic interaction to facilitate the oxidative chlorine transfer from N-chloramine to cell biological receptors leading to bacterial death. Even at half of the active chlorine on PMBAA-g-cotton-**1** or **5,** PMBAA-g-cotton-**4** showed comparable biocidal efficacy, if not better, within 5 minutes of contact. However, compared with PMBAA-g-cotton-**3**, the boosting effect was less significant. It is deduced that the long alkyl chain shields the electrostatic interaction between the cationic center on N-chloramine structure and negatively charged *E. coli* cells. The contact time was too short for the QAC moiety to complete the "bubble bursting" action. Under the experimental condition, no synergistic bacterial killing was found between the antibacterial QAC and the N-chloramine even when they were covalently bonded with each other.

Table 7. Antibacterial efficacy of modified cotton fabrics against MDR-*E.Coli* #70094.

Modified cotton Sample	Active chlorine (ppm)	Reduction of MDR-*E.coli* [a]	
		Percentage reduction	Log_{10} reduction
Cotton	0	0	0
PMBAA-g-cotton	51±5	5%	0.02
PMBAA-g-cotton-**1**	120±8	22.20%	0.11
PMBAA-g-cotton-**3**	152±12	90.20%	1
PMBAA-g-cotton-**3**	35±3	37.70%	0.21
PMBAA-g-cotton-**5**	107±2	18.90%	0.09
PMBAA-g-cotton-**4**	55±6	28.30%	0.14

a) Inoculum concentration was $2.12*10^6$ CFU/mL

The finding that a cationic charge center can boost the biocidal efficacy of N-chloramine has important applications. Even though previous research has shown that dimethyloldimethyl hydantoin-treated cotton fabrics with an active chlorine loading of 1100 ppm did not generate any erythema or edema on the bare skin of 8-week-old New Zealand male rabbits after a 4-hour skin contact, more evidence is needed to understand the safety and tolerability of N-chloramine modified fabrics before they can be used in close contact with skin. In this context, it is desirable to present more potent antibacterial activity with lower active chlorine loading as in the case of PMBAA-g-cotton-**3**. It is noteworthy that 33 ppm active chlorine on PMBAA-g-cotton-**3** was obtained using a NaClO chlorinating solution with only 10 ppm available chlorine, which is of a similar level to that in public swimming pools (2-5 ppm). It implies that the biocidal function of PMBAA-g-cotton-**3** can be easily activated to become self-disinfecting and useful in such settings as surgical gowns, nurse uniforms and hospital privacy curtains etc.

Since the dissociation constant of amide N-chloramine is less than 10^{-9},[136] its biocidal function is believed to proceed in a direct contact manner.[137] As for the N-Cl form of **3**, either free or after immobilization, the nature of N-Cl is identical to that of **1**. To further confirm the on-contact killing mechanism as depicted in **Scheme 6**, we designed a non-contact killing test. Chlorinated cotton and chlorinated PMBAA-g-cotton-**3** were first suspended in PBS (0.05 M, pH 7.0) under vortex conditions for 5 and 10 minutes. Then the extraction buffer was filtered through a syringe filter membrane and added to a bacterial suspension. Viable bacterial colonies were

counted to obtain almost constant bacterial concentration as outlined in **Figure 21**. No bacterial kill was observed when PMBAA-g-cotton-**3** was not in direct contact with the bacterial suspension. It indicated that contact between N-chloramines and bacteria is indispensable for the microorganism inactivation, lending support to the proposed mechanism of enhanced bacterial kill of PMBAA-g-cotton-**3 (Scheme 6)**.

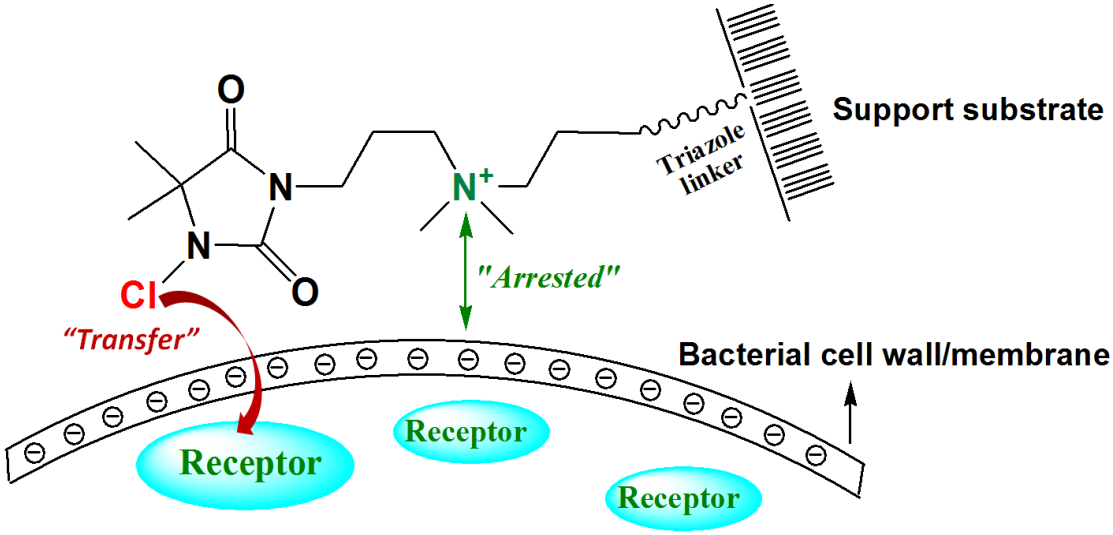

Scheme 6. Schematic illustration of boosting microbiocidal function between cation and N-chloramine.

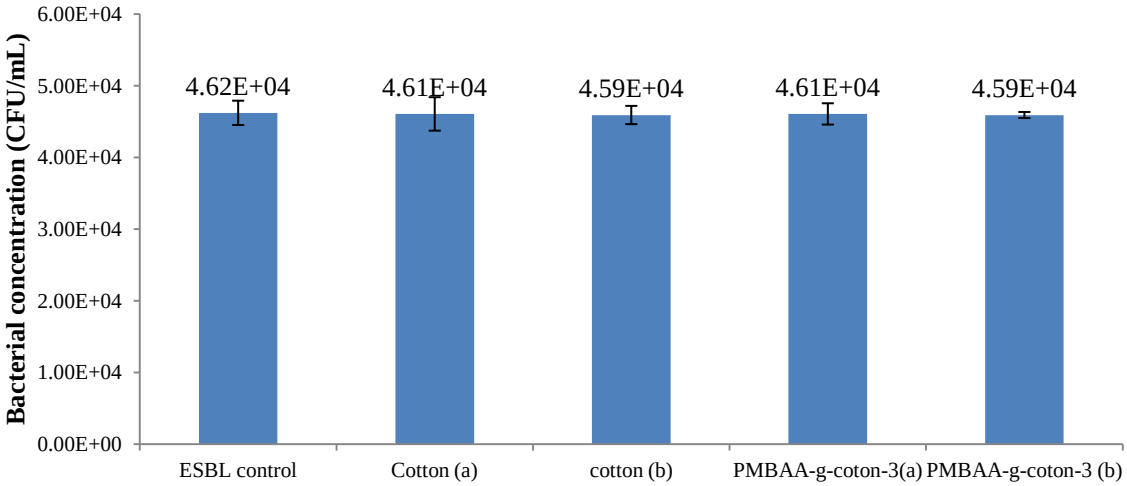

Figure 21. MDR-*E.coli* bacterial concentration after contact with soaking solution of corresponding cotton samples. (a) cotton fabric was shaken in PBS for 5 min; (b) cotton fabric was shaken in PBS for 10 min.

These modified cotton fabrics were also challenged with a Gram-positive bacterium healthcare associated (HA)-MRSA #77090. As shown in **Table 8**, PMBAA-g-cotton-**1** and PMBAA-g-cotton-**5** gave similar percent reductions of the tested bacterium: 75.0% and 82.3%. Again, it indicated negligible contribution from the negative charge to N-chloramine's biocidal function. A 6.3 log reduction was achieved by PMBAA-g-cotton-**3** with 141±8 ppm active chlorine. The 76.5 % bacterial reduction of PMBAA-g-cotton-**3** with the active chlorine loading of 33±5 ppm was comparable to that of PMBAA-g-cotton-**1** and PMBAA-g-cotton-**5**, which possessed a little over the twice active chlorine concentration (80±14 ppm and 84±1 ppm respectively). Sonohara and co-workers studied the electrophoretic mobility of *E.coli* and *S.aureus* in media with a range of pHs and ionic strengths. [138] Based on the mobility formula derived for biological cells by Ohshima and Kondo,[139] Sonohara extracted two parameters from the electrophoretic mobility results: charge density on the bacterial surface and resistance to liquid flow in the surface layer. Compared with *S.aureus*, the surfaces of *E.coli* cells are more negatively charged and more rigid, i.e. higher resistance to liquid flow in the surface layer. Since the number density of negative charges on *S.aureus* cells (0.025 m^{-3} at pH = 7) is much less than *E. coli* cells (0.145 m^{-3} at pH = 7),[138] the contribution of positive charge in the killing of *S. aureus* was not as obvious as in the case of *E. coli.* The same reason accounts for less effective antibacterial performance of PMBAA-g-cotton-**4**. When the contribution of positive charge diminished, the negative impact of hydrophobic alkyl chain magnified its effect. So unlike the case of *E. coli* reduction,

PMBAA-g-cotton-**4** appeared even less effective than PMBAA-g-cotton-**1** and -**5** in inactivating MRSA.

Based on the antibacterial studies against MDR-*E.coli* and HA-MRSA, the same conclusion could be drawn that the cation in **3** contributed greatly to bacterial kill while anion in **5** did not, and no synergistic effect between antibacterial QAC and N-chloramine was found. The long alkyl chain in QAC, on the contrary, contributed negatively to the antibacterial efficacy.

The mechanism for the enhanced antibacterial activity was proposed as follows: through an electrostatic attraction of opposite charges, the cation in PMBAA-g-cotton-**3** helps arrest negatively charged bacterial cells and hence facilitates the oxidative chlorine transfer from N-chlorohydantoin to cell biological receptors causing bacterial death (**Scheme 6**). Based on this hypothesis, it is possible that the antibacterial activity might be further enhanced if more than one cation were introduced to molecule **3**. We believe that such new products together with **3** are good candidates to challenge biofilms, a prominent form of microbial life that may cause many chronic infections and clinical environment contaminations.[132] Such designs and synthesis are currently being undertaken in our research group.

Table 8.Antibacterial efficacy of modified cotton fabrics against MRSA #77090.

Modified cotton Sample	Active chlorine (ppm)	Reduction of MRSA[a]	
		Percentage reduction	Log_{10} reduction
cotton	0	0.0%	0
PMBAA-g-cotton	66 ±3	27.2%	0.02
PMBAA-g-cotton-**1**	80 ±14	75.0%	0.6
PMBAA-g-cotton-**3**	141 ±8	100.0%	6.3
PMBAA-g-cotton-**3**	33 ±5	76.5%	0.63
PMBAA-g-cotton-**5**	84 ±1	82.3%	0.75
PMBAA-g-cotton-**4**	59 ±4	26.0%	0.11

[a)]Inoculum concentration was $2.0*10^6$CFU/mL and contact time was 5min.

5. CONCLUSIONS AND FUTURE STUDIES

Timely and effective wound management is critical for effective burn treatment. Important requirements for a burn wound dressing are infection control and low-adherence. Infection is a cause of failure in burn treatment and may be fatal if improperly treated. During a wound dressing change, if the newly formed tissue and cells have adhered to the wound and are peeled off along with the wound dressing, bleeding occurs and a larger wound size results, prolonging healing time and causing pain to the burn patient. Silver has long been recognized and used as an antimicrobial agent against a broad spectrum of bacteria, fungi, and viruses. Numerous reports have addressed the effectiveness of silver in burn wound infection control. However, there are also many reports of cytotoxicity of the silver ion, although a silver ion-containing wound dressing, such as Aquacel®, can inhibit the growth of both Gram-positive and Gram-negative bacteria, a cause of infection in burn wounds. Although antibacterial ability and nonadherence of Aquacel® are notable, cytotoxicity of the silver may cause a delay in wound epithelization. AgNP-containing wound dressings are available, but their nonadherence property needs to be enhanced. Another issue for current wound dressings is bacterial resistance to silver.

Since some of the AgNP-containing wound dressings are composed of knit PET, thus PET fabric was chosen as the substrate for surface modification. A hydrogel is a polymer composed mainly of water that is able to maintain a moist microenvironment between the dressing and the wound during the healing process. Moreover, it is a good structure in

which metal particles can be incorporated. Thus, the IPN method, developed in the Medical Surface Engineering Lab, was used to deposit PAM hydrogel onto PET fabric.

AgNPs were then successfully assembled onto modified PET with PAM IPN on the surface. The assembly of AgNPs on the modified PET (PAM-PET) fabrics can be attributed to the dimeric hydrogen bonding between the carboxylic group in the sodium citrate stabilizer and the amide groups in PAM IPN. The synthesized AgNPs were mainly about 3-4 nm and the average particle size was 6.74 nm. The content of self-assembled AgNPs on the modified fabrics ranged from 3.04% to 3.78%. The AgNP-containing PAM-PET fabrics were challenged by two bacteria, *P.aeruginosa* and MRSA, which are the main causes of infection in burn wounds. Due to the small diameter and the amount of particles incorporated in fabrics, the AgNP-containing PAM-PET proved its efficacy by reaching 3 log reduction with 2 hours of contact with the bacterial suspension and 6.7 log reduction could be reached after 4 hours. Those results indicate that the AgNP-containing PAM-PET is an effective antibacterial material with the potential of being used in treating burn wounds.

Results from peeling tests indicate that the surface modification achieved through grafting PAM onto PET greatly improved the swelling capacity of PET. Thus, when applied to a wound, the dressing is able to absorb exudates. With the increase of monomer concentration, the swelling capacity and nonadherent property were both improved. It was found that PAM IPN can form a hydrogel layer on the surface and lead to a 36.25% decrease in peeling force (PAM-PET-3) compared to untreated PET. The

adherence of PAM-PET-3 was further decreased by 81.24% when treated with water before the peeling test, and even a 87.53% reduction was achieved by using a surfactant. Low adherence is considered desirable and beneficial for wound dressings and brings less pain and damage to patients upon removal. It was proved that the hydrogel played an important role in reducing adherence. However, after the incorporation of AgNPs into PAM-PET fabrics, the properties of swelling and nonadherence were negatively influenced because AgNPs occupied some of the amide groups of PAM, meaning that fewer water molecules could form a hydrogen bond with the amide groups.

Because bacterial resistance to silver may be a problem in controlling infection, we synthesized a series of ionic DMH analogues and chlorinated these DMH derivatives to study their antibacterial activities. When the active chlorine was only 15 ppm in solution, the positively charged DMH derivative, which has a short alkyl chain, was found to have a total kill of different bacteria within 5 min, which was significantly faster than the negatively charged DMH derivative. It was also found that the positively charged DMH derivative (with short alkyl chain) resulted in the most effective antibacterial activity compared with other biocides when grafted on fabrics. The cotton grafted with this biocide killed 76.5% MRSA with only 33 ppm active chlorine whereas other samples need 80 ppm active chlorine or more to get similar antibacterial efficacy. There was boosting antibacterial effect for cationic charged QAC (with short alkyl chain) bonded DMH, but the synergistic effects of the long alkyl chain containing biocide was not found because of the short contact time, which was not enough for QAC to function. Moreover,

the antibacterial property can be regained when the fabric is washed and treated with bleach.

To summarize, effective antibacterial agents and nonadherent surfaces are the ultimate goal for an ideal burn wound dressing. This research used the IPN method to create a less adherent surface on PET fabric, into which AgNPs can be incorporated to kill bacteria and reduce infection. Also, new antibacterial precursors were grafted onto both PET and cotton fabrics. Fabrics grafted with the DMH derivative showed excellent antibacterial efficacy, which can be activated by dilute sodium hypochlorine, with low active chlorine. Specifically, the PMBAA-g-cotton-**3** can pick up positive chlorine atoms from only 10 ppm sodium hypochlorine solution. The dilute bleach used to activate the antibacterial property of fabrics,will lessen the environment burden which can lead to a wider use of N-chloramine based biocides to kill infectious bacteria. The wound dressing designed in this research is both antibacterial and less adherent; the new biocide containing fabric can be used as a second layer of wound dressing to decrease cross-infection. However, since the incorporation of AgNPs may compromise the nonadherence property, and the ideal peeling energy should be lower than 300-400 Jm^{-2}, further studies need to be carried out to develop less adherent surfaces. Studies on animals can also be conducted to observe wound healing and evaluate adherence. Since the IPN method is essentially applicable on all thermoplastic substrates, more attempts will be made to modify other materials so that these dressings could be applied to treat different burns or wounds at different parts of the human body. Ultimately, the

improvements in wound dressings will greatly improve the treatment and provide patients with quality of life.

6. REFERENCES

[1] Devgan, L.; Satyanarayan, B.; Aylward S.; Spence, R.J. Modalities for the assessment of burn wound depth. *J. Burns Wounds* **2006**, 5, 7-15.

[2] Souter, D. How to assess accurate burn depth. *Wound Essentials* **2010**, 5, 94-101.

[3] Sen, S.; Greenhalgh, D.; Palmieri, T. Review of Burn Injury Research for the Year 2009, *J Burn Care Res.* **2010**, 31, 836–848.

[4] Nguyen, T.T.; Gilpin, D.A.; Meyer, N.A.; Herndon, D.N. Current treatment of severely burned patients. *Ann. Surg.* **1996**, 223, 14-25.

[5] Church, D.; Elsayed, S.; Reid, O.; Winston, B.; Lindsay, R. Burn wound infections. *Clin. Microbiol. Rev.* **2006**, 19, 404-434.

[6] Sterling, J.P.; Heimbach, D.M. Hemostasis in burn surgery-a review. *Burns* **2011**, 37, 559-565.

[7] Rippon, M.; White, R.; Davies, P. Skin adhesives and their role in wound dressings. *Wounds UK* **2007**, 3, 76-86.

[8] Keen, E.F.; Robinson, B.J.; Hospenthal, D.R.; Aldous, W.K.; Wolf, S.E.; Chung, K.K.; Murray, C.K. Incidence and bacteriology of burn infections at a military burn center. *Burns* **2010**, 36, 461-468.

[9] Church, D.; Elsayed, S.; Reid, O.; Winston, B.; Lindsay, R. Burn wound infections. *Clin. Microbiol. Rev.* **2006**, 19, 403-434.

[10] Muller, M.J.; Herndon, D.N. The challenge of burns. *Lancet* **1994**, 343, 216-220.

[11] Soman, S.; Greenhalgh, D; Palmieri, T. Review of burn injury research. *J. Burn Care Res.* **2010**, 31, 836-848.

[12] Atiyeh, B.S; Gunn, S.W.; Hayek, S.N. State of the art in burn treatment. *World J. Surg.* **2005**, 29,131-148.

[13] Madhuri, A.G.; Deepika, A Evaluation of banana leaf dressing for partial thickness burn wounds. *Burns* **2003**, 29, 487–492.

[14] Shakespeare, P. Burn wound healing and skin substitutes. *Burns* **2001**, 27, 517-522.

[15] Boateng, J.S.; Matthews, K.H.; Stevens, H.N.E.; Eccleston, G.M. Wound healing dressings and drug delivery systems: a review. *J.Pharm. Sci.* **2008**, 97, 2892-2923.

[16] Stadelmann, W.K.; Digenis, A.G.; Tobin, G.R. Physiology and healing dynamics of chronic cutaneous wounds. *Am J.Surg.* **1998**, 176, 26-38.

[17] Ather, S.; Harding, K.G.; Thomas, S.; Gupta, B.S.; Edwards, J.V.; et al. *Advanced textiles for wounds*; Rajendran, S., eds.; CRC Press: Boca Raton, **2009**.

[18] Morris, C. Wound management and dressing selection. *Wound Essentials* **2006**, 1, 178-183.

[19] Wasiak, J.; Cleand, H.; Campbell, F. Dressings for superficial and partial thickness burns. *Cochrane Database Syst. Rev.* **2008**, 4, 1-53.

[20] Kagan, R.J.; Peck, M.D.; Aherenholz, D.H.; Hickerson, W.L.; Holmes, J.H.; Korentager, R.A.; Kraatz, J.J.; Kotoski, G.M. Surgical Management of the burn wound and use of skin substitutes. http://www.ameriburn.org/WhitePaperFinal.pdf (accessed JUL 1, 2012)

[21] Cameron, A.M.; Ruzehaji. N.; Cowin, A.J. Burn wound management: a surgical perspective. *Wound Prac. Res.* **2010**, 18, 35-40.

[22] Anon. Atraumatic Dressings. *Ostomy Wound Manage* **2003**, 49, 26-28.

[23] Van Rijswijk, L. Ingredient-based wound dressing classification: A paradigm shift that is passe and in need of replacement. *J. Wound Care* **2006**, 15, 11–14.

[24] Winter, G.D. Formation of scab and the rate of epithelization of superficial wound in the skin of the domestic pig. *Nature* **1962**, 193, 293-294.

[25] Greenhalgh, D.G. Topical antimicrobial agents for burn wounds. *Clin. Plastic Surg.* **2009**, 26, 597-606.

[26] Zhao, N.; Logsettty, S.; Liu, S. Durability of amide N-chloramine biocide to ethylene oxide sterilization. *J. Burn Care Res.* **2012**, 33, 201-206.

[27] Fong, J.; Wood Fiona. Nanocrystalline silver dressings in wound management: A review. *Int. J Med.* **2006**, 1, 441-449.

[28] Klasen, H.J. Historical review of the use of silver in the treatment of burns. I. Early uses. *Burns* **2000**, 26, 117-130.

[29] Klasen, H.J. Historical review of the use of silver in the treatment of burns. II. Renewed interest for silver. *Burns* **2000**, 26, 131-138.

[30] Leaper, J.D. Silver dressings: their role in wound management. *Int. Wound J.* **2006**, 3,282-294.

[31] Feng, Q.L.; Wu, J.; Chen, G.Q.; Cui, F.Z.; Kim, T.N.; Kim, J.O. A mechanistic study of the antibacterial effect of silver ions on *Escherichia coli* and *Staphylococcus*

aureus. J.Biomed. mater. Res. **2000**, 52, 662-668.

[32] Kim, J.S.; Kuk, E.; Yu, K.N.; Kim, J.H.; Park, S.J.; Lee, H.J.; et al. Antimicrobial effects of silver nanoparticles. *Nanomed-Nanotechnol.* **2007**, 3, 95-101.

[33] Pradhan, N.; Pal, A.; Pal, T. Silver nanoparticle catalyzed reduction of aromatic nitro compound. *Colloid Surface A.* **2002**, 196, 247-257.

[34] McFarland, A.D.; Van Duyne, R.P. Single silver nanoparticles as real-time optical sensors with zeptomole sensitivity. *Nano Letters* **2003**, 3, 1057-1062.

[35] Lok, C.N.; Ho, C.M.; Chen, R.; He, Q.Y.; Yu, W.Y.; et al. Proteomic analysis of the mode of antibacterial action of silver nanoparticles. *J. Proteome Res.* **2006**, 5, 916-924.

[36] Baker, C.; Pradhan, A.; Pakstis, L.; Pochan, D. J.; Shah, S.I. Synthesis and antibacterial properties of silver nanoparticles. *J. Nanosci. Nanotechnol.* **2005**, *5*, 244-249.

[37] Aymonier, C.; Schlotterbeck, U.; Antonietti, L.; Zacharias, P.; Thomann, R.; Tiller, J. C.; Mecking, S. Hybrids of silver nanoparticles with amphiphilic hyperbranched macromolecules exhibiting antimicrobial properties. *Chem. Commun.* **2002**, 3018-3019.

[38] Lok, C.N.; Ho, C.M.; Chen, R.; He, Q.Y.; Yu, W.Y.; Sun, H,; et al. Silver nanoparticles: partial oxidation and antibacterial activities. *J. Biol. Inorg. Chem*. **2007**, 12, 527-534.

[39] Kittler, S.; Greulich,C.; Koller. M.; Epple, M. Synthesis of PVP-coated silver

nanoparticles and their biological activity towards human mesenchymal stem cells. *Materialwissenschaft und Werkstofftechnik* **2009**, 40, 258-264.

[40] Kong, H.; Jang, J. Antibacterial Properties of Novel Poly (methylmethacrylate) Nanofiber Containing Silver Nanoparticles. *Langmuir* **2008**, 24, 2051-2056.

[41] Vimala, K.; Mohan, Y.M.; Sivudu, K.S.; Varaprasad, K.; Ravindra, S.; Reddy, N.N.; Padma, Y.; Sreedhar, B.; MohanaRaju, K. Fabrication of porous chitosan films impregnated with silver nanoparticles: A facile approach for superior antibacterial application. *Colloid Surface B.* **2010**, 76, 248–258.

[42] Simoncic, B.; Tomsic, B. Structures of novel antimicrobial agents for textiles-A review. *Textile Res. J.* **2010**, 80, 1721-1731.

[43] Gao, Y.; Granston, R. Recent advances in antimicrobial treatments of textile. *Textile Res. J.* **2008**, 78, 60-72.

[44] Tiller, J.C.; Liao, C.J.; Lewis, J.; Kilbanov, A.M. Designing surfaces that kill bacteria on contact. *Proc. Natl. Acad. Sci. U.S.A.* **2001**, 98, 5981-5985.

[45] Murugan, E.; Gopinath, P.; Shanmugayya, V.; Mathivanan, N. Antibacterial activity of novel insoluble bead-shaped polymer-supported multiquaternary ammonium salts. *J. Appl. Polym. Sci.* **2010**, 117, 3673-3678.

[46] Townsend, D.E.; Greed, I.; Ashdown, N.; Grubb, W.B. Plasmid-mediated resistance to quaternary ammonium compounds in *methicillin-resistant staphylococcus aureus*. *Med. J. Australia* **1983**, 2, 310.

[47] Tennent, J.M.; Lyon, B.R.; Gillespie, M.T. Cloning and expression of

Staphylococcus-aureus plasmid-medicated quaternary ammonium resistance in Escherichia-coli. *Antimicrob. Agents Chemother.* **1985**, 27, 1, 79-83.

[48] Williams, D.E.; Elder, E.D.; Worley, S.D. Is free halogen necessary for disinfection? *Appl. Environ. Microbiol*. **1988**, 54, 2583-2585.

[49] Sun, Y.Y.; Sun, G. Novel regenerable N-halamine polymeric biocides. I. Sythesis, characterization, and antibacterial activity of hydantoin-containing polymers. *J. Appl. Poly. Sci*. **2000**, 80, 2460-2467.

[50] Sun, Y.Y.; Sun, G. Novel regenerable N-halamine polymeric biocides. Ⅱ. Grafting hydantoin-containing monomers onto cotton cellulose. *J. Appl. Poly. Sci.* **2001**, 81, 617-624.

[51] Lin, J.; Cammarata, V.; Worley, S.D.; Broughton, R.M.; Tzou,Y. M.; Huang, T.S. Infrared charactrization of biocidal Nylon. *Polymer* **2001**, 42, 7903-7906.

[52] Efem, S.E.E. Clinical observations on the wound healing properties of honey. *Br H Surg*. **1988**, 75,679-681.

[53] Wilkinson,J.M.; Cavanagh,H.M.A. Antibacterial activity of 13 honey against *Escherichia coli* and *Pseudomonas aeruginosa*. *J. Med. Food* **2005**, 8, 100-103.

[54] Cooper, R.A.; Molan, P.C. Antibacterial activity of honey against strains of Staphylococcus aureus isolated from infected wound. *J Soc Med*. **1999**, 92, 283-285.

[55] Tim Cushnie, T.P.; Lamb, A.J. Antimicrobial activity of flavonoids. *Int. J. Antimicrob. agents* **2005**, 26, 343-356.

[56] Rabea, E.I.; Badawy, M.E.; Stevens, C.V.; et al. Chitosan as antimicrobial agent:

applications and mode of action. *Biomacromolecules* **2003**, 4, 1457-1456.

[57] Kong, M.; Chen, X.G.; Xing, K.; et al. Antimicrobial properties of chitosan and mode of action: a state of the art review. *Int. J. Food Microbiol*. **2010**, 144, 51-63.

[58] Dai, T.; Tanaka, M.; Huang, Y.Y.; Hamblin, M.R. Chitosan preparations for wounds and burns: antimicrobial and wound healing effects. *Expert Rev. Anti. Infect. Ther*. **2011**, 9, 857-879.

[59] Dong, H.; Wang, D.; Sun, G.; Hinestroza, J.P. Assembly of Metal Nanoparticles on Electrospun Nylon6 Nanofibers by Control of Interfacial Hydrogen-Bonding Interactions. *Chem. Mater.***2008**, 20, 6627-6632.

[60] Zhang, F.; Wu, X.; Chen, Y.; Lin, H. Application of Silver Nanoparticles to Cotton Fabric as an Antibacterial Textile Finish. *Fibers Polym.* **2009**, 10, 496-501.

[61] Thomas, V.; Namdeo, M.; Mohan, Y.M..; Bajpai, S.K.; Baipai, M. Review on polymer, hydrogel and microgel metal nanocomposites: A facile nanotechnological approach. *J. Macromolecular Sci. A.* **2008**, 45,107-119.

[62] Mohan, Y.M.; Premkumar, T.; Lee, K.; Geckeler, K.E. Fabrication of silver nanoparticles in hydrogel networks. *Macromol. Rapid Comm.*. **2006**, 27, 1346-1354.

[63] Uygun, M.; Kahveci, M.U.; Odaci, D.; Timur, S.; Yagci, Y. Antibacterial Acrylamide Hydrogels Containing Silver Nanoparticles by Simultaneous Photoinduced Free Radical Polymerization and Electron Transfer Processes. *Macromol. Chem. Phys*. **2009**, 210, 1867–1875.

[64] Murthy, P.S.K.; Mohan, Y.M.; Varaprasad. K.; Sreedhar, B.; Raju, K.M. First

successful design of semi-IPN hydrogel-silver nanocomposites: A facile approach for antibacterial application. *J. Colloid Interf. Sci.* **2008**, 318, 217-224.

[65] Varaprasad, K.; Mohan, Y.M.; Ravindra, S.; Reddy, N.N.; Vimala, K.; Monika, K.; Sreedhar, B.; Raju, K.M. Hydrogel-silver nanoparticle composites: A new generation of antimicrobials. *J. Appl. Polym.Sci.* **2010,** 115, 1199-1207.

[66] Bowler, P.; Jones, S.; Towers, V.; Booth, R.; Parson, D.; Walker, M. Dressing conformability and silver containing wound dressings. *Wounds UK* **2010**, 6, 14-20.

[67] Lu, G.; Wu, D.; Fu, R. Studies on the synthesis and antibacterial activities of polymeric quaternary ammonium salts from dimethylaminoethyl methacrylate. *React. Funct. Polym.* **2007**, 67,355-366.

[68] Owusu-Adom, K.; Guymon, C.A. Photopolymerization kinetics of poly(acrylate)-clay composites using polymerizable surfactants. *Polymer* **2008**, 49, 2636-2643.

[69] Marini, M.; Bondi, M.; Iseppi, R.; Toselli, M.; Pilati, F. Preparation and antibacterial activity of hybrid materials containing quaternary ammonium salts via Sol-Gel process. *Eur. Polym. J.* **2007,** 43, 3621-3628.

[70] Liu, S.; Sun, G. New Refreshable N-halamine Polymeric Biocides: N-Chlorination of Acyclic Amide Grafted Cellulose. *Ind. Eng. Chem. Res.* **2009**, 48, 613-618.

[71] Ren, X.; Kocer, H.B.; Kou, L.; Worley, S.D.; Broughton, R.M.; Tzou, Y.M.; Huang, T.S. Antimicrobial polyester. *J. App. Polym. Sci.* **2008**, 109. 2756-2761.

[72] Sun, Y.Y.; Sun, G. Novel refreshable N-halamine polymeric biocides: Grafting

hydantoin-containing monomers onto high performance fibers by a continuous process. *J. Appl. Polym. Sci*. **2003**, 88, 1032-1039.

[73] Liu, S.; Sun, G. Functional Modification of Poly(ethylene terephthalate) with an Allyl Monomer: Chemistry and Structure Characterization. *Polymer* **2008**, 49, 5225-5232.

[74] Mi, F.L.; Shyu, S.S.; Wu, Y.B.; Lee, S.T.; Shyong, J.Y.; Huang, R.N. Fabrication and characterization of a sponge-like asymmetric chitosan membrane as a wound dressing. *Biomaterials* **2001**, 22, 165-173.

[75] Ishihara, M.; Nakanishi, K.; Ono, K.; Sato, M.; et al. Photocrosslinkable chitosan as a dressing for wound occlusion and accelerator in healing process. *Biomaterials* **2002**, 23, 833-840.

[76] Jayakumar, R.; Prabaharan, M.; Sudheesh Kumar, P.T., Nair, S.V.; Tamura, H. Biomaterials based on chitin and chitosan in wound dressing applications. *Biotechn. Adv.* **2011**, 29, 322-337.

[77] Wijesinghe, M.; Weatherall, M.; Perrin,K.; Beasley, R. Honey in the treatment of burns: a systematic review and meta-analysis of its efficacy. *J. New Zealand Med. Associ.***2009**, 122,47-60.

[78] Subrahmanyam, M.A. Prospective randomized clinical and histological study of superficial burn wound healing with honey and silver sulfadiazine. *Burns* **1998**, 24, 157-161.

[79] Molan, P.C. Potential of honey in the treatment of wounds and burns. *Am. J. Clin.*

Dermatol. **2001**, 2, 13-19.

[80] Ahmed, A.K.; Hoekstra, M.J.; Hage, J.J. Honey medicated dressing: transformation of an ancient remedy into modern therapy. *Ann. Plast. Surg.* **2003**, 50, 143-148.

[81] Qin, Y. Silver-containing alginate fibers and dressings. *Int. Wound J.* **2005**, 2, 172-176.

[82] Barnea, Y.; Weiss, J.; Gur, E. A review of the applications of the hydrofiber dressing with silver (Aquacel Ag®). *Therapeut. Clin. Risk Manag.* **2010**, 6, 21-27.

[83] Karlsmark, T.; Agerslev, R.H.; Bendz, S.H.; Larsen, J.R.; Roed-Peterson, J.; Andersen, K.E. Clinical performance of a new silver dressing, Contreet Foam, for chronic exuding venous leg ulcers. *J. Wound Care* **2003**, 12, 351-354.

[84] Dowsett, C. An overview of Acticoat dressing in wound management. *Brit. J. Nur*. **2003**, 12, 44-49.

[85] Atiyeh, B.S.; Costagliola, M.; Hayek, S.N.; Dibo, S.A. Effect of silver on burn wound infection control and healing: Review of the literature. *Burns* **2007**, 33, 139-148.

[86] Rustogi, R.; Mill, J.; Fraser, J.F.; Kimble, R.M. The use of Acticoat™ in neonatal burns. *Burns* **2005**, 31, 878-882.

[87] Clare, M.; Panlene, E.; Elizabeth, M.; Frans, M.; Richard, W. Use of wound dressing with soft silicone adhesive technology. *Paediatr. Nurs.* **2009**, 21, 38-43.

[88] Koksal, C.; Bozkurt, A.K. Combination of hydrocolloid dressings and medical compression stocking versus Unna's boot for the treatment of venous leg ulcers.

Swiss Med. Wkly. **2003**, 364-368.

[89] Heffernan, A.; Martin, A.J. A comparison of a modified form of Granuflex (GranuflexExtra Thin) and a conventional dressing in the management of alcerations,abrasions and minor operation wounds in an accident and emergency department. *J. Accid. Emerg. Med.* **1994**, 11, 227-230.

[90] Bugmann, P.H.; Taylor, S.; Gyger, D. A silicone-coated nylon dressing reduces healing time in burned paediatric patients in comparison with standard sulfadiazine treatment: a prospective randomized trial. *Burns* **1998**, 24, 609-612.

[91] Barrett,B. Mepilex® Ag: an antimicrobial, absorbent foam dressing with Safetac® technology. *Brit. J. Nur.* **2009**, 18, 28-35.

[92] Fowler, A. Atraumatic dressings for non-complex burns. *Practice Nurs*. **2006**, 17, 193-196.

[93] Platt A.J.; Phipps, A.; Judkins, K. A comparative study of silicone net dressing and paraffin gauze dressing in skin-grafted sites. *Burns* **1996**, 22, 543-545.

[94] Heenan, A. Alginates: Frequently asked questions. *World Wide Wounds* **1998**, 1,1-7.

[95] Thomas, S. Alginate dressings in surgery and wound management-Part 1. *J. Wound Care* **2000**, 9, 56-60.

[96] Gilchrist, T.; Martin, A.M. Wound treatment with Sorbsan-An Alginate fiber dressing. *Biomaterials* **1983**, 4, 317-320.

[97] Abatangelo, G.; Akiyama, Y.; Ambrosio, L.; Barbucci, R.; Bartoli, C.; Borzacchiello, A.; et al. *Hydrogels-Biological properties and Applications;* Barbucci, R., Ed.;

Springer: New York, **2008**.

[98] Ferry, John D. *Viscoelastic Properties of Polymers*. Wiley: New York, **1980**.

[99] Razzak, M.T.; Zainuddin; Erizal; Dewi, S.P.; Lely, H.; Taty, E.; Sukirno. The characterization of dressing component materials and radiation formation of OVA-PVP hydrogel. *Radiat. Phys. Chem.* **1999**, 55, 153-165.

[100] Varshney, L. Role of natural polysaccharides in radiation formation of PVA-hydrogel wound dressing. *Nucl. Instru. Method. Phys. Res. B.* **2007**, 255, 343-349.

[101] Li, H.N.; Yang, J.; Hu, X.N.; Liang, J.; Fan, Y, J.; Zhang, X.D. Superabsorbent polysaccharide hydrogels based on pullulan derivate as antibacterial release wound dressing. *J. Biomed. Mater. Res. A.* **2011**, 98, 31-39.

[102] Zou, Y.; Reddy, N.; Yang, Y. Reusing polyester/cotton blend fabrics for composites. *Composite B* **2011**, 42, 763-770.

[103] Martin, L.; Wilson, C.G.; Koosha, F.; Tetley, L.; Gray, A.I.; Senel, S.; Uchegbu, I.F. The release of model macromolecules may be controlled by the hydrophobicity of palmitoyl glycol chitosan hydrogels. *J. Control Release* **2002**, 80, 87-100.

[104] Kiatamnuay, S.; Gettleman, L.; Khanand, Z.; Goldsmith, L.J. Effect of adhesive retention on maxillofacial prostheses. Part I: Skin dressings and solvent removers. *J. Prosthet. Dent.* **2000**, 84, 335-340.

[105] Dykes, P.J.; Heggie, R. The link between the peel force of adhesive dressings and subjective discomfort in volunteer subjects. *J. Wound Care* **2003**, 12, 260-262.

[106] Klode, J.; Schottler, L.; Stoffels, I.; Korber, A.; Schadendorf, A.; Dissemond, J. Polidocanol foam sclerotherapy is a new and effective treatment for post-operative lymphorrhea and lymphocele . *J. Eur. Acad. Dermatol.* **2010**, doi: 10.1111/j.1468-3083.2010.03886.

[107] Dykes, P.J.; Heggie, R.; Hill, S.A. Effects of adhesive dressings on the stratum corneum of the skin. *J. Wound Care* **2001**, 10, 7-10.

[108] Xu, H.; Ma, L.; Shi, H.; Gao, C.; Han, C. Chitosan-hyaluronic acid hybrid film as a novel wound dressing: in vitro and in *vivo* studies. *Polym. Adv. Technol.* **2007**, 18, 869-875.

[109] Dong, C.; Mead, E.; Skalak, R.; Fung, Y.C.; Debes, J.C.; Zapata-Sirvent, R.L.; et al. Development of a device for measuring adherence of skin grafts to the wound surface. *Ann. Biomed. Eng.* **1993**, 21, 51-55.

[110] Ansermino, M.; Hemsley, C. Intensive care management and control of infection. BMJ **2004**, 329, 220-223.

[111] Branski, L.K.; Mousawi, A.A.; Rivero, H., Jeschke, M.G.; et al. Emerging infections in burns. *Surg. Infection.* **2009**, 10, 389-396.

[112] Sondi, I.; Sondi, B.S. Silver nanoparticles as antimicrobial agent: a case study on *E.coli* as a model for gram-negative bacteria. *J. Colloid Interf. Sci.* **2004**, 275, 177-182.

[113] Morones, J.R.; Elechigurra, J.L.; Camacho, A.; Holt, K.; Kouri, J.B.; Ramirez, J.T.; Yacaman, M.J. The bactericidal effect of silver nanoparticles. *Nanotechnology*

2005, 16, 2346-2353.

[114] Fong, J.; Wood, F. Nanocrystalline silver dressings in wound management: a review. *Int. J. Nanomed.* **2006**, 1, 441-449.

[115] Panacek, A.; Kolar, M.; Vecerova, R.; Prucek, R.; Soukupova, J.; Srystof, V.; Hamal, P.; Zboril, R.; Kvitek, L. Antifungal activity of silver nanoparticles against Candida spp. *Biomaterials* **2009**, 30, 6333-6340.

[116] Silver, S. Bacterial silver resistance: molecular biology and uses and misuses of silver compounds. *FEMS Microbiol. Rev.* **2003**, 27,341-353.

[117] Loh, J.V.; Percival, S.L.; Woods, E.J.; Williams, N.J.; Cochrane, C.A. Silver resistance in MRSA isolated from wound and nasal sources in humans and animals. *Int. Wound J*. **2009**, 6, 32-38.

[118] Townsend, D.E.; Greed, L.; Ashdown, N.; Grubb, W.B. Plasmid-mediated Resistance to Quaternary Ammonium-compounds in Methicillin-resistant *Staphylococcus-aureus*. *Med. J. Australia*. **1983**, 2, 310.

[119] Tennent, J.M.; Lyon, B.R.; Gillespie, M.T.; May, J.W.; Skurray, R.A. Cloning and Expression of *Staphylococcus-aureus* Plasmid-mediated Quaternary Ammonium Resistance in *Escherichia-coli*. *Antimicrob. agents Chemother.* 1985, 27, 79-83.

[120] Li, L.; Zhao, N.; Liu, S. Versatile Surface Biofunctionalization of Poly(ethylene terephthalate) (PET) by Interpenetrating Polymerization of a butynyl Monomer Followed by “Click” Chemistry. *Polymer* **2012**, 53, 67-78.

[121] Andrews, E.H.; Kamyab, I. Adhesion of surgical dressings to wounds. A new *in*

vitro model. *Clin. Mater.* **1986** 1, 9-21.

[122] Gottesman, R.; Shukla, S.; Perkas, N.; Solovyov, L.A.; Nitzan, Y.; Gedanken, A. Sonochemical coating of paper by microbiocidal silver nanoparticles. *Langmuir* **2011**, 27, 720-726.

[123] Branski, L.K.; Al-Mousawi, A.; Rivero, H.; Jeschke, M.G.; Sanford, A.P.; Herdon, D.N. Emerging infection in burns. *Surg. Infection.* **2009**, 10,389-397.

[124] Zhanel, G.G.; Rossnagel, E.; Nichol, K.; Karlowsky, J.A.; Zelenitsky, S.; Noreddin, A.M.; Hoban, D.J. Ceftsroline pharmacodynamic activity verus community-associated and healthcare-associated methicillin-resistant *Staphylococcus aureus*, heteroresistant vancomycin-intermediate *S.aureus*, vancomycin-intermediate *S.aureus* and vancomyin-resistant *S.aureus* using an *in vitro* model. *J. Antimicrob. Chemother.* **2011**, 66, 1301-1305.

[125] Rudenja, S.; Zhao, N.; Liu, S. Surface Interpenetrating Networks of Polyacrylamide in Poly(ethylene terephthalate) as a Means of Surface Modification. *Eur. Polym. J.* **2010**, 46, 2078-2084.

[126] Hagendoefer, H.; Kaegi, R.; Parlinska, M.; Ludwig, C.; Ulrich, A. Characterization of silver nanoparticle products using asymmertirc flow field flow fractionation with a multidetector approach-a comparison to transmission electron microscopy and batch dynamic light scattering. *Anal. Chem.* **2012**, 74, 2678-2685.

[127] Sharabaty, T.; Biguenet, F.; Dupuis, D.; Viallier, P. Investigation on moisture transport through plyester/cotton fibrics. *Indian J. Fiber Textile Res.* **2008**, 33,

419-425.

[128] Thomas, S. Wound dressing materials-testing and control. *Pharm. J.* **1982**, 228,576.

[129] Larmour, C.J; McCabe, J.F; Gordon, P.H. An ex vivo investigation into the effects of chemical solvents on the debond behavior of ceramic orthodontic brackets. *Brit.J. orthodontics* **1998**, 25, 35-39.

[130] Martinez-Castanon, G.A; Nino-Martinez, N.; Martinez-Guiterrez, F.; Martinez-Mendoza, J.R.; Facundo, R. Synthesis and antibacterial activity of silver nanoparticles with difference sizes. *J. Nanopart. Res.* **2008**, 10, 1343-1348.

[131] Lu, X.Q.; Bittman, R. Synthesis of a photoactivatable (2S,3R)-sphingosylphosphorylcholine analogue. *J. Org. Chem*. **2005**, 70, 4746-4750.

[132] Hall-Stoodley, L.; Costerton, J.W.; Stoodley, P. Bacterial biofilms: From the natural environment to infectious diseases. *Nat. Rev. Microbiol.* **2004**, 2, 95-108.

[133] Angelos, S.; Yang, Y.W.; Patel, K.; Stoddart, J.F.; Zink, J.I. pH-responsive supramolecular nanovalves based on cucurbit[6]uril pseudorotaxanes. *Angew. Chem. Int. Ed*. **2008**, 47, 2222-2226.

[134] Liu, S.; Sun, G. Radical Graft Functional Modification of Cellulose with Allyl Monomers: Chemistry and Structure Characterization. *Carbohydr. Polym*. **2008**, 71, 614-625.

[135] Mauger, R.P.; Soper, F.G. Acid catalysis in the formation of chloroamides from hypochlorous acid-N-chlorination by hypochilorire ions and by acyl hypochlorites. *J.*

Chem. Soc. **1946**,71-75.

[136] Qian, L.; Sun, G. Durable and regenerable antimicrobial textiles: Synthesis and applications of 2-methylol-2,2,5,5-tetramethylimidazolidin-4-one (MTMIO). *J. appl. Polym. Sci*. **2003**, 89, 2418-2425.

[137] Williams, D.E.; Elder, E.D.; Worley, S.D. Is free halogen necessary for disinfection. *Appl. Environ. Microbiol*. **1988**, 54, 2583-2585.

[138] Sonohara. R.; Muramatsu, N.; Ohshima, H.; Kondo, T. Difference in surface-properties between *Escherichia-coli* and *Staphylococcus-aureus* as revealed by electrophoretic mobility. *Biophys. Chem.* **1995**, 55, 273-277.

[139] Ohshima, H.; Kondo, T. Approximate analytic-expression for the electrophoretic mobility of colloidal particles with surface-charge layers. *J. Colloid Interf. Sci.***1989**, 130, 281-282.

SUPPORTING INFORMATION

TEM images

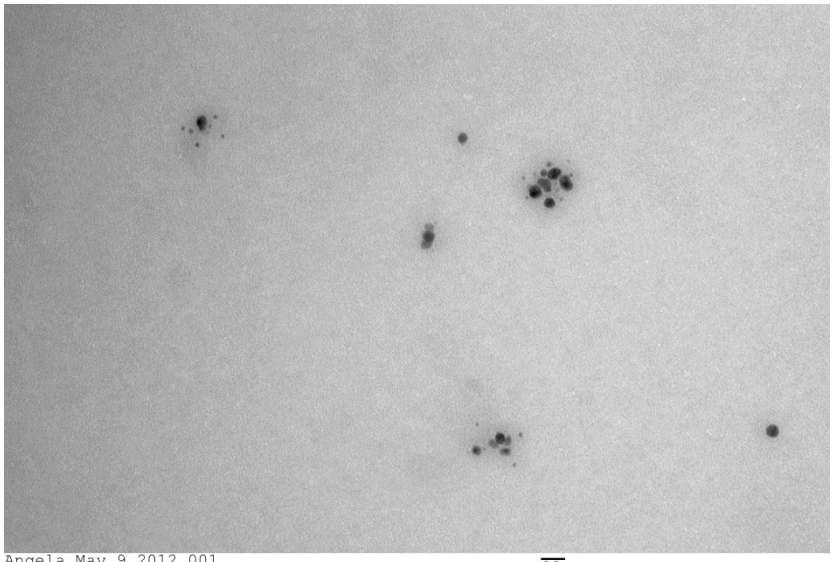

Angela May 9 2012_001
Ag nanoparticle
Cal: 0.139938 nm/pix
10:51:08 a 05/09/12

20 nm
HV=75.0kV
Direct Mag: 80000x
UM Biological Science

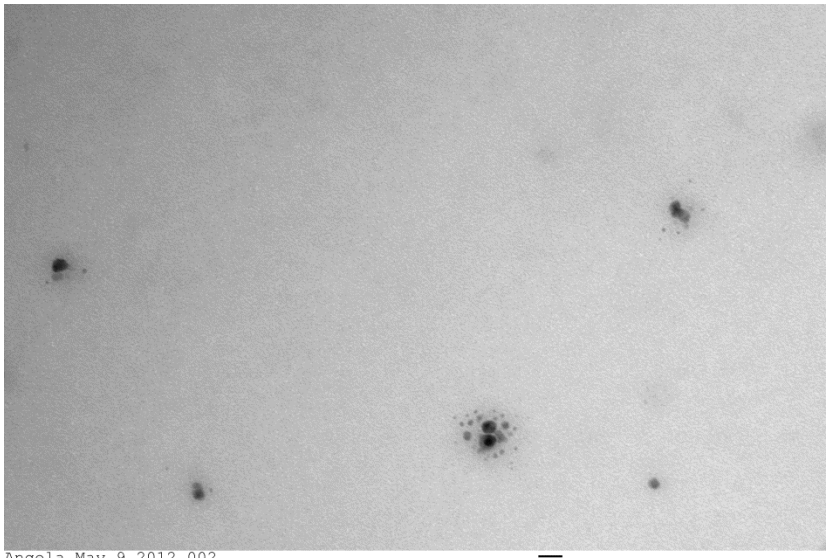

Angela May 9 2012_002
Ag nanoparticle
Cal: 0.139938 nm/pix
10:53:17 a 05/09/12

20 nm
HV=75.0kV
Direct Mag: 80000x
UM Biological Science

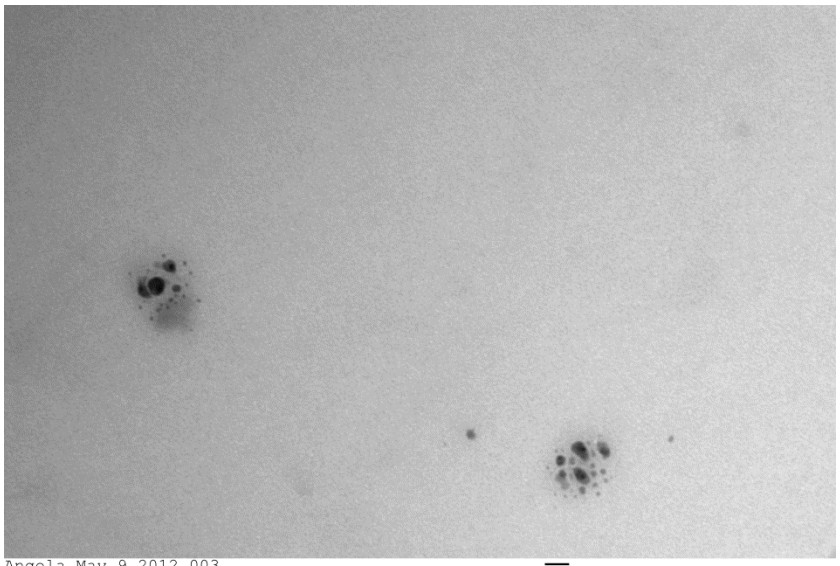

Angela May 9 2012_003
Ag nanoparticle
Cal: 0.139938 nm/pix
10:54:15 a 05/09/12

20 nm
HV=75.0kV
Direct Mag: 80000x
UM Biological Science

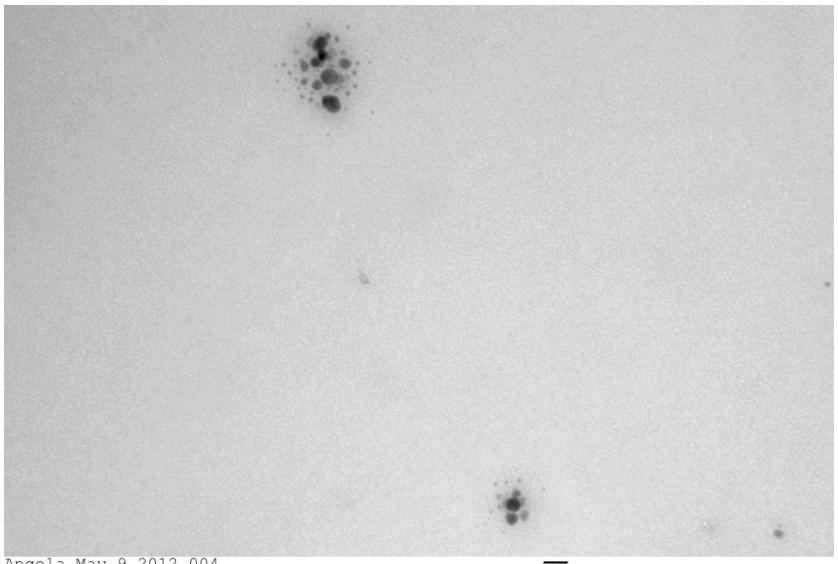

Angela May 9 2012_004
Ag nanoparticle
Cal: 0.139938 nm/pix
10:55:23 a 05/09/12

20 nm
HV=75.0kV
Direct Mag: 80000x
UM Biological Science

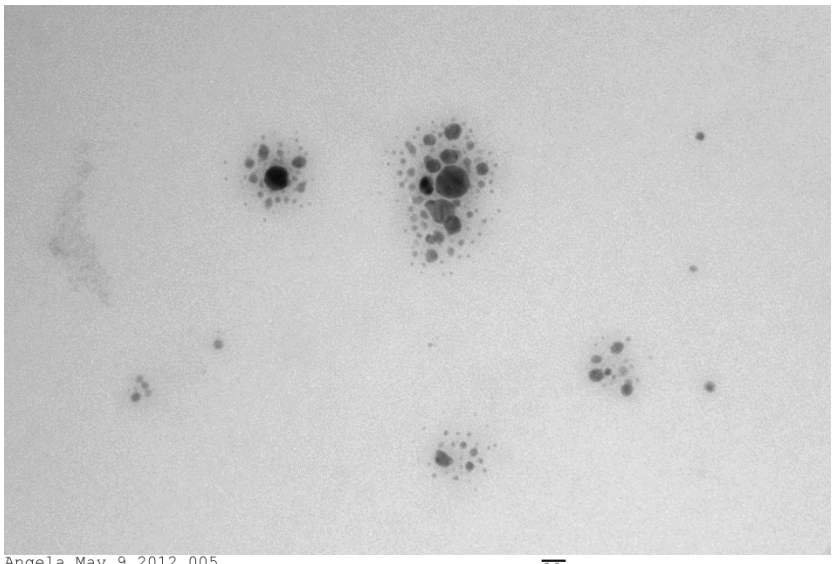

Angela May 9 2012_005
Ag nanoparticle
Cal: 0.139938 nm/pix
10:57:52 a 05/09/12

20 nm
HV=75.0kV
Direct Mag: 80000x
UM Biological Science

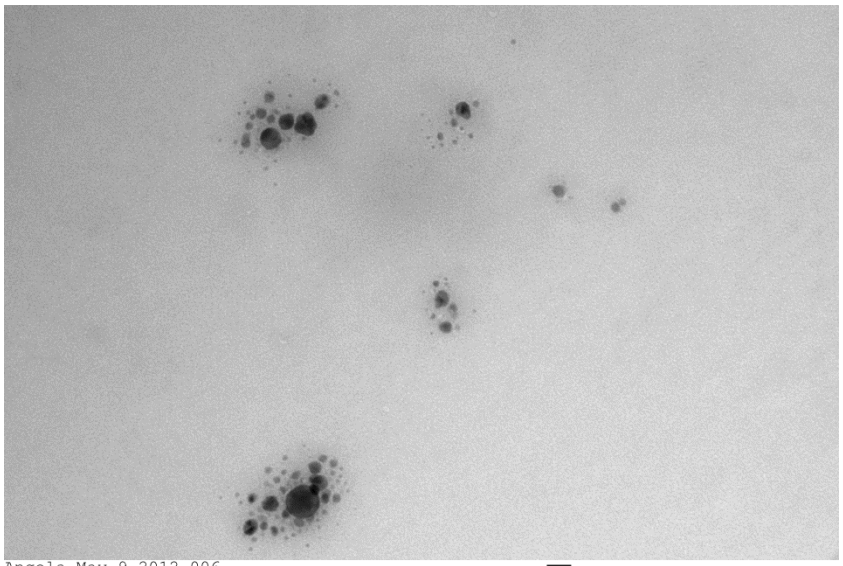

Angela May 9 2012_006
Ag nanoparticle
Cal: 0.139938 nm/pix
11:00:11 a 05/09/12

20 nm
HV=75.0kV
Direct Mag: 80000x
UM Biological Science

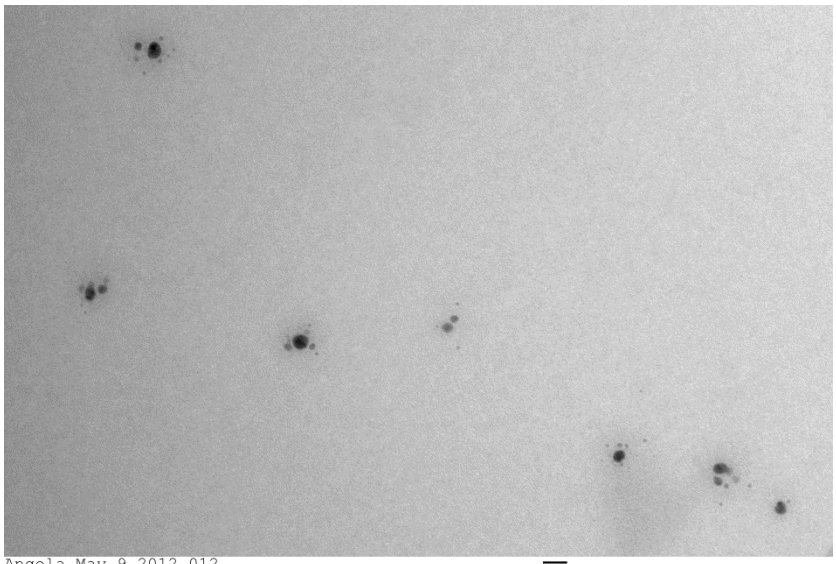

Angela May 9 2012_012
Ag nanoparticle
Cal: 0.139938 nm/pix
11:20:42 a 05/09/12

20 nm
HV=75.0kV
Direct Mag: 80000x
UM Biological Science

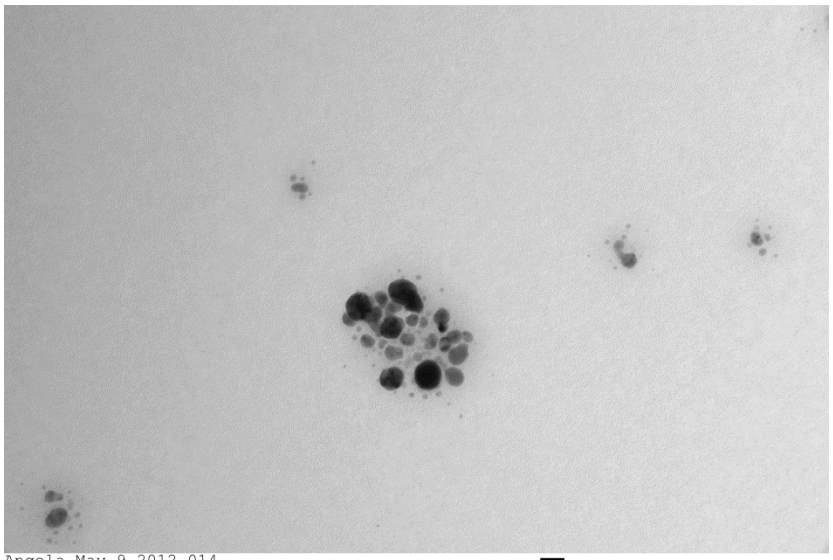

Angela May 9 2012_014
Ag nanoparticle
Cal: 0.139938 nm/pix
11:26:04 a 05/09/12

20 nm
HV=75.0kV
Direct Mag: 80000x
UM Biological Science

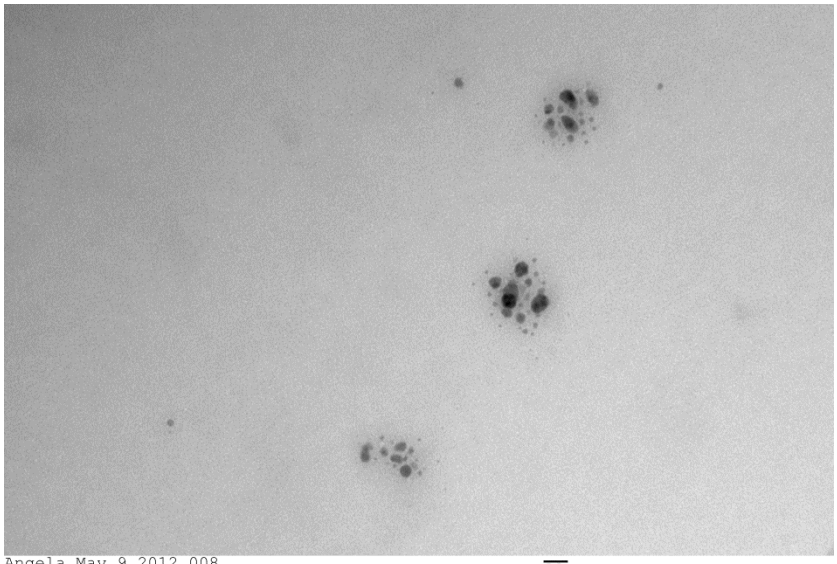

Angela May 9 2012_008
Ag nanoparticle
Cal: 0.139938 nm/pix
11:02:45 a 05/09/12

20 nm
HV=75.0kV
Direct Mag: 80000x
UM Biological Science

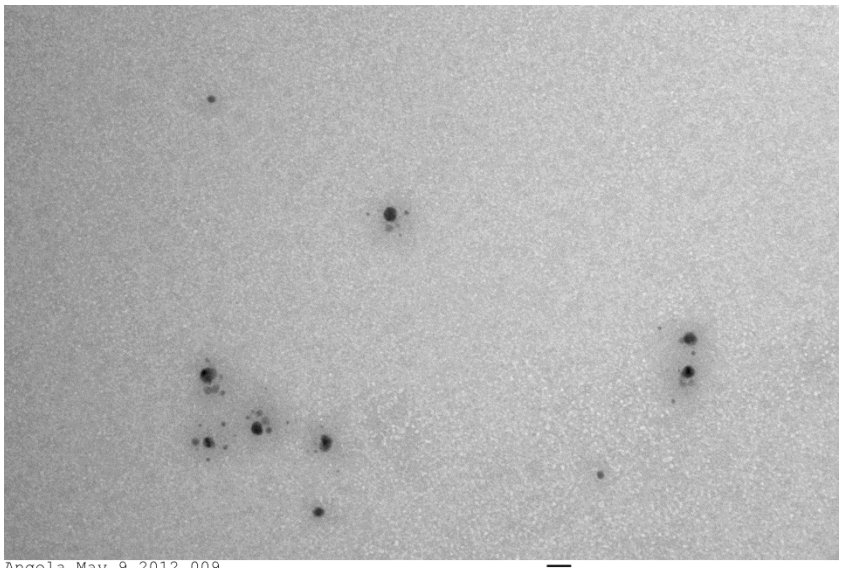

Angela May 9 2012_009
Ag nanoparticle
Cal: 0.139938 nm/pix
11:09:04 a 05/09/12

20 nm
HV=75.0kV
Direct Mag: 80000x
UM Biological Science

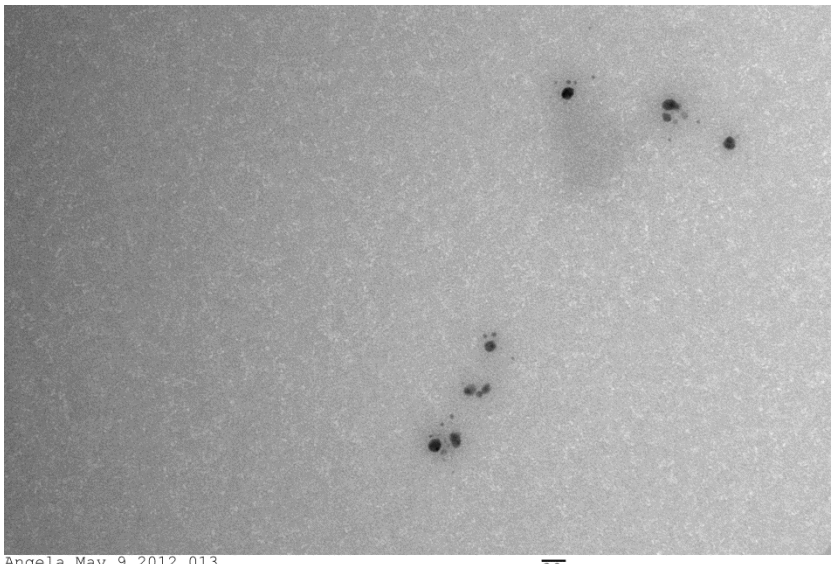

Angela May 9 2012_013
Ag nanoparticle
Cal: 0.139938 nm/pix
11:24:02 a 05/09/12

20 nm
HV=75.0kV
Direct Mag: 80000x
UM Biological Science

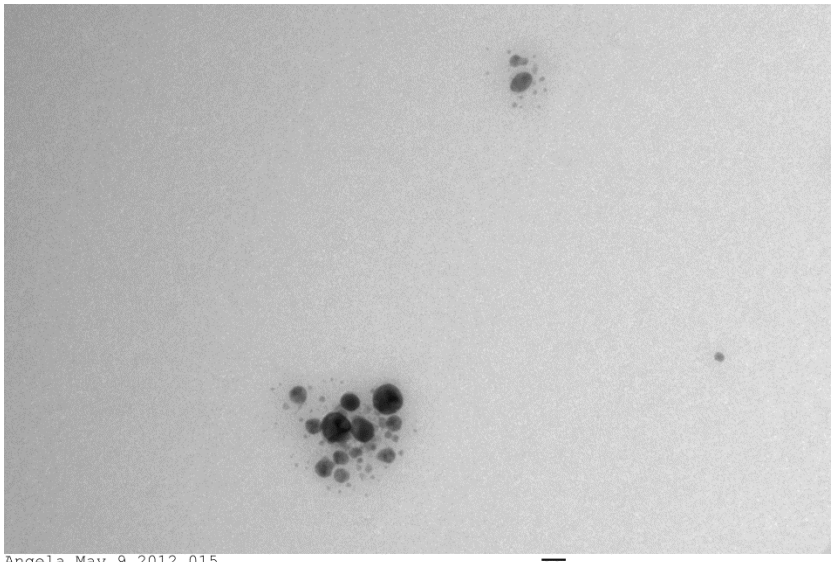

Angela May 9 2012_015
Ag nanoparticle
Cal: 0.139938 nm/pix
11:27:08 a 05/09/12

20 nm
HV=75.0kV
Direct Mag: 80000x
UM Biological Science

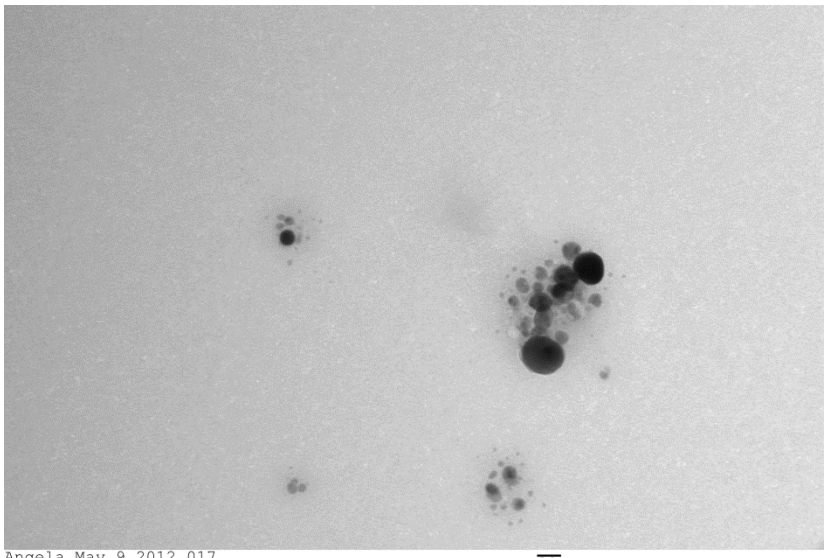

Angela May 9 2012_017
Ag nanoparticle
Cal: 0.139938 nm/pix
11:28:56 a 05/09/12

20 nm
HV=75.0kV
Direct Mag: 80000x
UM Biological Science

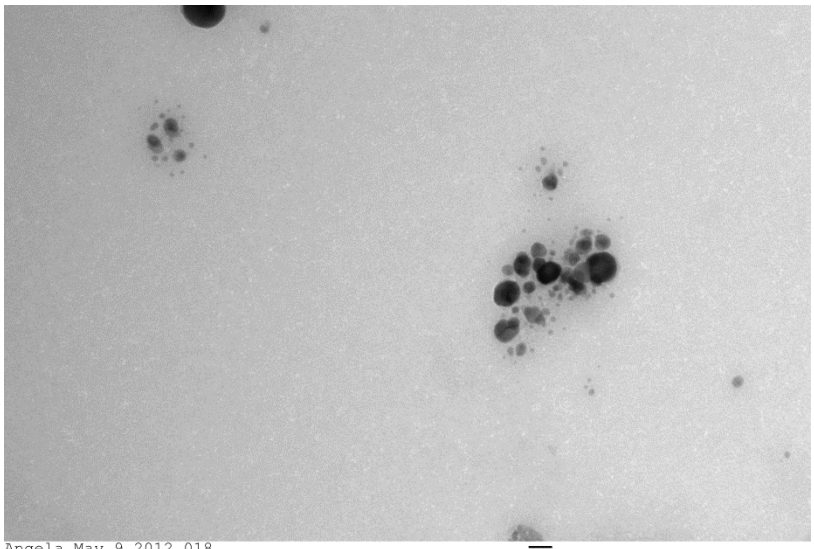

Angela May 9 2012_018
Ag nanoparticle
Cal: 0.139938 nm/pix
11:30:20 a 05/09/12

20 nm
HV=75.0kV
Direct Mag: 80000x
UM Biological Science

The example size measuring screen shot